Classical/Quantum Dynamics of a Particle in Free Fall

Thesis sketch for Tomoko Ishihara

Introduction. Every student of mechanics encounters discussion of the idealized one-dimensional dynamical systems

$$F(x) = m\ddot{x} \quad \text{with} \quad F(x) = \begin{cases} 0 & : \text{ FREE PARTICLE} \\ -mg & : \text{ PARTICLE IN FREE FALL} \\ -k\,x & : \text{ HARMONIC OSCILLATOR} \end{cases}$$

at a very early point in his/her education, and with the first & last of those systems we are never done: they are—for reasons having little to do with their physical importance—workhorses of theoretical mechanics, traditionally employed to illustrated formal developments as they emerge, one after another. But—unaccountably—the motion of particles in uniform gravitational fields[1] is seldom treated by methods more advanced than those accessible to beginning students.[2] It is true that terrestrial gravitational forces are so relatively weak that they can usually be dismissed as irrelevant to the phenomenology studied by physicists in their laboratories,[3] but it will my thesis that the 1-dimensional free fall problem has very much to teach us of a *formal* nature.

[1] It is to avoid that cumbersome phrase that I adopt the "free fall" locution, though technically *free fall presumes neither uniformity nor constancy of the ambient gravitational field*.

[2] The place to insert reference to the results of a bibliographic search, listing both a sampling of the classical/quantum texts that (like Goldstein's *Classical Mechanics*) conspicuously *fail* to mention the free fall problem, and the most important of those relatively few texts that *do* treat aspects of the problem.

[3] There are exceptions: I am thinking of experiments done several decades ago where neutron diffraction in crystals was found to be sensitive to the value of g: would be good to track down such references.

1. Free fall trajectories in spacetime. The general solution of

$$\ddot{x} + g = 0 \tag{1}$$

can be described

$$x(t) = a + bt - \tfrac{1}{2}gt^2 \tag{2}$$

where a and b are arbitrary constants. Standardly we associate a and b with *initial data*

$$a \equiv x(0) \quad : \quad b \equiv \dot{x}(0)$$

but other interpretations are sometimes more useful: from stipulated endpoint conditions

$$x_0 = a + bt_0 - \tfrac{1}{2}gt_0^2$$
$$x_1 = a + bt_1 - \tfrac{1}{2}gt_1^2$$

we compute (its easy by hand if we compute b first, but ask *Mathematica*)

$$\left.\begin{aligned} a &= \frac{x_0t_1 - x_1t_0}{t_1 - t_0} - \tfrac{1}{2}gt_0t_1 \\ b &= \frac{x_1 - x_0}{t_1 - t_0} + \tfrac{1}{2}g(t_0 + t_1) \end{aligned}\right\} \tag{3}$$

giving

$$\begin{aligned} x(t; x_1, t_1; x_0, t_0) = &\left\{\frac{x_0t_1 - x_1t_0}{t_1 - t_0} - \tfrac{1}{2}gt_0t_1\right\} \\ &+ \left\{\frac{x_1 - x_0}{t_1 - t_0} + \tfrac{1}{2}g(t_0 + t_1)\right\}t - \tfrac{1}{2}gt^2 \end{aligned} \tag{4}$$

which checks out: $x(t_0; x_1, t_1; x_0, t_0) = x_0$, $x(t_1; x_1, t_1; x_0, t_0) = x_1$.

2. Translational equivalence in spacetime. Spacetime translation of what we will agree to call the "primitive solution"

$$x = -\tfrac{1}{2}gt^2 \tag{5.1}$$

gives

$$(x - x_0) = -\tfrac{1}{2}g(t - t_0)^2 \tag{5.2}$$

or

$$x = (x_0 - \tfrac{1}{2}gt_0^2) + (gt_0)t - \tfrac{1}{2}gt^2$$

To say the same thing another way: if into (2) we introduce the notation

$$\left.\begin{aligned} b &= gt_0 \\ a &= x_0 - \tfrac{1}{2g}b^2 = x_0 - \tfrac{1}{2}gt_0^2 \end{aligned}\right\} \tag{6}$$

then we achieve (5.2). In short: *every solution is translationally equivalent to the primitive solution*. In this regard the free fall problem is distinguished from both the FREE PARTICLE PROBLEM

> General solution of $\ddot{x} = 0$ reads $x(t) = a + bt$. Take $x(t) = Bt$ to be the primitive solution (B a prescribed constant "velocity"). To bring $a + bt$ to the form Bt one must
> - translate in space and
> - rescale the time coordinate

and the HARMONIC OSCILLATOR

> General solution of $\ddot{x} = -\omega^2 x$ reads $x(t) = a\cos\omega t + (b/\omega)\sin\omega t$. Take $x(t) = (B/\omega)\sin\omega t$ to be the primitive solution (here B is again a prescribed constant "velocity": we have arranged to recover free particle conventions in the limit $\omega \downarrow 0$). To bring the general solution to primitive form one must
> - translate in time and
> - rescale the space coordinate

REMARK: Some figures here would make everything clear. Figure 1 captures the situation as it relates specifically to the free fall problem.

The preceding observations motivate the following

> CONJECTURE: If $x(t) = x_0 + f(t - t_0)$ describes the general solution of a differential equation of the form $\ddot{x} = F(x)$ then necessarily $F(x) =$ constant.

—the proof of which is, in fact, easy. The conjecture identifies a seldom-remarked **uniqueness property of the free fall problem**, the effects of which will haunt this work.

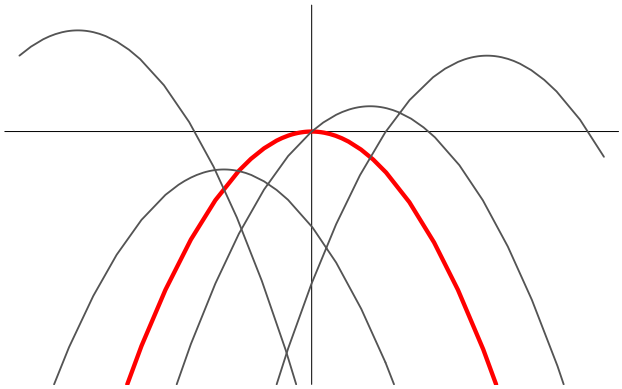

FIGURE 1: *Shown in red is a graph of the "primitive" free fall solution* (5.1). *Other solutions of* $\ddot{x} + g = 0$ *are seen to have the same shape; i.e., to be translationally equivalent.*

3. Lagrangian, Hamiltonian and 2-point action. If, as is most natural, we take the free fall Lagrangian to be given by

$$L(\dot{x}, x) \equiv \tfrac{1}{2}m\dot{x}^2 - U(x) \tag{7.1}$$

$$U(x) = mgx \tag{7.2}$$

then

$$p \equiv \partial L/\partial\dot{x} = m\dot{x}$$

and the Hamiltonian becomes

$$H(p,x) = p\dot{x} - L(\dot{x},x) = \tfrac{1}{2m}p^2 + mgx \tag{8}$$

The *action* associated with any test path $x(t)$ is given by

$$S[x(t)] \equiv \int_{t_0}^{t_1} L\big(\dot{x}(t), x(t)\big)\, dt$$

Take $x(t)$ to be in fact a *solution* of the equation of motion. Take it, more particularly, to be the solution described at (2). Then

$$\begin{aligned} S[a+bt-\tfrac{1}{2}gt^2] &= \int_{t_0}^{t_1} L(b-gt, a+bt-\tfrac{1}{2}gt^2)\, dt \\ &= m\Big\{(\tfrac{1}{2}b^2 - ag)(t_1-t_0) - bg(t_1^2-t_0^2) + \tfrac{1}{3}g^2(t_1^3-t_0^3)\Big\} \end{aligned}$$

Take a and b to be given by (3). Then *Mathematica* supplies[4]

$$S(x_1,t_1;x_0,t_0) = \tfrac{1}{2}m\left\{\frac{(x_1-x_0)^2}{t_1-t_0} - g(x_0+x_1)(t_1-t_0) - \tfrac{1}{12}g^2(t_1-t_0)^3\right\} \tag{9}$$

This is the action functional associated with (not must some arbitrary "test path" linking $(x_0,t_0) \longrightarrow (x_1,t_1)$ but with) the *dynamical path* linking those spacetime points: it is not a functional but a *function* of the parameters $(x_1,t_1;x_0,t_0)$ that serve by (4) to define the path, and is, for reasons now obvious, called the "2-point action function."

It becomes notationally sometimes convenient to drop the $_1$'s from x_1 and t_1, and to write $S(x,t;x_0,t_0)$. We observe that the free fall action function (9) gives back the more frequently encountered free particle action

$$\begin{aligned} &\downarrow \\ &= \tfrac{1}{2}m\frac{(x_1-x_0)^2}{t_1-t_0} \end{aligned} \quad \text{when the gravitational field is turned off: } g \downarrow 0$$

4. Energy & momentum. The total energy of our freely falling particle is given by

$$\begin{aligned} E(t) &= \tfrac{1}{2}m\dot{x}^2(t) + mgx(t) \\ &= \tfrac{1}{2m}p^2(t) + mgx(t) \\ &= \text{instantaneous numerical value of the Hamiltonian} \end{aligned} \tag{10}$$

Taking $x(t)$ to be given by (2) we compute

$$E(t) = \tfrac{1}{2}m(b^2+2ga) = \text{constant} \tag{11}$$

[4] For the first occurance of this result in my own writing, see QUANTUM MECHANICS (1967), Chapter 1, page 21. But beware: one must reverse the sign of g to achieve agreement with results quoted there.

Energy conservation is no surprise: it follows directly from the t-independence of the Hamiltonian (which is to say: from the t-independence of the potential).

Working from (2) we find that the momentum

$$p(t) = m(b - gt) \tag{12}$$

which follows also from

$$\begin{aligned} p(t) &= \sqrt{2m[E - mg\,x(t)]} \\ &= \sqrt{m^2(b^2 + 2ga) - 2m^2g(a + bt - \tfrac{1}{2}gt^2)} \\ &= \sqrt{m^2(b^2 - 2gbt + g^2t^2)} \\ &= \sqrt{m^2(b - gt)^2} \end{aligned}$$

Working from (4)—or (more simply) by drawing upon (3)—we obtain

$$p(t) = m\Big\{\frac{x_1 - x_0}{t_1 - t_0} + \tfrac{1}{2}g(t_0 - 2t + t_1)\Big\} \tag{13}$$

which means that a particle that moves along the trajectory $(x_0, t_0) \longrightarrow (x_1, t_1)$ must be launched with momentum

$$p(t_0) = m\Big\{\frac{x_1 - x_0}{t_1 - t_0} + \tfrac{1}{2}g\,(t_1 - t_0)\Big\}$$

and arrives with momentum

$$p(t_1) = m\Big\{\frac{x_1 - x_0}{t_1 - t_0} - \tfrac{1}{2}g\,(t_1 - t_0)\Big\}$$

General theory asserts, and computation confirms, that these equations could also have been obtained from

$$\left.\begin{aligned} p(t_1) &= +\frac{\partial S(x_1, t_1; x_0, t_0)}{\partial x_1} \\ p(t_0) &= -\frac{\partial S(x_1, t_1; x_0, t_0)}{\partial x_0} \end{aligned}\right\} \tag{14}$$

Notice that

$$\Delta p \equiv p(t_1) - p(t_0) = -mg\,(t_1 - t_0) = \int_{t_0}^{t_1} (-mg)\,dt = \text{impulse}$$

and that, according to (13), $p(t)$ interpolates *linearly* between its initial and final values.

5. Noether's theorem. It is to a mathematician (Emmy Noether, 1918) that physicists owe recognition of an illuminating connection between

- an important class of conservation laws and
- certain invariance properties ("symmetries") of the dynamical action.

We look here only to some particular instances of that connection, as they relate specifically to the free fall problem.

We saw in §2 that **time translation** generally, and infinitesimal time translation $(x,t) \longmapsto (x, t+\delta t)$ more particularly,[5] maps solutions to other solutions of the free fall equations:

$$(x-x_0) + \tfrac{1}{2}g(t-t_0)^2 = 0 \quad \longmapsto \quad (x-x_0) + \tfrac{1}{2}g(t-(t_0-\delta t))^2 = 0$$

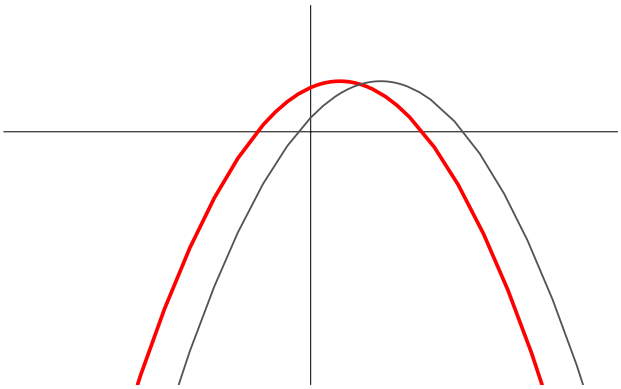

FIGURE 2: *Graphs of a free fall and of its temporal translate. If the initial motion is identified by specification of its endpoints then to identify its translate one must modify <u>both</u> endpoints:*

$$(x_1,t_1;x_0,t_0) \longmapsto (x_1,t_1+\delta t;x_0,t_0+\delta t)$$

Noether argues[6] that

$$\begin{aligned}\delta S &= S(x_1,t_1+\delta t;x_0,t_0+\delta t) - S(x_1,t_1;x_0,t_0)\\ &= J(\dot x,x)\Big|_{t_0}^{t_1}\cdot\delta t \quad \text{with} \quad J(\dot x,x) \equiv -\Big[p(\dot x,x)\dot x - L(\dot x,x)\Big]\end{aligned}$$

But it is a manifest implication of (9) that

$$\delta S = 0 \quad : \quad \text{the dynamnical action is } t\text{-translation } \textit{invariant}$$

and from this it follows that

$$\Big[p(\dot x,x)\dot x - L(\dot x,x)\Big]_{t_1} = \Big[p(\dot x,x)\dot x - L(\dot x,x)\Big]_{t_0}$$

which asserts simply that *energy is conserved*.

[5] Noether worked within the framework provided by the calculus of variations, so found it natural to assign special importance to *infinitesimal* transformations.

[6] See CLASSICAL MECHANICS (1983), page 163.

Similarly . . . we saw in §2 that **space translation** generally, and infinitesimal space translation $(x,t) \longmapsto (x+\delta x, t)$ more particularly, maps solutions to other solutions of the free fall equations:

$$(x-x_0)+\tfrac{1}{2}g(t-t_0)^2=0 \quad \longmapsto \quad (x-(x_0-\delta x))+\tfrac{1}{2}g(t-t_0)^2=0$$

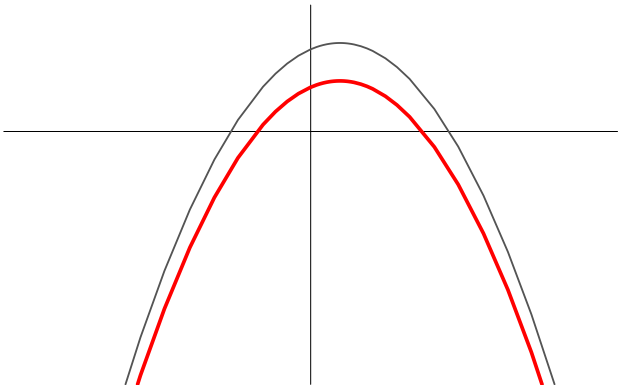

FIGURE 3: *Graphs of a free fall and of its spatial translate. Again, if we adopt endpoint specification then we must write*

$$(x_1,t_1;x_0,t_0) \longmapsto (x_1+\delta x, t_1; x_0+\delta x, t_0)$$

Noether's argument in this instance supplies

$$\begin{aligned}\delta S &= S(x_1,t_1+\delta t;x_0,t_0+\delta t)-S(x_1,t_1;x_0,t_0)\\ &= J(\dot x,x)\Big|_{t_0}^{t_1}\cdot\delta t \quad \text{where now} \quad J(\dot x,x)\equiv p(\dot x,x)\end{aligned}$$

But it is a manifest implication of (9) that—owing to the presence of the (x_0+x_1)-term (which vanishes in the free particle limit $g\downarrow 0$)—

$$\delta S\neq 0 \quad : \quad \text{the dynamnical action is not } \underline{x\text{-translation invariant}}$$

and from this it follows that

$$\Big[p(\dot x,x)\Big]_{t_1} \neq \Big[p(\dot x,x)\Big]_{t_0} \quad : \quad \text{momentum is } \textit{not conserved}$$

Evidently it is not the "symmetry of the space of motions" that matters: it is *symmetry of the dynamical* <u>*action*</u> that gives rise to conservation laws.

6. 2-point Hamilton-Jacobi equations. Classical mechanics, pursued to its depths, supplies the information that the dynamical action function satisfies a pair of (generally non-linear) partial differential equations—namely, the

Hamilton-Jacobi equation

$$H\big(\tfrac{\partial S(x_1,t_1;\bullet,\bullet)}{\partial x_1}, x_1\big) + \tfrac{\partial S(x_1,t_1;\bullet,\bullet)}{\partial t_1} = 0$$

and its time-reversed companion

$$H\big(\tfrac{\partial S(\bullet,\bullet;x_0,t_0)}{\partial x_0}, x_0\big) - \tfrac{\partial S(\bullet,\bullet;x_0,t_0)}{\partial t_0} = 0$$

In the present context those equations read

$$\tfrac{1}{2m}\big(\tfrac{\partial S(x_1,t_1;\bullet,\bullet)}{\partial x_1}\big)^2 + mg\,x_1 + \tfrac{\partial S(x_1,t_1;\bullet,\bullet)}{\partial t_1} = 0 \tag{15.1}$$

$$\tfrac{1}{2m}\big(\tfrac{\partial S(\bullet,\bullet;x_0,t_0)}{\partial x_0}\big)^2 + mg\,x_0 - \tfrac{\partial S(\bullet,\bullet;x_0,t_0)}{\partial t_0} = 0 \tag{15.2}$$

and *Mathematica* confirms that the $S(x_1,t_1;x_0,t_0)$ of (9) does in fact satisfy those equations.

There are, of course, infinitely many *other* bi-functions $F(x_1,t_1;x_0,t_0)$ that satisfy the H-J system (15). We have yet to describe the sense in which S occupies a distinguished place within that population.

7. Separated solutions of the 1-point Hamilton-Jacobi equation. In some respects deeper, and in all respects simpler and more transparent ... than the theory of 2-point H-J functions is the theory of 1-point H-J functions, central to which is the (solitary) Hamilton-Jacobi equation

$$H\big(\tfrac{\partial S(x,t)}{\partial x}, x\big) + \tfrac{\partial S(x,t)}{\partial x} = 0 \tag{16}$$

As—briefly—to the meaning of that equation: given a function $S(x) \equiv S(x,0)$ the fundamental relation

$$p(x) = \tfrac{\partial S(x,0)}{\partial x} \tag{17}$$

serves to describe a *curve* $\mathcal{C}_0$ on phase space (*i.e.*, on (x,p)-space). The H-J equation (16) describes the *dynamical motion of that curve*:

$$\mathcal{C}_0 \xrightarrow[\text{Hamiltonian-induced phase flow}]{} \mathcal{C}_t \tag{18}$$

We will have occasion later to describe concrete instances of (18).

In the case of interest (16) reads

$$\tfrac{1}{2m}\big(\tfrac{\partial S(x,t)}{\partial x}\big)^2 + mg\,x + \tfrac{\partial S(x,t)}{\partial t} = 0 \tag{19}$$

What happens if we attempt to solve that non-linear partial differential equation by separation of variables? Write

$$S(x,t) = W(x) + F(t)$$

and obtain

$$\tfrac{1}{2m}\big(\tfrac{\partial W(x)}{\partial x}\big)^2 + mg\,x = -\tfrac{\partial F(t)}{\partial t}$$

whence

$$\left.\begin{aligned} \tfrac{1}{2m}\big(\tfrac{dW(x)}{dx}\big)^2 + mg\,x &= +E \\ \tfrac{dF(t)}{dt} &= -E \end{aligned}\right\} \quad : \quad E \text{ is a separation constant}$$

Immediately

$$\begin{aligned} F(t) &= F_0 - Et \\ W(x) &= \int^x \sqrt{2m[E - mg\xi]}\, d\xi \\ &= \tfrac{2}{3mg}\sqrt{2m[E - mgx]^3} + W_0 \end{aligned}$$

which supply this E-parameterized family of particular H-J functions

$$S(x,t;E) = \tfrac{2}{3mg}\sqrt{2m[E - mgx]^3} - Et + S_0 \tag{20}$$

Here we have lumped the additive constants: $S_0 \equiv W_0 + F_0$.[7]

We will revisit this topic after we have acquired quantum mechanical reason to do so: for the moment I must be content mere to set the stage. We are in the habit of thinking that *solutions obtained by separation can be combined to produce the general solution* of a partial differential equation. How is that to be accomplished in the present instance? Quantum theory will motivate us to ask this sharper question: How can the H-J functions $S(x,t;E)$ be combined to produce the $S(x_1,t_1;x_0,t_0)$ of (9)?[8]

8. Hamiltonian methods. The free fall Hamiltonian

$$H(p,x) = \tfrac{1}{2m}p^2 + mgx$$

supplies canonical equations

$$\left.\begin{aligned} \dot{x} &= +\partial H/\partial p = \tfrac{1}{m}p \\ \dot{p} &= -\partial H/\partial x = -mg \end{aligned}\right\} \tag{21}$$

which are transparently equivalent to (1). The motion of an arbitrary observable $A(p,x,t)$ is therefore given by

$$\dot{A} = \frac{\partial A}{\partial x}\frac{\partial H}{\partial p} - \frac{\partial A}{\partial p}\frac{\partial H}{\partial x} + \frac{\partial A}{\partial t} \equiv [A,H\,] + \frac{\partial A}{\partial t} \tag{22}$$

Energy conservation is, from this point of view, immediate

$$\dot{H} = [H,H\,] = 0$$

and so is momentum non-conservation:

$$\dot{p} = [\,p,H\,] = [\,p,mgx] = -mg \neq 0$$

---

[7] Because it is always useful to inquire "What happens in the free particle limit to the gravitational result in hand?" we expand in powers of g and obtain the curious result

$$S = \big\{S_0 - \tfrac{4}{3}\tfrac{E^2}{P}g^{-1}\big\} + \big\{Px - Et\big\} - \tfrac{1}{2}\tfrac{m^2x^2}{P}g + \cdots$$

where $P \equiv \sqrt{2mE}$.

[8] General theory relating to those questions is developed in Appendix B: "Legendre transformation to/from the 'energy representation' and its Fourier-analytic quantum analog" to the class notes cited in footnote 6.

Phase flow carries

$$(x,p)_0 \xrightarrow[\text{phase flow}]{} (x,p)_t = (x_0 + \tfrac{1}{m}p_0 t - \tfrac{1}{2}gt^2,\, p_0 - mgt) \qquad (23)$$

Necessarily $(x,p)_0$ and $(x,p)_t$ lie on the same isoenergetic curve, and those E-parameterized curves

$$\tfrac{1}{2m}p^2 + mgx = E$$

are parabolic, oriented as shown in the following figure:

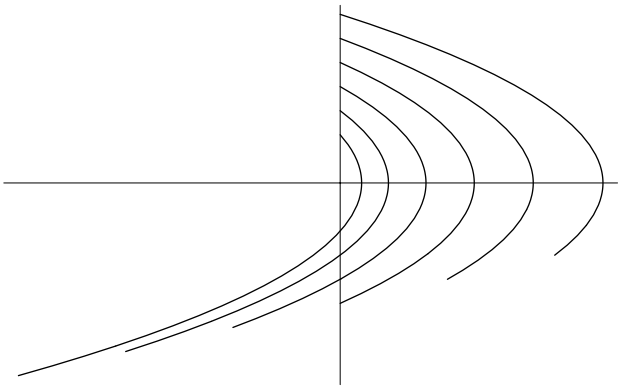

FIGURE 4: *Effect of phase flow on a representative population of phase points, computed on the basis of* (23). *The x-axis runs $\rightarrow$, the p-axis runs $\uparrow$. I have set $m = g = 1$ and assigned to the phase points the initial coordinates* $(0, 0.4)$, $(0, 0.6)$, $(0, 0.8)$, $(0, 1.0)$, $(0, 1.2)$ *and* $(0, 1.4)$. *The coaxial parabolas all have the same shape, and are conveniently distinguished/identified by their x-intercepts*: $x_E = E/mg$.

We now adjust our viewpoint, agreeing to look upon ...

9. Gravitation as an artifact of non-inertiality. The root idea is that when we encounter an equation of motion of the form

$$\boldsymbol{F} + m\boldsymbol{G} = m\ddot{\boldsymbol{x}}$$

we should think of the $m\boldsymbol{G}$-term not as a "force that happens to adjust its strength in proportion to the mass of the particle upon which it acts" (shades of Galileo!)—indeed, not as a "force" at all—but as an "acceleration term" that has slipped to the wrong side of the equality: that we should instead write

$$\boldsymbol{F} = m(\ddot{\boldsymbol{x}} - \boldsymbol{G})$$

and interpret the non-Newtonian structure of the expression on the right to signal that $\boldsymbol{x}$ must refer to a *non-inertial coordinate system*. To adopt such a view[9] is to dismiss gravitation as a "fictitious force," akin to the centrifugal

[9] Hard to do if, as I have, you've every been hospitalized by a fall, though we speak here of nothing less than Einstein's lofty Equivalence Principle.

and Coriolis "forces." The idea can be implemented, in a degree of generality sufficient for the purposes at hand,[10] as follows:

Let x and x, which refer to Cartesian coordinatizations of 1-space, stand in the simple relation

$$\mathrm{x} = x + a(t)$$

Evidently $a(t)$ describes the instantaneous location, relative to the $\mathcal{X}$-frame, of the $\mathcal{X}$-origin (conversely, $-a(t)$ describes the instantaneous location, relative to the $\mathcal{X}$-frame, of the $\mathcal{X}$-origin):

$$\mathrm{x}(0,t) = +a(t)$$
$$x(0,t) = -a(t)$$

Assume $\mathcal{X}$ to be inertial: assume, in other words, that the force-free motion of a mass m relative to $\mathcal{X}$ can be described

$$m\ddot{\mathrm{x}} = 0$$

In x-coordinates that statement becomes

$$m(\ddot{x} + \ddot{a}) = 0$$

To recover (1) we have only to set $a(t) = \frac{1}{2}gt^2$. (We might, more generally, set $a(t) = a_0 + a_1 t + \frac{1}{2}gt^2$ but in the interest of simplicity I won't.) Then

$$\mathrm{x} = x + \tfrac{1}{2}gt^2$$
$$x = \mathrm{x} - \tfrac{1}{2}gt^2$$

Motion which is seen to be free with respect to $\mathcal{X}$ is seen as free fall to the left when referred to the $\mathcal{X}$-frame which $\mathcal{X}$ sees to be accelerating to the right.

Turning now from the kinematic to the Lagrangian dynamical aspects of the problem, and taking

$$L(\dot{\mathrm{x}}, \mathrm{x}) = \tfrac{1}{2}m\dot{\mathrm{x}}^2 \quad : \quad \text{FREE PARTICLE LAGRANGIAN}$$

as an obvious point of departure, we construct

$$L(\dot{x}, x, t) \equiv L(\dot{x} + gt, x + \tfrac{1}{2}gt^2) = \tfrac{1}{2}m(\dot{x} + gt)^2$$

which (gratifyingly, but not at all to our surprise) gives back (1):

$$\tfrac{d}{dt}m(\dot{x} + gt) = m(\ddot{x} + g) = 0$$

The Lagrangian $L(\dot{x}, x, t)$ does not much resemble the Lagrangian encountered at (7), but in fact they *differ only by a gauge term*:

$$\left[\tfrac{1}{2}m(\dot{x} + gt)^2\right] = \left[\tfrac{1}{2}m\dot{x}^2 - mgx\right] + \tfrac{d}{dt}\left(mgxt + \tfrac{1}{6}mg^2t^3\right)$$

[10] For a fairly detailed general account of the theory of fictitious forces see pages 101–110 in the class notes cited several times previously.[6]

Our program—the objective of which is to recover all the unfamiliar details of free fall physics from the simpler details of free particle physics—proceeds from the elementary device of stepping from an inertial frame to a uniformly accelerated frame, but is seen now to involve rather more than a simple change of coordinates $x \longrightarrow x = x - \frac{1}{2}gt^2$: it is a 2-STEP PROCESS

$$\begin{aligned} x &\longrightarrow x = x - \tfrac{1}{2}gt^2 \\ L &\longrightarrow L = L + \tfrac{d}{dt}\Lambda \end{aligned}$$

involving a coordinate transformation *and a synchronized gauge transformation*. We must attend carefully to conceptual/notational distinctions at risk of becoming confused (or—which is almost as bad—confusing). I spell out the detailed meaning and some of the immediate implications of the second of the preceding statements:

$$\begin{aligned} L(\dot{x}) &\equiv \tfrac{1}{2}m\dot{x}^2 \\ &\downarrow \\ L(\dot{x},x) &\equiv \tfrac{1}{2}m\dot{x}^2 - mgx \\ &= L(\dot{x}+gt) + \tfrac{d}{dt}\Lambda(x,t) \\ &\qquad\qquad \Lambda(x,t) \equiv -mgxt - \tfrac{1}{6}mg^2t^3 \\ &= \tfrac{1}{2}m(\dot{x}+gt)^2 - mg\big[\dot{x}t + x + \tfrac{1}{2}gt^2\big] \end{aligned}$$

Collaterally

$$\begin{aligned} p \equiv \partial L/\partial\dot{x} &= m\dot{x} \\ &\downarrow \\ p \equiv \partial L/\partial\dot{x} &= m\dot{x} \\ &= (\partial L/\partial\dot{x})\underbrace{(\partial\dot{x}/\partial\dot{x})}_{=(\partial x/\partial x)=1} + (\partial\Lambda/\partial x) \\ &= p - mgt \end{aligned}$$

Look now to the transformation of the Hamiltonian. Generally, the fact that the Lagrangian responds as a scalar to coordinate transformations implies that the Hamiltonian does too: that would give

$$\begin{aligned} H(p,x) &\equiv p\dot{x} - L = \tfrac{1}{2m}p^2 \\ &\downarrow \\ H(p,x) &\equiv p\dot{x} - \tfrac{1}{2}m(\dot{x}+gt)^2\Big|_{\dot{x}\to p/m} \\ &= \tfrac{1}{2m}p^2 - pgt - \tfrac{1}{2}mg^2t^2 \end{aligned}$$

But gauge adjustment of the Lagrangian is found[11] to cause the Hamiltonian to pick up an subtractive t-derivative of the gauge function, which in the present

[11] See page 198 in CLASSICAL MECHANICS (1983).

instance supplies

$$\begin{aligned}&\downarrow\\&= \tfrac{1}{2m}p^2 - pgt - \tfrac{1}{2}mg^2t^2 - \tfrac{d}{dt}\Big[-mgxt - \tfrac{1}{6}mg^2t^3\Big]_{\dot{x}\to p/m}\\&= \tfrac{1}{2m}p^2 + mgx\end{aligned}$$

10. Contact with the theory of canonical transformations. From

$$\left.\begin{aligned}x &\longrightarrow x = x - \tfrac{1}{2}gt^2\\ p &\longrightarrow p = p - mgt\end{aligned}\right\} \tag{24}$$

it follows trivially that

$$[x,p] \equiv \frac{\partial x}{\partial x}\frac{\partial p}{\partial p} - \frac{\partial p}{\partial x}\frac{\partial x}{\partial p} = 1$$

which is to say: the transformation (24) is *canonical*. At any given t the equations (24) describe a *rigid translation of the phase plane*, and it is because of that "rigidity" that the t-parameterized curves traced by individual phase points are congruent (see again Figure 4).

Classical mechanics supplies two distinct techniques for "generating" canonical transformations—one associated with the name of Legendre, the other with that of Lie. We look first to the former:[12]

Legendre recognizes generators of four standard types

$$F_1(x,x), \quad F_2(x,p), \quad F_3(p,x), \quad F_4(p,p)$$

—each of which is a function of "half the old phase coordinates (x,p) and half the new (x,p)." A moment's tinkering leads us to the Type 2 generator

$$F_2(x,p) \equiv (x - \tfrac{1}{2}gt^2)(p + mgt) \tag{25}$$

from which we recover (24) by writing

$$\left.\begin{aligned}p &= \partial F_2/\partial x = p + mgt\\ x &= \partial F_2/\partial p = x - \tfrac{1}{2}gt^2\end{aligned}\right\} \tag{26}$$

Notice that in the limit $g \downarrow 0$ we are left with a well-known "generator of the identity": $F_2(x,p) = xp$.

Lie would have us undertake to achieve (24) not "all at once" (as Legendre did) but incrementally, by iteration of *infinitesimal* canonical transformations. His idea can be implemented as follows: in place of (24) write

[12] See pages 224–234 in CLASSICAL MECHANICS (1983).

$$\left.\begin{aligned} x(u) &= x - \tfrac{1}{2}gt^2u \\ p(u) &= p - mgtu \end{aligned}\right\} \tag{27}$$

Here u is a dimensionless parameter that in effect "tunes the strength" of the gravitational field and enables us to *smoothly interpolate* between free particle physics and free fall physics: more particularly

$$\begin{aligned} x(0) &= x \\ p(0) &= p \end{aligned} \qquad \text{and} \qquad \begin{aligned} x(1) &= x \\ p(1) &= p \end{aligned}$$

It follows from (27) that

$$\begin{aligned} \tfrac{d}{du}x(u) &= -\tfrac{1}{2}gt^2 \\ \tfrac{d}{du}p(u) &= -mgt \end{aligned}$$

These equations can be made to assume the design of Hamilton's canonical equations of motion

$$\left.\begin{aligned} \tfrac{d}{du}x(u) &= +\tfrac{\partial}{\partial p}K(p,x) = -[K,x] \\ \tfrac{d}{du}p(u) &= -\tfrac{\partial}{\partial x}K(p,x) = -[K,p] \end{aligned}\right\} \tag{28}$$

provided we set

$$K(p,x) = mgtx - \tfrac{1}{2}gt^2p \tag{29}$$

Formal iteration[13] leads to this description of the *solution* of (28):

$$\begin{aligned} x(u) &= x - u[K,x] + \tfrac{1}{2!}u^2[K,[K,x]] - \tfrac{1}{3!}u^3[K,[K,[K,x]]] + \cdots \\ &= x - u\tfrac{1}{2}gt^2 \\ p(u) &= p - u[K,p] + \tfrac{1}{2!}u^2[K,[K,p]] - \tfrac{1}{3!}u^3[K,[K,[K,p]]] + \cdots \\ &= p - umgt \end{aligned}$$

from which we recover (24) at $u = 1$. It is the fact that x and p enter *linearly* into the design of $K(p,x)$ that accounts for the exceptional simplicity of these results (*i.e.*, for the disappearance of terms of $O(u^2)$).

Turning now from discussion of what the transformation does to phase coordinates to discussion of what it does to the expression of the physics ... if we start from

$$H(p) = \tfrac{1}{2m}p^2 \quad : \quad \text{gives canonical equations} \begin{cases} \dot{x} = p/m \\ \dot{p} = 0 \end{cases}$$

then the theory of canonical transformations[12] informs us we should construct

$$\begin{aligned} H(p,x) &= H + \tfrac{\partial}{\partial t}F_2 \\ &= \left[\tfrac{1}{2m}(p+mgt)^2\right] + mg(x + \tfrac{1}{2}gt^2) - gt(p+mgt) \\ &= \tfrac{1}{2m}p^2 + mgx \end{aligned}$$

[13] See pages 234–239 in CLASSICAL MECHANICS (1983).

The resulting equations

$$\left.\begin{aligned}\dot{x} &= p/m\\ \dot{p} &= -mg\end{aligned}\right\} \quad : \quad \text{canonical equations of free fall} \tag{30}$$

could alternatively have been obtained from the original equations, since when expressed in terms of transformed phase coordinates (x, p) they become

$$\begin{aligned}\dot{x} + gt &= (p + mgt)/m\\ \dot{p} + mg &= 0\end{aligned}$$

which after trivial simplifications give back (30).

The canonical transformations (27) can be recovered from the following $(u - u)$-parameterized *family* of Legendre generators:[14]

$$F(p, u; x, u) \equiv [x - \tfrac{1}{2}g(u - u)t^2][p + mg(u - u)t] \tag{31.1}$$

Acting on the basis of a Hamilton-Jacobi-inspired hunch, we compute

$$\begin{aligned}K\big(p, \tfrac{\partial F(p,u;x,u)}{\partial p}\big) &= \quad mgt[x - \tfrac{1}{2}g(u - u)t^2] - \tfrac{1}{2}gt^2p\\ &= \quad mgtx - \tfrac{1}{2}gt^2p - \tfrac{1}{2}mg^2t^3(u - u)\\ \tfrac{\partial F(p,u;x,u)}{\partial u} &= +[mgtx - \tfrac{1}{2}gt^2p - \quad mg^2t^3(u - u)]\end{aligned}$$

$$\begin{aligned}K\big(\tfrac{\partial F(p,u;x,u)}{\partial x}, x\big) &= \quad mgtx - \tfrac{1}{2}gt^2[p + mg(u - u)t]\\ &= \quad mgtx - \tfrac{1}{2}gt^2p - \tfrac{1}{2}mg^2t^3(u - u)\\ \tfrac{\partial F(p,u;x,u)}{\partial u} &= -[mgtx - \tfrac{1}{2}gt^2p - \quad mg^2t^3(u - u)]\end{aligned}$$

which give

$$\begin{aligned}K\big(p, \tfrac{\partial F(p,u;x,u)}{\partial p}\big) - \tfrac{\partial F(p,u;x,u)}{\partial u} &= \tfrac{1}{2}mg^2t^3(u - u)\\ K\big(\tfrac{\partial F(p,u;x,u)}{\partial x}, x\big) + \tfrac{\partial F(p,u;x,u)}{\partial u} &= \tfrac{1}{2}mg^2t^3(u - u)\end{aligned}$$

What are we to make of the non-0's on the right sides of those equations? They can be dismissed as artifacts, "gauged away." For just as

$$\text{Lagrangian} \quad \& \quad \text{Lagrangian + arbitrary function of } t$$

give rise to the same Lagrange equations, and

$$\text{Hamiltonian} \quad \& \quad \text{Hamiltonian + arbitrary function of } t$$

give rise to the same canonical equations of motion, so do

[14] Here I write $u \to u - u$ to introduce a "floating initial value of the evolution parameter" and make other slight notational adjustments—all to facilitate comparison in a moment with the H-J equations encountered in §6.

Legendre generator & Legendre generator
+ arbitrary function of the evolution parameter u

Lie generator & Lie generator
+ arbitrary function of the evolution parameter u

—this because the Legendre generator does its work not nakedly, but through the agency of its derivatives $\partial F/\partial$(old, new arguments), the Lie generator does its work not nakedly, but through the agency of its derivatives $\partial K/\partial$(x's, p's). With that license we reassign the work formerly done by $F(p,u;x,u)$ to

$$\mathcal{F}(p,u;x,u) \equiv F(p,u;x,u) + \tfrac{1}{4}mg^2t^3(u-u)^2 \tag{31.2}$$

and obtain

$$\left.\begin{aligned} K\big(p, \tfrac{\partial \mathcal{F}(p,u;x,u)}{\partial p}\big) - \tfrac{\partial \mathcal{F}(p,u;x,u)}{\partial u} = 0 \\ K\big(\tfrac{\partial \mathcal{F}(p,u;x,u)}{\partial x}, x\big) + \tfrac{\partial \mathcal{F}(p,u;x,u)}{\partial u} = 0 \end{aligned}\right\} \tag{32}$$

We will remain alert for *other, independent, & more convincing grounds* on which to argue that $\mathcal{F}$ is "more natural" than F. But the essential lesson here[15] is that

> The Hamilton-Jacobi equations (15) have only incidentally to do with dynamics, and that only because phase flow happens to be a t-parameterized *canonical* transformation. More deeply, they serve to establish a relationship between the Lie generator (which does its work iteratively) and the Legendre generator (which does its work "all at once, beginning to end") of any given parameterized family of canonical transformations.

My "incidentally" is not intended to be dismissive, for the fact of the matter is that phase flow is canonical, and the H-J equations say what is arguably the deepest thing that can be said about classical motion.

11. Recovery of gravitational Hamilton-Jacobi theory from that of a free particle. The motion $(x_0,t_0) \longrightarrow (x_1,t_1)$ of our free particle is described

$$\begin{aligned} x(t;x_1,t_1;x_0,t_0) &= x_0 + \frac{x_1-x_0}{t_1-t_0}(t-t_0) \\ &= \left\{\frac{x_0t_1 - x_1t_0}{t_1-t_0}\right\} + \left\{\frac{x_1-x_0}{t_1-t_0}\right\}t \end{aligned} \tag{33}$$

which when inserted into

$$S(x_1,t_1;x_0,t_0) = \int_{t_0}^{t_1} \tfrac{1}{2}m\dot{x}^2(t)\,dt$$

gives the free dynamical action

$$= \tfrac{1}{2}m\left\{\frac{(x_1-x_0)^2}{t_1-t_0}\right\} \tag{34}$$

[15] The point is elaborated on pages 245–252 in CLASSICAL MECHANICS (1983).

which is readily seen to satisfy the Hamilton-Jacobi equations

$$\begin{aligned}\tfrac{1}{2m}\tfrac{\partial S}{\partial x_1}+\tfrac{\partial S}{\partial t_1}&=0\\ \tfrac{1}{2m}\tfrac{\partial S}{\partial x_0}-\tfrac{\partial S}{\partial t_0}&=0\end{aligned}$$

These statements could have been obtained from their free fall counterparts (4) and (9), but our objective here is to proceed in the reverse of that direction: to obtain the physics of uniformly accelerated free fall from the simpler physics of unaccelerated free motion.

The recovery of (4) from (33) follows straightforwardly from $x = x + \frac{1}{2}gt^2$: we verify by computation that

$$x(t;x_1+\tfrac{1}{2}gt_1^2,t_1;x_0+\tfrac{1}{2}gt_0^2,t_0)=x(t;x_1,t_1;x_0,t_0)+\tfrac{1}{2}gt^2$$

The recovery of (9) from (34) is more interesting:

Action integrals S[path], like (say) length integrals ℓ[curve], respond to coordinate transformations by numerical invariance: that is a principle source of their formal utility (responsible for the general covariance of Lagrange's equations). But in the present context (see again page 12) the coordinate transformation is understood to be accompanied by a gauge transformation

$$L = L + \tfrac{d}{dt}\Lambda$$

which entails

$$S = S + \Lambda\Big|_{t_0}^{t_1} \quad \text{with} \quad \Lambda(x,t) = -mgxt - \tfrac{1}{6}mg^2t^3$$

Computation now supplies

$$\begin{aligned}S(x_1+\tfrac{1}{2}gt_1^2,t_1;x_0+\tfrac{1}{2}gt_0^2,t_0) - mg\big[x_1t_1+\tfrac{1}{6}mg^2t_1^3\big]&\\ + mg\big[x_0t_0+\tfrac{1}{6}mg^2t_0^3\big] &= S(x_1,t_1;x_0,t_0)\end{aligned}$$

12. Bouncing ball basics. Erect now a prefectly reflective barrier at $x = 0$, the intended effect of which is to cause the particle ("ball") to "bounce" elastically whenever its descent brings it into contact with the barrier (Figure 5). Evidently

$$x_{\max}(E) = \tfrac{E}{mg} \tag{35}$$

and the E-dependent period (computed from $x_{\max}(E) = \frac{1}{2}g[\frac{1}{2}\tau]^2$) is given by

$$\tau(E) = \sqrt{\tfrac{8E}{mg^2}} \tag{36}$$

If we start the clock at the time of a bounce, then the flight up until the time of the next bounce can be described

$$x(t) = \tfrac{1}{2}gt(\tau - t) \quad : \quad 0 < t < \tau \tag{37.1}$$

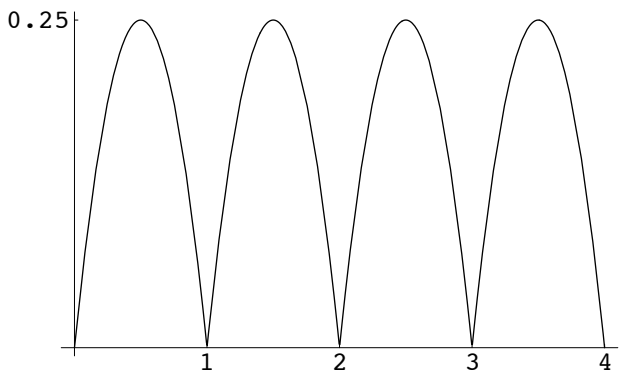

FIGURE 5: *Flight of a bouncing ball, computed from* (37.2) *with the parameters* g *and* τ *both set equal to unity.*

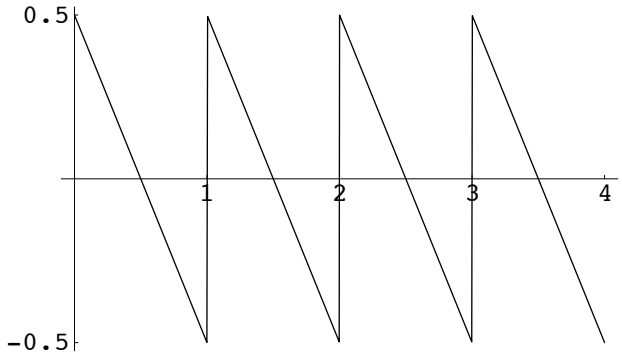

FIGURE 6: *Time-derivative of the preceding figure, computed from* (38.2): *the velocity decreases uniformly between bounces.*

To notate the "bounce-bounce-bounce..." idea we might write

$$x(t) = \tfrac{1}{2}g\sum_n [t-n\tau][(n+1)\tau - t]\cdot \texttt{UnitStep[}[t-n\tau][(n+1)\tau-t]\texttt{]} \quad (37.2)$$

but there is seldom reason to do so. Between bounces the velocity decreases uniformly

$$\dot{x}(t) = \tfrac{1}{2}g\tau - gt \quad : \quad 0<t<\tau \quad (38.1)$$

so we have

$$\dot{x}(t) = \sum_n \left[\tfrac{1}{2}g\tau - g(t-n\tau)\right]\cdot \texttt{UnitStep[}[t-n\tau][(n+1)\tau-t]\texttt{]} \quad (38.2)$$

which describes a sawtooth (Figure 6). The τ-dependence of $x_{\max}$ is described

$$x_{\max} = x(\tfrac{1}{2}\tau) = \tfrac{1}{8}g\tau^2 \quad (39)$$

13. Probabilistic aspects of the bouncing ball problem. We proceed from the idea that the probability $Q(x)dx$ that a bouncing ball will be found in the neighborhood dx of x $(0 \leqslant x \leqslant x_{\max})$ is the same as the *fraction of the time* that the particle spends in that neighborhood. Working from the figure

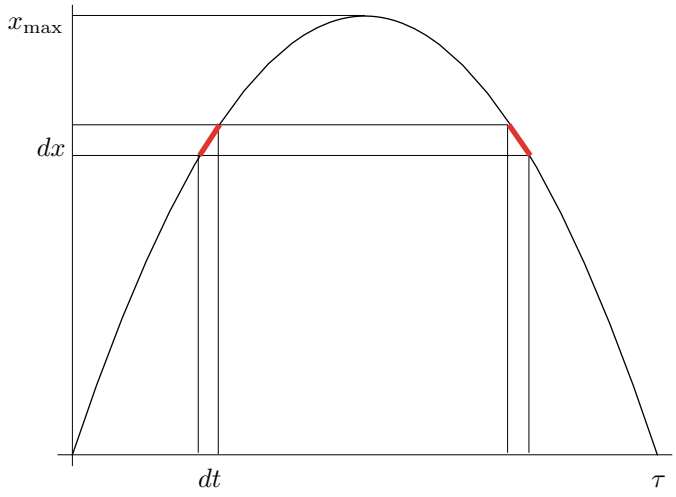

FIGURE 7: *Construction used to compute* $Q(x)$.

we have

$$Q(x)dx = Q(x)\tfrac{1}{2}g(\tau - 2t)dt = \frac{2dt}{\tau}$$

giving

$$Q(x) = \frac{4}{g\tau(\tau - 2t)}$$

But $2t(x) = \tau \pm \sqrt{(g\tau^2 - 8x)/g}$ so

$$\begin{aligned} Q(x) &= \frac{1}{2\sqrt{\tfrac{1}{8}g\tau^2}\sqrt{\tfrac{1}{8}g\tau^2 - x}} \\ &= \frac{1}{2\sqrt{x_{\max}}\sqrt{x_{\max} - x}} \quad : \quad 0 \leqslant x \leqslant x_{\max} \end{aligned} \tag{40}$$

This "ballistic distribution function" is plotted in Figure 8. Calculation confirms that (as expected/required)

$$\int_0^{x_{\max}} Q(x)\,dx = 1$$

On the other hand, momentum decreases uniformly during the course of a flight (see again Figure 6), ranging from $+\frac{1}{2}mg\tau$ down to $-\frac{1}{2}mg\tau$, so the momentum distribution $P(p)$ is *flat* on that interval, where it has constant value $(mg\tau)^{-1}$.

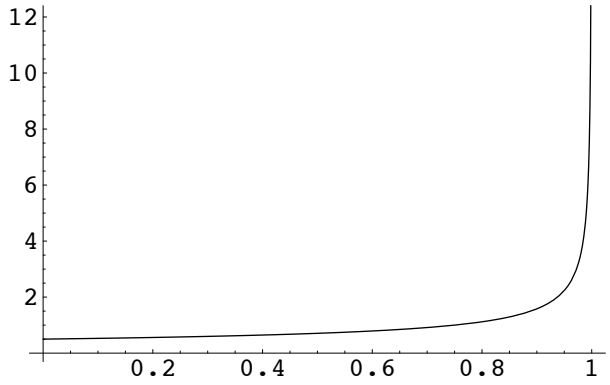

FIGURE 8: *The "ballistic distribution function" $Q(x)$, displayed as a function of the dimensionless variable $x/x_{\max}$. The singularity at $x = x_{\max}$ reflects the tendency of ballistic particles to linger at the apex of their flight.*

14. Action per bounce. Working from (9) we have

$$\begin{aligned} S(0,\tau;0,0) &= \text{value of the bounce-to-bounce action} \\ &= \tfrac{1}{2}m\Big\{ -\tfrac{1}{12}g^2\tau^3 \Big\} \end{aligned} \tag{41}$$

But we can approach this issue also from another angle:

Between one bounce and the next the phase flow is ballistic, and can be described

$$\begin{aligned} x(t) &= \tfrac{1}{2}gt(\tau - t) \\ p(t) &= \tfrac{1}{2}mg(\tau - 2t) \end{aligned}$$

Eliminating t between those equations gives

$$x - x_{\max} = -x_{\max}\cdot(p/p_0)^2 \quad \text{with} \quad p_0 \equiv \tfrac{1}{2}mg\tau \tag{42}$$

which inscribes on phase space a parabola that opens to the left (Figure 9). Equivalently

$$p(x) = p_0\sqrt{1-(x/x_{\max})} \tag{43}$$

It follows that the *area* of the region bounded by (42) can be described

$$\begin{aligned} \text{enveloped area } A = \oint p\,dx &= 2\int_0^{x_{\max}} p_0\sqrt{1-(x/x_{\max})}\,dx \\ &= \tfrac{4}{3}p_0 x_{\max} \\ &= \tfrac{4}{3}\cdot\tfrac{1}{2}mg\tau\cdot\tfrac{1}{8}g\tau^2 \\ &= \tfrac{1}{12}mg^2\tau^3 \end{aligned} \tag{44}$$

We are presented here with a problem, which I have been thus far unable to resolve: Why are (41) and (44) not in agreement?

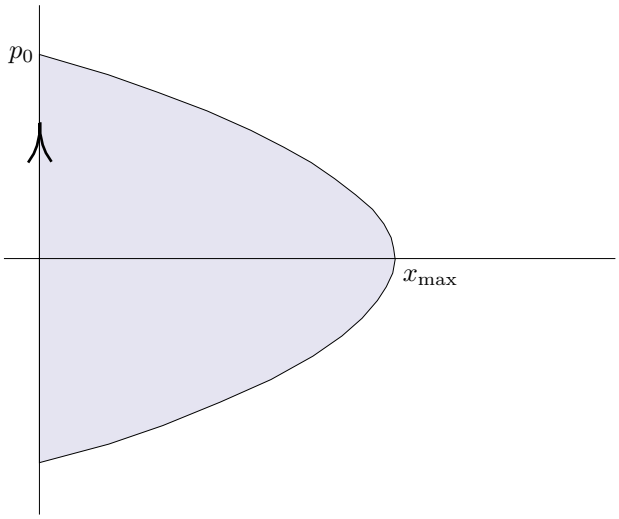

FIGURE 9: *The phase space representation of bounce-bounce-bounce consists of going round* ↻ *and round the parabolically bounded region shown. We have interest in the area of that region.*

15. Planck quantization. We have arrived here at the historic birthplace of quantum mechanics. For Planck (1900), in order to account mechanically for the successful description of the blackbody radiation spectrum to which he had been led by other (interpolative thermodynamic) means, was forced to dismiss all classical oscillator motions except those that conformed to the quantization condition

$$\oint p\,dx = nh \quad : \quad n = 1, 2, 3, \ldots \tag{45}$$

Bringing that condition to the bouncing ball problem, we on the basis of (44) have

$$\tfrac{1}{12}mg^2\tau^3 = nh$$

according to which only bounces of certain discrete periods

$$\tau_n = \left[12nh/mg^2\right]^{\frac{1}{3}} \quad : \quad n = 1, 2, 3, \ldots$$

are "allowed." This, by (36), is equivalent to the assertion that a ball can bounce only with certain discrete energies

$$\begin{aligned} E_n &= \tfrac{mg^2}{8}\tau_n^2 \\ &= \mathcal{E}\,n^{\frac{2}{3}} \quad \text{with} \quad \mathcal{E} \equiv \left[\tfrac{9}{64}mg^2h^2\right]^{\frac{1}{3}} \end{aligned} \tag{46}$$

We expect a refinement of (46) to emerge from the *exact* quantum theory of a bouncing ball—the theory achieved by Schrödinger quantization of the classical physics. But before turning to the details of the latter theory we look to an aspect of the classical problem that is directly relevant to *Feynman's alternative to Schrödinger quantization*.

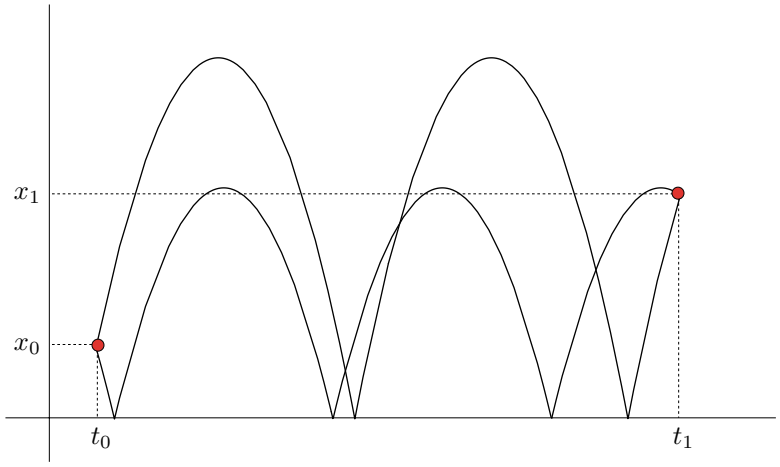

FIGURE 10: *Two of the distinct bounce paths that link a specified pair of spacetime points. Implementation of Feynman quantization program would require us to ennumerate the totality of such paths, in the general case.*

16. Multiple paths & the ennumeration problem. It is clear from figures such as the one shown above that, in general, a *finite multitude* of bounce paths link $(x_0, t_0) \longrightarrow (x_1, t_1)$. To ennumerate the members of the population one has to discover all the values of τ and δ such that (see again (37.2))

$$x(t;\tau,\delta) \equiv \tfrac{1}{2}g \sum_n \xi(t - n\tau + \delta) \cdot \texttt{UnitStep[}\xi(t - n\tau + \delta)\texttt{]}$$
$$\xi(t) \equiv t(\tau - t)$$

conforms to the endpoint conditions

$$x(t_0;\tau,\delta) = x_0 \quad \text{and} \quad x(t_1;\tau,\delta) = x_1$$

Though the problem appears on its face to be difficult (intractable?), these pertinent facts are immediately evident:

- It must be the case that $x_{\max} \geqslant$ (greater of x_0, x_1). This (by $x_{\max} = \frac{1}{8}g\tau^2$) sets a limit on how small τ can be:

$$\tau \geqslant \tau_{\min} \equiv \sqrt{\frac{8(\text{greater of } x_0,\, x_1)}{g}}$$

- This sets a limit on how many bounces can occur in the available time:

$$\text{maximal number } N_{\max} \text{ of bounces} = 1 + \text{integral part of } \frac{t_1 - t_0}{\tau_{\min}}$$

- I conjecture (the demonstratiuon may not be difficult, but at the moment does not tempt me) that there exists always

$$\begin{aligned}&\text{exactly one 0-bounce path}^*\\&\text{exactly one 1-bounce path}^*\\&\text{exactly one 2-bounce path}\\&\qquad\vdots\\&\text{exactly one } N_{\max}\text{-bounce path}\end{aligned}$$

  linking (x_0, t_0) to (x_1, t_1), and that the paths marked * *always* exist (this becomes clear when one looks to the limit $g \downarrow 0$).

17. Close companion of the bouncing ball problem: the wedge potential. Slight adjustments of results appropriate to the bouncing ball problem

$$U(x) = \begin{cases} mgx & : \quad x \geqslant 0 \\ \infty & : \quad x < 0 \end{cases}$$

give results appropriate to the more "oscillator-like" system

$$U(x) = mg|x| \tag{47}$$

I call this (for graphically obvious reasons) the "wedge potential," but in the literature it is often called the "vee potential." The associated force law is

$$F(x) = \begin{cases} -mg & : \quad x > 0 \\ +mg & : \quad x < 0 \end{cases}$$

18. Quantum mechanical free fall according to Schrödinger. The Schrödinger equation reads

$$\Big\{ -\tfrac{\hbar^2}{2m}\big(\tfrac{\partial}{\partial x}\big)^2 + mgx \Big\}\Psi(x,t) = i\hbar\tfrac{\partial}{\partial t}\Psi(x,t) \tag{48}$$

The basic problem is to display the normalized solution of (48)

$$\int_{-\infty}^{+\infty} |\Psi(x,t)|^2\, dx = 1$$

that conforms to the prescribed initial data $\Psi(x, t_0)$.

If $\Psi(x,t)$ is assumed to possess the separated structure

$$\Psi(x,t) = \Psi(x) \cdot e^{-\frac{i}{\hbar}E\,t}$$

then (48) requires that $\Psi(x)$ be a solution of the t-independent Schrödinger equation

$$\Big\{ -\tfrac{\hbar^2}{2m}\big(\tfrac{d}{dx}\big)^2 + mgx \Big\}\Psi(x) = E\,\Psi(x) \tag{49}$$

which will serve as our point of departure.

Let (49) be written

$$\left(\tfrac{d}{dx}\right)^2\Psi(x) = \tfrac{2m^2g}{\hbar^2}\left(x - \tfrac{E}{mg}\right)\Psi(x)$$

Now introduce the shifted/rescaled new independent variable $z = k\left(x - \frac{E}{mg}\right)$ and assume Ψ to transform as a scalar density of weight $\frac{1}{2}$:

$$\begin{aligned}\Psi(x) \to \psi(z) \equiv \left|\tfrac{dx}{dz}\right|^{\frac{1}{2}}\Psi(x(z)) \;\;:\;\; &\text{this to achieve } \textstyle\int |\psi(z)|^2\,dz = \int |\Psi(x)|^2\,dx \\ &= \tfrac{1}{\sqrt{k}}\Psi(x)\end{aligned}$$

The differential equation then becomes

$$\left(\tfrac{d}{dz}\right)^2\psi(z) = \tfrac{2m^2g}{\hbar^2}k^{-3}z\,\psi(z)$$

which motivates us to assign to k the particular value $k = \left(\frac{2m^2g}{\hbar^2}\right)^{\frac{1}{3}}$. The t-independent Schrödinger equation is brought thus to the strikingly simple form

$$\left(\tfrac{d}{dz}\right)^2\psi(z) = z\,\psi(z) \tag{50}$$

where—remarkably—the value of E has been absorbed into the definition of the (dimensionless!) independent variable:

$$z \equiv \left(\tfrac{2m^2g}{\hbar^2}\right)^{\frac{1}{3}}\left(x - \tfrac{E}{mg}\right) \tag{51}$$

At (50) we have *Airy's differential equation*, first encountered in George Airy's "Intensity of light in the neighborhood of a caustic" (1838).[16] The solutions are linear combinations of the *Airy functions* $\mathrm{Ai}(z)$ and $\mathrm{Bi}(z)$, which are close relatives of the Bessel functions of orders $\pm\frac{1}{3}$, and of which (since $\mathrm{Bi}(z)$ diverges as $z \to \infty$) only the former

$$\mathrm{Ai}(z) \equiv \tfrac{1}{\pi}\int_0^\infty \cos\left(zu + \tfrac{1}{3}u^3\right)du \tag{52}$$

will concern us.[17] To gain insight into the origin of Airy's construction, write

$$f(z) = \tfrac{1}{2\pi}\int_{-\infty}^{+\infty} g(u)e^{izu}\,du$$

and notice that $f'' - zf = 0$ entails

$$\tfrac{1}{2\pi}\int_{-\infty}^{+\infty}\left[-u^2g(u) + ig(u)\tfrac{d}{du}\right]e^{izu}\,du = 0$$

---

[16] At this point I begin to borrow directly from material that begins on page 22 of Chapter 2: "Weyl Transform and the Phase Space Formalism" in ADVANCED QUANTUM TOPICS (2000).

[17] For a summary of the properties of Airy functions see Chapter 56 in Spanier & Oldham.[21] Those functions are made familiar to students of quantum mechanics by their occurance in the "connection formulæ" of simple WKB approximation theory: see Griffiths' §8.3, or C. M. Bender & S. A. Orszag, *Advanced Mathematical Methods for Scientists & Engineers* (1978), §10.4.

Integration by parts gives

$$\tfrac{1}{2\pi} ig(u) e^{izu}\Big|_{-\infty}^{+\infty} - \tfrac{1}{2\pi}\int_{-\infty}^{+\infty} \big[u^2 g(u) + ig'(u)\big] e^{izu}\, du = 0$$

The leading term vanishes if we require $g(\pm\infty) = 0$. We are left then with a first-order differential equation $u^2 g(u) + ig'(u) = 0$ of which the general solution is $g(u) = A \cdot e^{i\frac{1}{3}u^3}$. So we have

$$f(z) = A \cdot \tfrac{1}{2\pi}\int_{-\infty}^{+\infty} e^{i\,(zu + \frac{1}{3}u^3)}\, du = A \cdot \tfrac{1}{\pi}\int_0^{\infty} \cos\Big(zu + \tfrac{1}{3}u^3\Big)\, du$$

It was to achieve

$$\int_{-\infty}^{+\infty} \mathrm{Ai}(y)\, dy = 1 \tag{53}$$

that Airy assigned the value $A = 1$ to the constant of integration.

Returning with this mathematics to the quantum physics of free fall, we see that solutions of the Schrödinger equation (49) can be described

$$\Psi_{\mathcal{E}}(x) = N \cdot \mathrm{Ai}\big(k(x - a_{_E})\big) \tag{54}$$

where N is a normalization factor (soon to be determined), and where

$$k \equiv \big(\tfrac{2m^2 g}{\hbar^2}\big)^{\frac{1}{3}} = \frac{1}{\text{“natural length” of the quantum free fall problem}}$$
$$a_{_E} \equiv \tfrac{E}{mg} = \text{classical turning point of a particle lofted with energy } E$$
$$\mathcal{E} \equiv k a_{_E} = \tfrac{E}{mg(\text{natural length})} \equiv \text{dimensionless energy parameter}$$

We observe that

$$mg \cdot (\text{natural length}) = mg\,\big(\tfrac{2m^2 g}{\hbar^2}\big)^{-\frac{1}{3}} = \big(\tfrac{mg^2\hbar^2}{2}\big)^{\frac{1}{3}}$$

differs only by a numerical factor from the $\mathcal{E} \equiv \big[\tfrac{9}{64} mg^2\hbar^2\big]^{\frac{1}{3}} = \big[\tfrac{9}{32}\big]^{\frac{1}{3}} \big(\tfrac{mg^2\hbar^2}{2}\big)^{\frac{1}{3}}$ encountered at (46), and that we confront now the question: *Why the factor*?[18]

It is a striking fact—evident in (54)—that the eigenfunctions $\Psi_{_E}(x)$ *all have the same shape* (*i.e.*, are translates of one another: see Figure 11), and remarkable also that the *the energy spectrum is continuous, and has no least member*: the system possesses no ground state. One might dismiss this highly unusual circumstance as an artifact, attributable to the physical absurdity of the idealized free-fall potential

$$U(x) = mgx \quad : \quad -\infty < x < +\infty$$

[18] $\big[\tfrac{9}{32}\big]^{\frac{1}{3}} = 0.655185.$

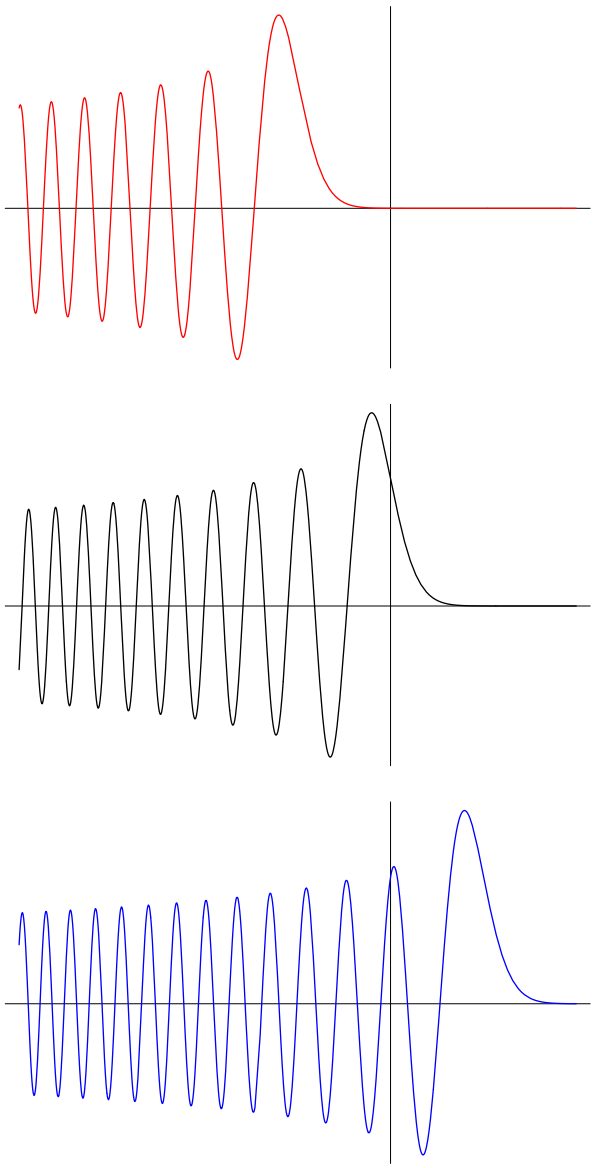

FIGURE 11: *Free fall eigenfunctions* $\Psi_E(x)$ *with* $E < 0$, $E = 0$, $E > 0$, *in descending order. The remarkable translational similarity of the eigenfunctions can be understood as a quantum manifestation of the self-similarity evident at several points already in the classical physics of free fall (see again §2 and Figure 4).*

but then has to view with surprise the major qualitative difference between the cases $g^2 \neq 0$ (no ground state) and $g = 0$ (ground state abruptly springs into existence). I prefer to adopt the notion that *"free fall" is free motion relative to a non-inertial frame*, and to trace that "major qualitative difference" to the major difference between being/not being inertial.

The eigenfunctions $\Psi_{\mathcal{E}}(x)$ share with the free particle functions $e^{\pm\frac{i}{\hbar}\sqrt{2mE}x}$ the property that they are not individually normalizable,[19] but require assembly into "wavepackets." They do, however, comprise a complete orthonormal set, in the sense which I digress now to establish. Let

$$f(z,m) \equiv \mathrm{Ai}(z-m)$$

To ask of the m-indexed functions $f(z,m)$

- Are they *orthonormal*: $\int f(z,m)f(z,n)\,dz = \delta(m-n)$?
- Are they *complete*: $\int f(x,m)f(y,m)\,dm = \delta(x-y)$?

is, in fact, to ask the same question twice, for both are notational variants of this question: Does

$$\int_{-\infty}^{+\infty} \mathrm{Ai}(z-m)\,\mathrm{Ai}(z-n)\,dy = \delta(m-n)?$$

An affirmative answer (which brings into being a lovely "Airy-flavored Fourier analysis") is obtained as follows:

$$\begin{aligned}
&= \left(\tfrac{1}{2\pi}\right)^2 \iiint e^{i\left[(z-m)u+\frac{1}{3}u^3\right]} e^{i\left[(z-n)v+\frac{1}{3}v^3\right]}\,dudvdz \\
&= \tfrac{1}{2\pi}\iint e^{i\frac{1}{3}(u^3+v^3)} e^{-i(mu+nv)} \underbrace{\left\{\tfrac{1}{2\pi}\int e^{iz(u+v)}\,dz\right\}}_{\delta(u+v)} dudv \\
&= \tfrac{1}{2\pi}\int \underbrace{e^{i\frac{1}{3}(v^3-v^3)}}_{1} e^{iv(m-n)}\,dv = \delta(m-n)
\end{aligned}$$

So for our free fall wave functions we have the "orthogonality in the sense of Dirac:"

$$\begin{aligned}
\int_{-\infty}^{+\infty} \Psi^*_{\mathcal{E}'}(x)\,\Psi_{\mathcal{E}''}(x)\,dx &= N^2 \int_{-\infty}^{+\infty} \mathrm{Ai}\big(k(x-a_{E'})\,\mathrm{Ai}\big(k(x-a_{E''})\,dx \\
&= N^2\tfrac{1}{k}\cdot\delta(\mathcal{E}'-\mathcal{E}'') \\
&\downarrow \\
&= \delta(\mathcal{E}'-\mathcal{E}'') \quad \text{provided we set } N=\sqrt{k} \qquad (55.1)
\end{aligned}$$

The functions thus normalized are complete in the sense that

$$\int_{-\infty}^{+\infty} \Psi^*_{\mathcal{E}}(x')\,\Psi_{\mathcal{E}}(x'')\,d\mathcal{E} = \delta(x'-x'') \qquad (55.2)$$

---

[19] Asymptotically $\mathrm{Ai}^2(z) \sim \frac{1}{\pi\sqrt{|z|}}\sin^2\left(\frac{2}{3}|z|^{\frac{3}{2}}+\frac{\pi}{4}\right)$ dies as $z \downarrow -\infty$, but so slowly that the limit of $\int_z^0 \mathrm{Ai}^2(u)\,du$ blows up.

19. Construction & structure of the free fall propagator. Quite generally (subject only to the assumption that the Hamiltonian is t-independent), eigenvalues E_n and eigenfunctions $\psi_n(x)$, when assembled to produce the "propagator"

$$K(x_1,t_1;x_0,t_0) \equiv \sum_n \Psi_n(x_1)\Psi_n^*(x_0)e^{-\frac{i}{\hbar}E_n(t_1-t_0)} \tag{56}$$

permit one to describe the dynamical evolution of any prescribed initial state:

$$\Psi(x,t_0) \longmapsto \Psi(x,t) = \int K(x,t;x_0,t_0)\Psi(x_0,t_0)\,dx_0 \tag{57}$$

The propagator, looked upon as an (x_0,t_0)-parameterized function of x and t, is a solution of the t-dependent Schrödinger equation, distinguished from other solutions by the property

$$\lim_{t\downarrow t_0} K(x,t;x_0,t_0) = \delta(x-x_0)$$

In the present context (56) supplies

$$K(x,t;x_0,0) = \int_{-\infty}^{+\infty} \Psi_{\mathcal{E}}(x)\Psi_{\mathcal{E}}^*(x_0)e^{-\frac{i}{\hbar}E(\mathcal{E})\,t}\,d\mathcal{E}$$

where, in the notation introduced on page 25, $E(\mathcal{E}) \equiv (mg/k)\mathcal{E}$. Working from

$$\Psi_{\mathcal{E}}(x) = N\cdot\mathrm{Ai}\big(k[x-a]\big) = N\cdot\tfrac{1}{2\pi}\int_{-\infty}^{+\infty} e^{i\,(\frac{1}{3}u^3+k[x-a]u)}\,du$$

with $N=\sqrt{k}$ and $a=\mathcal{E}/k$, we have[20]

$$\begin{aligned}
K &= \big(\tfrac{N}{2\pi}\big)^2 \iiint e^{i\,(\frac{1}{3}u^3+k[x-a]u)}e^{i\,(\frac{1}{3}v^3+k[x_0-a]v)}e^{-ikwa}\,dudvda \\
&= \big(\tfrac{N}{2\pi}\big)^2 \iiint e^{i\,\frac{1}{3}(u^3+v^3)}e^{ik(xu+x_0v)}e^{-i(ku+kv+kw)a}\,dadudv \\
&= \tfrac{N^2}{2\pi}\iint e^{i\,\frac{1}{3}(u^3+v^3)}e^{ik(xu+x_0v)}\,\underbrace{\delta(ku+kv+kw)}_{=\,k^{-1}\delta(u+v+w)}\,dudv \\
&= \tfrac{N^2}{2\pi k}\int e^{i\,\frac{1}{3}[v^3-(v+w)^3]}e^{ik[x_0v-x(v+w)]}\,dv
\end{aligned}$$

But $v^3-(v+w)^3 = -3v^2w-3vw^2-w^3$ so

$$= \tfrac{N^2}{2\pi k}e^{-i(\frac{1}{3}w^3+kxw)}\cdot\int e^{-iwv^2-i[w^2+k(x-x_0)]}\,dv$$

[20] The following argument was taken from page 32 of some informal notes "Classical/quantum mechanics of a bouncing ball" (March 1994) that record the results of my first excursion into this problem area.

The sole surviving integral is (formally) Gaussian, and its elementary evaluation supplies

$$\begin{aligned} K &= \tfrac{N^2}{2\pi k} e^{-i(\frac{1}{3}w^3+kxw)} \cdot \sqrt{\tfrac{2\pi}{2iw}}\, e^{-\frac{1}{4iw}[w^2+k(x-x_0)]^2} \\ &= \tfrac{1}{2\pi}\sqrt{\tfrac{2\pi}{2iw}}\,\exp\!\left\{ i\left[\frac{k^2(x-x_0)^2}{4w} + \left[\frac{2k(x-x_0)}{4} - kx\right]w + \left[\tfrac{1}{4}-\tfrac{1}{3}\right]w^3 \right] \right\} \end{aligned}$$

When—tacitly—I elected to use a rather than $\mathcal{E}$ as my "eigenfunction identifier" and wrote $\frac{1}{\hbar}(mga) = kwa$ I assigned to w the enforced value $w = (mg^2/2\hbar)^{\frac{1}{3}}t$. Inserting this and $k = (2m^2g/\hbar^2)^{\frac{1}{3}}$ into the preceding equation we (after a good bit of simplification) obtain

$$= \sqrt{\tfrac{m}{2\pi i\hbar t}}\,\exp\!\left\{ \tfrac{i}{\hbar}\left[\tfrac{m}{2t}(x-x_0)^2 - \tfrac{1}{2}mg(x+x_0)t - \tfrac{1}{24}mg^2t^3 \right] \right\} \tag{58}$$

whence (after a trivial notational adjustment: $t \mapsto t_1 - t_0$)

$$K(x_1,t_1;x_0,t_0) = \sqrt{\tfrac{m}{2\pi i\hbar(t_1-t_0)}}\cdot e^{\frac{i}{\hbar}S(x_1,t_1;x_0,t_0)} \tag{59}$$

where $S(x_1,t_1;x_0,t_0)$ is precisely the classical free-fall action function first encountered at (9) on page 4. Some theoretical importance attaches also to the fact that

$$\sqrt{\tfrac{m}{2\pi i\hbar(t_1-t_0)}} \quad \text{can be written} \quad \sqrt{\tfrac{i}{\hbar}\tfrac{\partial^2 S}{\partial x_1 \partial x_0}}$$

By way of commentary: If, into the Schrödinger equation (48), we insert

$$\psi = A\, e^{\frac{i}{\hbar}S}$$

we obtain

$$A\left\{ \tfrac{1}{2m}(S_x)^2 + mgx + S_t \right\} - i\hbar \underbrace{\left\{ \tfrac{1}{2m}\left[AS_{xx} + 2A_xS_x \right] + A_t \right\}}_{= \frac{1}{2A}\left\{ (\frac{1}{m}S_xA^2)_x + (A^2)_t \right\}} - \hbar^2 \tfrac{1}{2m}A_{xx} = 0$$

Returning with this information to (59) we find that

- the leading $\{\}$ vanishes because S satisfies the Hamilton-Jacobi equation
- the final term vanishes because A is x-independent
- the the middle $\{\}$—which brings to mind a "continuity equation," of precisely the sort that $A^2 = |\psi|^2$ is known in quantum mechanics to satisfy (as a expression of the "conservation of probability")—vanishes by computation:

$$\left(\tfrac{1}{m}\left[\tfrac{m}{t}(x-x_0) - \tfrac{1}{2}mgt \right]\tfrac{1}{t} \right)_x + \left(\tfrac{1}{t} \right)_t = \tfrac{1}{t^2} - \tfrac{1}{t^2} = 0$$

20. Dropped Gaussian wavepacket. Let Ψ be given initially by

$$\Psi(x,0) = \tfrac{1}{\sqrt{s\sqrt{2\pi}}}\, e^{-\frac{1}{4}[x/s]^2} \tag{60}$$

Then

$$|\Psi(x,0)|^2 = \tfrac{1}{s\sqrt{2\pi}}\, e^{-\frac{1}{2}[x/s]^2}$$

is a normalized Gaussian

$$\int_{-\infty}^{+\infty} |\Psi(x,0)|^2\, dx = 1$$

with second moment

$$\langle x^2 \rangle = \int_{-\infty}^{+\infty} x^2 |\Psi(x,0)|^2\, dx = s^2$$

Returning with (58) and (60) to (57), we confront the messy Gaussian integral

$$\Psi(x,t) = \sqrt{\tfrac{m}{iht}\tfrac{1}{s\sqrt{2\pi}}} \int \exp\Big\{ \tfrac{i}{\hbar}\Big[\tfrac{m}{2t}(x-x_0)^2 - \tfrac{1}{2}mg(x+x_0)t - \tfrac{1}{24}mg^2t^3\Big] - \tfrac{1}{4s^2}x_0^2 \Big\}\, dx_0$$

Mathematica responds with a result

$$= \sqrt{\tfrac{m}{iht}\tfrac{1}{s\sqrt{2\pi}}}\, 2\sqrt{\pi}\Big[\tfrac{1}{s^2} - i\tfrac{2m}{\hbar t}\Big]^{-\frac{1}{2}} \cdot \exp\Big\{ \tfrac{m}{24\hbar} \tfrac{12gt^2x\hbar - 12x^2\hbar + g^2t^4\hbar - 48igms^2xt - 8ig^2ms^2t^3}{2ms^2 + i\hbar t} \Big\}$$

which we have now to disentangle. Look first to the prefactor, which after simplifications becomes

$$\sqrt{\tfrac{m}{iht}\tfrac{1}{s\sqrt{2\pi}}}\, 2\sqrt{\pi}\Big[\tfrac{1}{s^2} - i\tfrac{2m}{\hbar t}\Big]^{-\frac{1}{2}} = \sqrt{\tfrac{1}{S(t)\sqrt{2\pi}}}$$

$$S(t) \equiv s\big[1 + i\tfrac{\hbar}{2ms^2}t\big] = s\sqrt{1 + \big(\tfrac{\hbar t}{2ms^2}\big)^2}\cdot e^{i\alpha(t)} \equiv s(t)\cdot e^{i\alpha(t)}$$

with $\alpha(t) \equiv \arctan\big(\tfrac{\hbar t}{2ms^2}\big)$. Look next to the argument of the exponential: we find

$$\Big\{\text{etc.}\Big\} = -\tfrac{[x - \frac{1}{2}gt^2]^2}{4s^2(t)} - i\beta(t)$$

where $\beta(x,t)$ is a complicated term the details of which need not concern us. We now have

$$\Psi(x,t) = \tfrac{1}{\sqrt{s(t)\sqrt{2\pi}}}\, \exp\Big\{ -\tfrac{1}{4}\Big[\frac{x - \frac{1}{2}gt^2}{s(t)}\Big]^2 - i\theta(x,t)\Big\}$$

with $\theta \equiv \frac{1}{2}\alpha + \beta$. The phase factor is of no present interest because it disappears

when we look to the probability density

$$|\Psi(x,t)|^2 = \tfrac{1}{s(t)\sqrt{2\pi}}\,\exp\!\left\{-\tfrac{1}{2}\Big[\frac{x-\frac{1}{2}gt^2}{s(t)}\Big]^2\right\} \tag{61.1}$$

An even more tedious variant[20] of the same argument serves to establish that if—in place of (60)—we had taken[21]

$$\Psi(x,0) = e^{-\frac{i}{\hbar}p\,x}\cdot\tfrac{1}{\sqrt{s\sqrt{2\pi}}}\,e^{-\frac{1}{4}[x/s]^2}$$

as our starting point we would have been led to

$$|\Psi(x,t)|^2 = \tfrac{1}{s(t)\sqrt{2\pi}}\,\exp\!\left\{-\tfrac{1}{2}\Big[\frac{x+vt-\frac{1}{2}gt^2}{s(t)}\Big]^2\right\} \tag{61.2}$$

with $v \equiv p/m$, from which we recover (61.1) as a special case. Equations (61) describe Gaussian distributions the centers of which move ballistically, but which disperse hyperbolically[22]—*just what you would expect to see if the standard free particle result were viewed from a uniformly accelerated frame.*

21. Other dropped wavefunctions. What happens when you drop the familiar free particle eigenfunction

$$\Psi(x,0) = \tfrac{1}{\sqrt{h}}e^{\frac{i}{\hbar}p\,x} \quad : \quad p \text{ an adjustable real constant}$$

Immediately

$$\begin{aligned}\Psi(x,t) &= \sqrt{\tfrac{m}{iht}\tfrac{1}{\hbar}}\int \exp\!\left\{\tfrac{i}{\hbar}\Big[\tfrac{m}{2t}(x-x_0)^2 - \tfrac{1}{2}mg(x+x_0)t \right.\\ &\qquad\qquad \left. - \tfrac{1}{24}mg^2t^3\Big] + \tfrac{i}{\hbar}px_0\right\}dx_0\\ &= \tfrac{1}{\sqrt{h}}\exp\!\left\{\tfrac{i}{\hbar}\Big[px - \tfrac{1}{2m}p^2t - g\big\{mxt - \tfrac{1}{2}pt^2 + \tfrac{1}{6}mgt^3\big\}\Big]\right\}\end{aligned} \tag{62}$$

I have not been able to account term-by-term in an intuitively satisfying way for the design of this result, but have verified that $S(x,t;p) \equiv \big[\text{etc.}\big]$ does in fact satisfy the Hamilton-Jacobi equation (equivalently: $\psi(x,t)$ does satisfy the Schrödinger equation).

---

[21] See page 9 in "Gaussian wavepackets" (1998).

[22] I say "hyperbolically" because

$$s(t) = s_0\sqrt{1+(t/\tau)^2} \quad : \quad \tau \equiv 2ms_0^2/\hbar$$

can be written

$$(s/s_0)^2 - (t/\tau)^2 = 1$$

Note that the dispersion law is g-independent.

It is a curious (though self-evident!) fact that when you drop a free-fall eigenfunction

$$\Psi(x,0) \equiv \Psi_{\mathcal{E}}(x)$$

it does not fall: it simply "stands there and buzzes"

$$\Psi(x,0) \quad \longrightarrow \quad \Psi(x,t) = \Psi(x,0)\cdot e^{-\frac{i}{\hbar}E(\mathcal{E})t} \tag{63}$$

I have described elsewhere a "quantum calculus of moments"[23] that can be used to show—very simply—that the phenomenon illustrated at (61) is in fact not special to Gaussian wavepackets: *every* wavepacket falls in such a way that $\langle x\rangle$ moves ballistically, and Δx grows hyperbolically. Equations (62) and (63) do not provide counterexamples, for they refer to wavefunctions that are not normalizable, do not describe quantum states—are, in short, not wavepackets.

22. The free particle limit of the quantum mechanics of free fall. Trivially

$$\Big\{-\tfrac{\hbar^2}{2m}\big(\tfrac{\partial}{\partial x}\big)^2 + mgx\Big\}\Psi(x,t) = i\hbar\tfrac{\partial}{\partial t}\Psi(x,t) \tag{48}$$

$$\downarrow$$

$$\Big\{-\tfrac{\hbar^2}{2m}\big(\tfrac{\partial}{\partial x}\big)^2\Big\}\Psi(x,t) = i\hbar\tfrac{\partial}{\partial t}\Psi(x,t) \quad : \text{ free particle Schrödinger equation}$$

and

$$K_g(x,t;x_0,0) = \sqrt{\tfrac{m}{2\pi i\hbar t}}\exp\Big\{\tfrac{i}{\hbar}\Big[\tfrac{m}{2t}(x-x_0)^2 - \tfrac{1}{2}mg(x+x_0)t - \tfrac{1}{24}mg^2t^3\Big]\Big\} \tag{58}$$

$$\downarrow$$

$$K_0(x,t;x_0,0) = \sqrt{\tfrac{m}{2\pi i\hbar t}}\exp\Big\{\tfrac{i}{\hbar}\Big[\tfrac{m}{2t}(x-x_0)^2\Big]\Big\} \quad : \text{ free particle propagator}$$

when gravity is turned off: $g^2 \downarrow 0$. More interesting is the question: What happens to the eigenfunctions? How do the Airy functions manage to become exponentials? The following remarks have been abstracted from the discussion that appears on pages 48–52 of the notes already cited,[20] where I found the problem to be surprisingly ticklish.

Borrowing from page 28, we have

$$\Psi_E(x) = \sqrt{k}\cdot\mathrm{Ai}\big(k[x-a]\big) = \sqrt{k}\cdot\tfrac{1}{2\pi}\int_{-\infty}^{+\infty} e^{i\left(\frac{1}{3}u^3 + k[x-a]u\right)}\,du$$

with

$$k \equiv \big(\tfrac{2m^2g}{\hbar^2}\big)^{\frac{1}{3}}$$
$$a \equiv \tfrac{E}{mg} \quad : \text{ becomes } \infty \text{ as } g \downarrow 0$$

from which we would like to recover $\frac{1}{\sqrt{2\pi\hbar}}\exp(\frac{i}{\hbar}\sqrt{2mE}\,x)$ as $\lim g^2 \downarrow 0$.

[23] ADVANCED QUANTUM TOPICS (2000) Chapter 2, page 51. The method is an elaboration of the idea central to Ehrenfest's theorem.

A slight notational adjustment gives

$$\psi_E(x) = \sqrt{k}\cdot\tfrac{1}{2\pi}\int_{-\infty}^{+\infty} e^{ia\,(\frac{1}{3a}u^3+k[\frac{x}{a}-1]u)}\,du$$

which by a change of variable $u \mapsto w : w^3 \equiv \frac{1}{a}u^3$ becomes

$$= \tfrac{1}{2\pi\sqrt{k}}\,ka^{\frac{1}{3}}\int_{-\infty}^{+\infty} e^{ia\,(\frac{1}{3}w^3+ka^{1/3}[\frac{x}{a}-1]w)}\,du$$

Here

$$ka^{\frac{1}{3}} = \big[\tfrac{2m^2g}{\hbar^2}\cdot\tfrac{E}{mg}\big]^{\frac{1}{3}} = \big[\tfrac{2mE}{\hbar^2}\big]^{\frac{1}{3}} \equiv B$$

so we have

$$= \tfrac{1}{2\pi\sqrt{k}}\,B\int_{-\infty}^{+\infty} e^{iah(w)}\,dw \tag{64}$$

with

$$h(w) \equiv \tfrac{1}{3}w^3 + B\big[\tfrac{x}{a}-1\big]w$$

which we want to evaluate in the limit $a \equiv E/mg \uparrow \infty$. Now (64) is of such a form as to invite attack by the "method of stationary phase,"[24] which would give

$$\sim \tfrac{1}{2\pi\sqrt{k}}\,B\Big[\frac{2\pi}{ah''(w_0)}\Big]^{\frac{1}{2}} e^{i[ah(w_0)+\frac{\pi}{4}]}$$

where w_0 marks the point where $h(w)$ assumes its minimal value. From

$$h'(w) = w^2 + B\big[\tfrac{x}{a}-1\big] = 0 \quad \text{we have} \quad w_0 = \pm\sqrt{B\big[1-\tfrac{x}{a}\big]}$$

and $h''(w_0) = 2w_0 > 0$ requires us (i) to select the upper sign and (ii) to enforce the restriction $a - x > 0$. We now have

$$= \tfrac{1}{2\pi\sqrt{k}}\,B\left[\frac{2\pi}{a2\sqrt{B\big(1-\frac{x}{a}\big)}}\right]^{\frac{1}{2}} e^{i\frac{\pi}{4}}\cdot e^{iah(w_0)}$$

with

$$\begin{aligned} h(w_0) &= -\tfrac{2}{3}\Big[B\big(1-\tfrac{x}{a}\big)\Big]^{\frac{3}{2}} \\ &= B^{\frac{3}{2}}\Big\{-\tfrac{2}{3}+\tfrac{x}{a}-\tfrac{1}{4}\big(\tfrac{x}{a}\big)^2+\cdots\Big\} \\ B^{\frac{3}{2}} &= \tfrac{\sqrt{2mE}}{\hbar} \equiv \tfrac{1}{\hbar}p \end{aligned}$$

Thus do we obtain

$$\begin{aligned} \psi_E(x) &\sim \tfrac{1}{2\pi\sqrt{ka}}\sqrt{2\pi}B^{\frac{3}{4}}\big\{1+O(g)\big\}e^{ia\{-\frac{2}{3}B^{\frac{3}{2}}+\frac{\pi}{4}\}}\cdot e^{iB^{\frac{3}{2}}\{x+O(g)\}} \\ &= \sqrt{\tfrac{p}{ka}}\cdot\tfrac{1}{\sqrt{h}}e^{\frac{i}{\hbar}px}\cdot e^{i\,(\text{phase})} \end{aligned} \tag{65}$$

[24] See A. Erdélyi, *Asymptotic expansions* (1956), page 51. Also of special relevance is Erdélyi's §2.6.

I am willing to discard the phase factor as an unphysical artifact, but have been unable to argue that the factor $\sqrt{p/ka}$ is effectively unity. So not only is the argument tediously "ticklish"—it elludes me. The problem, I suspect, has to do with enforcement of the restriction $a - x > 0$.

There is, however, a work-around, every step of which is feasible in the present instance. It can be diagramed

$$\begin{array}{ccc} K_g & \xrightarrow[g\downarrow 0]{\qquad\qquad\qquad\qquad} & K_0 \\ \uparrow & & \downarrow \\ \text{free fall eigenfunctions} & & \text{free motion eigenfunctions} \end{array} \tag{66}$$

where the unproblematic meaning of $K_g \longrightarrow K_0$ was described already on page 32.

23. Recovery of the quantum mechanics of free fall from free particle theory. The problem studied in the preceding section

$$\text{free fall eigenfunctions} \xrightarrow[g \text{ turned OFF}]{\qquad\qquad\qquad\qquad} \text{free motion eigenfunctions}$$

(and found there to be difficult) is of less interest to me than its inversion:

$$\text{free fall eigenfunctions} \xleftarrow[g \text{ turned ON}]{\qquad\qquad\qquad\qquad} \text{free motion eigenfunctions}$$

The motivating question: *How—in detail—does the quantum motion of a free particle come to look "gravitational" when viewed from an accelerated frame*? I do not propose to address that problem here . . . except to remark that it clearly calls for new methods (one cannot turn asymptotic analysis "inside out"), and that the scheme (66) can be run in reverse: the hard work, from this point of view, is entirely classical, and was accomplished in §§10 & 11 when we showed how to achieve

$$S_g(x_1,t_1;x_0,t_0) \xleftarrow[g \text{ turned ON}]{\qquad\qquad\qquad\qquad} S_0(x_1,t_1;x_0,t_0)$$

We have only to exponentiate that result, and read off the eigenfunctions. But that exsercise would leave much of the relevant theory still in shadow.

24. A first look at the quantum bouncer problem. The quantum mechanical free fall and bouncer problems take identical Schrödinger equations as their points of departure. But in the latter case we require

$$\psi(x<0,t) = 0 \quad : \quad \text{all } t$$

This amounts to a requirement that the

$$\text{probability current} = i\tfrac{\hbar^2}{2m}(\psi_x^*\psi - \psi_x\psi^*)\Big|_{x=0} = 0 \quad : \quad \text{all } t$$

which we achieve by imposing the boundary condition

$$\psi(0,t) = 0 \quad : \quad \text{all } t \tag{67}$$

It is the presence of that boundary condition that serves to distinguish the one problem from the other, and it makes all the difference: it renders the energy spectrum discrete, and the eigenfunctions normalizable. And it is to acquire the technique needed to work out the detailed implications of that condition that we look not to some of the (semi-miraculous!) ...

25. Detailed properties of the Airy function. ... and of certain functions derived from it.

Reading rough estimates of the locations of the zeros of $Ai(\xi)$ from a graph of the function (Figure 12), we feed that data into *Mathematica* commands of

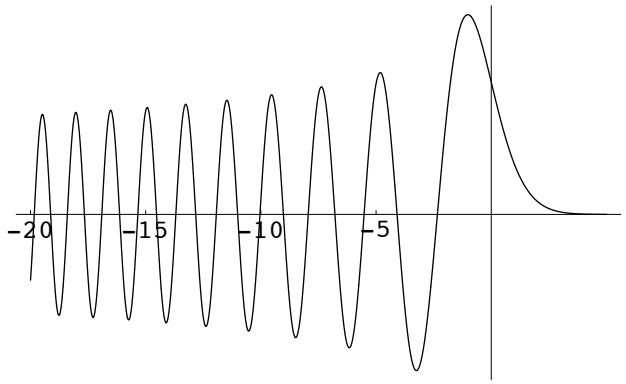

FIGURE 12: *Graph of* $\mathrm{Ai}(\xi)$*, used to obtain rough estimates of the locations of the zeros:* $0 > \xi_1 > \xi_2 > \cdots$.

the form `FindRoot[AiryAi[ξ],{ξ,-2}]` and obtain the data tabulated on the following page. Concerning the data in the third column: Spanier & Oldham (*An Atlas of Functions* (1987), page 559) report that

$$Z(n) \equiv -\tfrac{1}{4}q - \tfrac{5}{3}q^{-2} \quad \text{with} \quad q \equiv [3\pi(4n-1)]^{\frac{2}{3}} \tag{68.1}$$

provides (in their words) "excellent approximations to ξ_n for $n \geqslant 5$."[25] So I have tabulated

$$\Delta_n \equiv Z(n) - \xi_n$$

in support of that claim.[26] The implication is that for n very large (which is to say: in the classical limit) we can expect to have

$$\xi_n \sim z(n) \equiv -\tfrac{1}{4}[12\pi n]^{\frac{2}{3}}$$

[25] For an elaborately refined description of $Z(n)$ see Abramowitz & Stegun: **10.4.105**.

[26] I do not know how to account for the hiccup at $n = 11$, which so far as I have been able to determine is real.

TABLE OF THE LEADING ZEROS OF THE AIRY FUNCTION

n	ξ_n	Δ_n
1	-2.338107	-1.492×10^{-3}
2	-4.087949	-1.126×10^{-4}
3	-5.520560	-2.618×10^{-5}
4	-6.786708	-9.466×10^{-6}
5	-7.944134	-4.337×10^{-6}
6	-9.022651	-2.304×10^{-6}
7	-10.040174	-1.353×10^{-6}
8	-11.008524	-8.551×10^{-7}
9	-11.936016	-5.664×10^{-7}
10	-12.828777	-3.985×10^{-7}
11	-13.691489	-5.088×10^{-7}
12	-14.527830	-2.142×10^{-7}
13	-15.340755	-1.566×10^{-7}
14	-16.132685	-1.007×10^{-7}
15	-16.905634	-1.005×10^{-7}
16	-17.661300	-9.653×10^{-8}
17	-18.401133	-5.686×10^{-8}
18	-19.126381	-5.422×10^{-8}
19	-19.838130	-4.550×10^{-8}
20	-20.537333	-3.831×10^{-8}

Convergence is very slow

$$
\begin{aligned}
Z(10^2) - z(10^2) &= 0.217725 \\
Z(10^3) - z(10^3) &= 0.046847 \\
Z(10^4) - z(10^4) &= 0.021744 \\
Z(10^5) - z(10^5) &= 0.010093 \\
Z(10^6) - z(10^6) &= 0.004685 \\
Z(10^7) - z(10^7) &= 0.002174
\end{aligned}
$$

but convergence in the *fractional* sense—which is to say, the convergence of

$$F(n) \equiv \frac{Z(n) - z(n)}{Z(n)}$$

—is quite rapid:

$$\begin{aligned} F(10^1) &= -1.697 \times 10^{-2} \\ F(10^2) &= -1.670 \times 10^{-3} \\ F(10^3) &= -1.667 \times 10^{-4} \\ F(10^4) &= -1.667 \times 10^{-5} \\ F(10^5) &= -1.667 \times 10^{-6} \\ F(10^6) &= -1.667 \times 10^{-7} \end{aligned}$$

Julio Gea-Banacloche[27] adopts this intermediate approximation

$$\xi_n \approx -\tfrac{1}{4}q = -[\tfrac{3\pi}{8}(4n-1)]^{\frac{2}{3}} = -\big[\tfrac{3\pi}{2}(n-\tfrac{1}{4})\big]^{\frac{2}{3}} \tag{68.2}$$

to the zeros of $\mathrm{Ai}(\xi)$. See "Theory of a transcendental equation encountered in the theory of single slit diffraction" (1997) for some related material.

We now use `NIntegrate[]` to compute normalization factors

$$N_n \equiv \left[\int_0^\infty [\mathrm{Ai}(\xi + \xi_n)]^2 \, d\xi \right]^{-\frac{1}{2}}$$

and with their aid construct normalized functions

$$f_n(\xi) \equiv N_n \, \mathrm{Ai}(\xi + \xi_n) \quad : \quad n = 1, 2, 3, \ldots \tag{69.1}$$

Thus do we obtain

$$\left.\begin{aligned} f_1(\xi) &= 1.426105 \, \mathrm{Ai}(\xi - 2.338107) \\ f_2(\xi) &= 1.245157 \, \mathrm{Ai}(\xi - 4.087949) \\ f_3(\xi) &= 1.155797 \, \mathrm{Ai}(\xi - 5.520560) \\ f_4(\xi) &= 1.097875 \, \mathrm{Ai}(\xi - 6.786708) \\ f_5(\xi) &= 1.055592 \, \mathrm{Ai}(\xi - 7.944134) \\ f_6(\xi) &= 1.022576 \, \mathrm{Ai}(\xi - 9.022651) \\ f_7(\xi) &= 0.995649 \, \mathrm{Ai}(\xi - 10.040174) \\ f_8(\xi) &= 0.973010 \, \mathrm{Ai}(\xi - 11.008524) \\ f_9(\xi) &= 0.953543 \, \mathrm{Ai}(\xi - 11.936016) \\ &\vdots \end{aligned}\right\} \tag{69.2}$$

though those constructions are stored in *Mathematica*'s memory with a good deal more precision that I have displayed: for example, the command

$$\texttt{InputForm[}f_9\texttt{]}$$

produces

$$0.9535427774272334 * \texttt{AiryAi[}-11.936015568074044 + \xi\texttt{]}$$

[27] "A quantum bouncing ball," AJP **67**, 776 (1999).

To Gea-Banacloche we are indebted for the "little guesswork" that led him to the discovery that the normalization factors are well approximated by the remarkably simple construction[28]

$$N(n) \equiv \Big[\frac{\pi}{\sqrt{-\xi_n}}\Big]^{\frac{1}{2}} \approx \Big[\frac{\pi}{[\frac{3}{8}\pi(4n-1)]^{\frac{1}{3}}}\Big]^{\frac{1}{6}} = \Big[\frac{8\pi^2}{3(4n-1)}\Big]^{\frac{1}{6}} \tag{70}$$

—the accuracy of which can be gauged from the following table:

n	N_n	$N(n)$
1	1.426105	1.423372
2	1.245157	1.246518
3	1.155797	1.156323
4	1.097875	1.098146
5	1.055592	1.055755
6	1.022576	1.022684
7	0.995649	0.995725
8	0.993020	0.973067
9	0.953543	0.953586

The functions (69) are normalized by construction, so we are not surprised that `NIntegrate[`$f_1 f_1, \{\xi, 0, \infty\}$`]` yields output 1., to which `InputForm` assigns the expanded meaning 1.0000000000000002. But (though it is, by general principle, a quantum mechanical necessity) I find it to be function-theoretically amazing—an astounding property of the Airy function—that the functions $f_n(\xi)$ are *orthogonal*:

$$\int_0^\infty f_m(\xi) f_n(\xi)\, d\xi = 0 \quad : \quad m \neq n$$

I would not know how to construct an analytic proof, but the numerical evidence is quite convincing: *Mathematica* does complain that "NIntegrate failed to converge to prescribed accuracy after 7 recursive bisections" and that it "suspects one of the following: highly oscillatory integrand or the true value of the integral is 0," but reports that (for example)

$$\texttt{NIntegrate[}f_1 f_3, \{x, 0, \infty\}\texttt{]} = -4.55018 \times 10^{15}$$

Here follow graphs of the normalized functions (69):

[28] Gea-Banacloche remarks that he was unable to find any such formulæ in the literature, and in his Appendix sketches "the details of the 'derivation' [in the hope that] they might inspire somebody to find a better approximation."

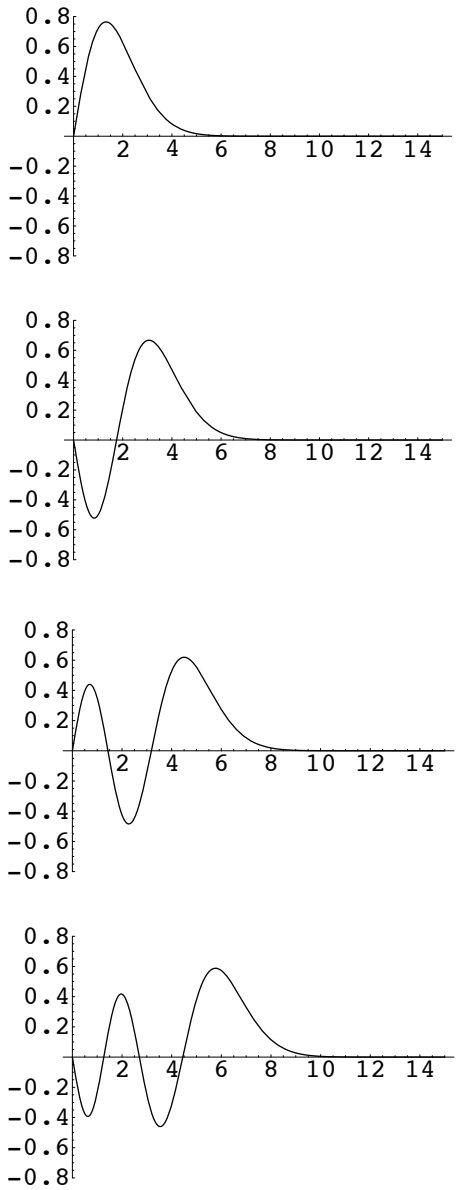

FIGURE 13: *Graphs of (reading top to bottom)* $f_1(\xi)$, $f_2(\xi)$, $f_3(\xi)$ *and* $f_4(\xi)$. *Notice that*

$$\text{order} = \text{number of zero crossings} + 1$$

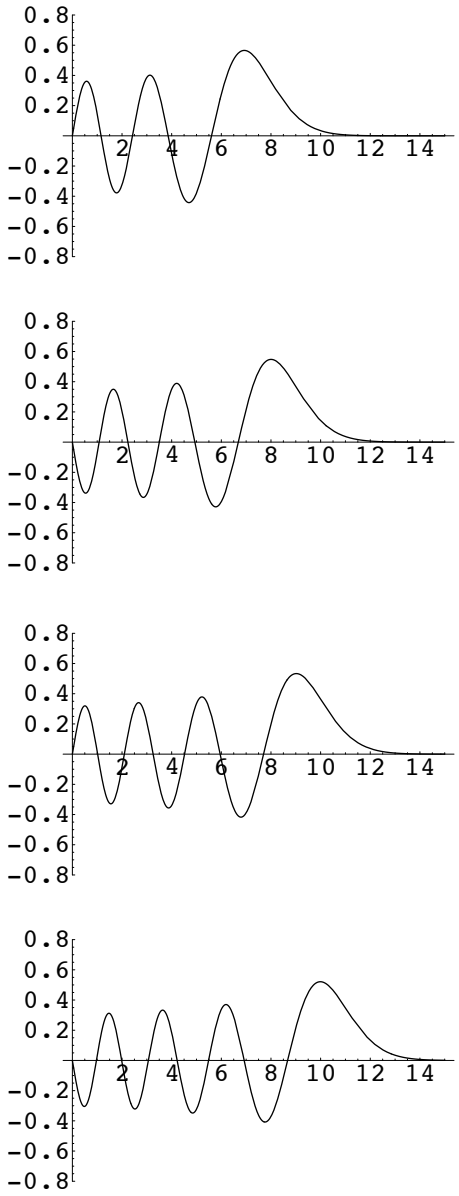

FIGURE 14: *Graphs of (reading top to bottom)* $f_5(\xi)$, $f_6(\xi)$, $f_7(\xi)$ *and* $f_8(\xi)$.

26. Eigenvalues and eigenfunctions of the quantum bouncer. The quantum bouncer presents a situation in which the eigenfunctions and eigenvalues are "folded together" in way which—though characteristic of all variants of the quantum free fall problem—is (or so I believe) quantum mechanically unique.

Solutions of the Schrödinger equation (49) are all of the form (54), but constrained by the boundary condition (67):

$$\psi(x) = N\cdot\mathrm{Ai}\big(k(x-\tfrac{E}{mg})\big) \quad \text{with} \quad \psi(0) = N\cdot\mathrm{Ai}\big(-k\tfrac{E}{mg}\big) = 0$$

Immediately $-k\frac{E}{mg} = \xi_n$, which by $mg/k = mg\big(\frac{\hbar^2}{2m^2g}\big)^{\frac{1}{3}}$ gives

$$E_n = -\big(\tfrac{mg^2\hbar^2}{2}\big)^{\frac{1}{3}}\xi_n \quad : \quad n = 1, 2, 3, \ldots$$

└recall that the ξ_n are themselves negative

which for large values of n ($n \gtrsim 5$) is well approximated[29]

$$E_n \approx \big(\tfrac{mg^2\hbar^2}{2}\big)^{\frac{1}{3}}\big[\tfrac{3\pi}{2}(n-\tfrac{1}{4})\big]^{\frac{2}{3}} = \big[\tfrac{9}{8}\pi^2\big]^{\frac{1}{3}}(mg^2\hbar^2)^{\frac{1}{3}}\cdot(n-\tfrac{1}{4})^{\frac{2}{3}}$$

$$\downarrow$$

$$= \big[\tfrac{9}{32}mg^2h^2\big]^{\frac{1}{3}}n^{\frac{2}{3}} \quad \text{for } n \text{ very large}$$

Notice that "for n very large" we have obtained a result in precise agreement with the result (46) of Planck's old quantization procedure.[30]

---

[29] We notice in the following connection that

$$(n-\tfrac{1}{4})^{\frac{2}{3}} = n^{\frac{2}{3}}\cdot\Big\{1 - \tfrac{1}{6n} - \tfrac{1}{144n^2} - \tfrac{1}{1296n^3} - \cdots\Big\}$$

[30] I digress to remark that, while Planck's procedure over-estimates the

$$\text{ground state energy of an oscillator} = \begin{cases} \hbar\omega & : \ \text{PLANCK} \\ \frac{1}{2}\hbar\omega & : \ \text{SCHRÖDINGER} \end{cases}$$

... in the case of a bouncer it *under*-estimates:

$$\text{bouncer ground state energy} = \begin{cases} \big[\frac{9}{32}\big]^{\frac{1}{3}}(mg^2h^2)^{\frac{1}{3}} \\ 0.655185\,(mg^2h^2)^{\frac{1}{3}} \quad : \ \text{PLANCK} \end{cases}$$

$$\text{bouncer ground state energy} = \begin{cases} \big[\frac{1}{2}\big]^{\frac{1}{3}}\xi_1(mg^2h^2)^{\frac{1}{3}} \\ 1.855760\,(mg^2h^2)^{\frac{1}{3}} \quad : \ \text{SCHRÖDINGER} \end{cases}$$

I find this surprising ... for, I guess, the admittedly irrelevant reason that I have echoing in my head the central lesson of the variational method: "imperfect guesses (and procedures?) always overestimate." I acquire increased interest now in the "wedge potential," since (as was remarked in §17) it is "more oscillator-like" than the bouncer.

It is natural to write

$$E_n = mg\,a_n$$

where

$$\begin{aligned} a_n &= \text{maximal excursion of a } \textit{classical} \text{ bouncer with energy } E_n \\ &= -\left(\tfrac{\hbar^2}{2m^2g}\right)^{\frac{1}{3}}\xi_n \approx \left(\tfrac{\hbar^2}{2m^2g}\right)^{\frac{1}{3}}\left[\tfrac{3\pi}{2}(n-\tfrac{1}{4})\right]^{\frac{2}{3}} \end{aligned}$$

The normalized eigenfunctions of the quantum bouncer can be described

$$\psi_n(x) = \sqrt{k}\,f_n(kx)$$

and when graphed have the form already illustrated (Figures 13 & 14).

27. Comparison of quantum with classical probability density. Adopt units in which $k = 1$, and assign to n a value large enough to make the point at issue, yet not so large as to be computationally burdensome or graphically opaque: $n = 20$ will do nicely. Drawing upon (68.2) and (70) we then have

$$\psi_{20}(x) = (0.83261)\,\mathrm{Ai}(-20.537 + x)$$

In this instance (*i.e.*, when $x_{\max} = a_{20} = 20.537$) the classical distribution $Q(x)$—the classical counterpart to $|\psi_{20}(x)|^2$—is given by

$$Q(x) = \begin{cases} \dfrac{1}{2\sqrt{20.537}\sqrt{20.537 - x}} & : \quad 0 \leqslant x \leqslant 20.537 \\ 0 & : \quad 20.537 < x \end{cases}$$

Superimposed graphs of those distributions are shown in the following figure:

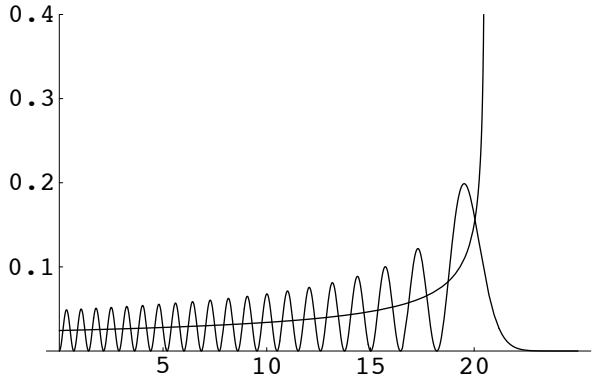

FIGURE 15: *Superposition of the graphs of* $|\psi_{20}(x)|^2$ *and of its classical counterpart. More commonly encountered is a figure taken from the theory of harmonic oscillators*: *see, for example, Figure 2.5b on page 42 in Griffiths'* Introduction to Quantum Mechanics.

The likelihood that the particle will be found *farther from the origin than is classically allowed* is in this instance given by

$$\int_{20.537}^{\infty} |\psi_{20}(x)|^2 \, dx = 0.04644$$

which is to say: we have in this instance a 4% quantum violation of what we might classically expect. Pretty clearly: as n increases the "quantum violation" decreases, which is the upshot of the familiar assertion that "classical mechanics is not so much 'quantum mechanics in the (necessarily only formal!) limit $\hbar \downarrow 0$' as it is 'quantum mechanics in the limit that the quantum numbers have become large.' "

28. A first look at the quantum wedge-potential problem. Our recent subject—the quantum physics of a bouncing ball—is far from exhausted: in fact, we are only now within sight of "the good stuff" (construction of the propagator, motion of wavepackets, study of the recurrence phenomenon, other more esoteric topics[31]). But it will become increasingly natural to treat the "bouncer" and "wedge-potential" problems in comparative conjunction, so I digress now to develop the basics of the latter system. The following diagram underscores the close relationship between the two systems:

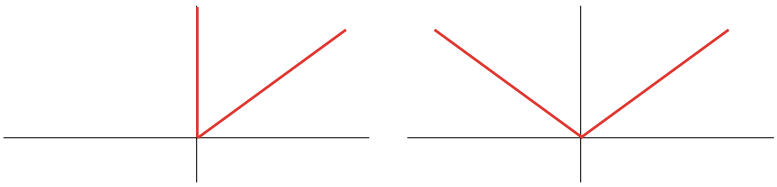

Bouncer potential *Wedge potential*

The two systems share the same (free fall) Schrödinger equation, and are distinguished by

- the fact that x assumes only positive values for the bouncer, but for the wedge is allowed to assume both positive and negative values
- boundary conditions: for the bouncer we were led at (67) to require that ψ vanish at $x = 0$; for the wedge we are led by ultimately the same physical consideration (the requirement that probability current be continuous at the points where the potential displays kinks) to require that

$$\text{both } \psi \text{ and } \psi' \equiv \tfrac{\partial}{\partial x}\psi \text{ must be } \textit{continuous} \text{ at } x = 0 \qquad (71)$$

The latter condition brings into play two classes of eigenfunctions:

[31] I am thinking here mainly of the possible relation between some remarkable identities presented at the end of the essay cited on page 37 and properties of the "quantum zeta function" that arises from bouncer physics.

- **odd eigenfunctions**: $\psi(-x) = -\psi(x)$. These turn out to be close asssociates of the bouncer eigenfunctions, and to have "bouncer eigenvalues;"
- **even eigenfunctions**: $\psi(-x) = +\psi(x)$. These require a fresh extension of our former line of argument. They lead to interdigitated eigenvalues and a lowered groundstate energy.

29. Detailed properties of the Airy function—continued. Proceeding in imitation of the pattern established in §25 ... we read rough estimates of the locations of the zeros of $\frac{d}{d\xi}\,\mathrm{Ai}(\xi)$—known to *Mathematica* as `AiryAiPrime`—from a graph

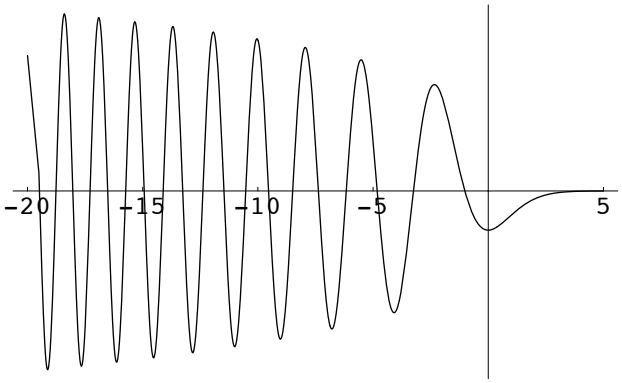

FIGURE 16: *Graph of* $d\mathrm{Ai}(\xi)/d\xi$*, used to obtain rough estimates of the locations of the points* $0 > \eta_0 > \eta_1 > \cdots$ *at which the derivative of the Airy function vanishes.*

of that function obtain the "seed data" that we use to construct the following

SHORT TABLE OF ZEROS OF THE DERIVATIVE OF THE AIRY FUNCTION

n	η_n	$-[\frac{3\pi}{8}(4n+1)]^{\frac{2}{3}}$
0	− 1.01879	− 1.11546
1	− 3.24820	− 3.26163
2	− 4.82010	− 4.82632
3	− 6.16331	− 6.16713
4	− 7.37218	− 7.37485
9	− 12.38479	− 12.38574
14	− 16.52050	− 16.52104
19	− 20.18863	− 20.18899

The third column is intended to establish the credentials of the claim (compare (68.2)) that asymptotically

$$\eta_n \approx -[\tfrac{3\pi}{8}(4n+1)]^{\frac{2}{3}} \tag{72}$$

which is a truncated version of the much more elaborate formula given by Abramowitz & Stegun.[25] I have adopted $0, 1, 2, \ldots$ indexing in place of our former $1, 2, 3, \ldots$ indexing to conform to the quantum mechanical convention that assigns the subscript $_0$ to the ground state. We are not surprised, after a glance back to Figure 12, to observe that

$$\cdots < \xi_3 < \eta_2 < \xi_2 < \eta_1 < \xi_1 < \eta_0 < 0$$

(whence my use of the word "interdigitated" on the preceding page).

Now construct the odd wedge functions[32]

$$f_n(y) \equiv \theta(y)\,\mathrm{Ai}(\xi_n + y) - \theta(-y)\,\mathrm{Ai}(\xi_n - y) \quad : \quad n = 1, 2, 3, \ldots$$

and the even wedge functions

$$g_n(y) \equiv \theta(y)\,\mathrm{Ai}(\eta_n + y) + \theta(-y)\,\mathrm{Ai}(\eta_n - y) \quad : \quad n = 0, 1, 2, \ldots$$

and use `NIntegrate[]` to evaluate the normalization constants

$$N_n^{\mathrm{odd}} \equiv \left[\int_{-\infty}^{+\infty} [f_n(y)]^2\,dy\right]^{-\frac{1}{2}} \quad \text{and} \quad N_n^{\mathrm{even}} \equiv \left[\int_{-\infty}^{+\infty} [g_n(y)]^2\,dy\right]^{-\frac{1}{2}}$$

Use that information to construct the normalized functions

$$F_n(y) \equiv N_n^{\mathrm{odd}} \cdot f_n(y) \quad : \quad n = 1, 2, 3, \ldots$$
$$G_n(y) \equiv N_n^{\mathrm{even}} \cdot g_n(y) \quad : \quad n = 0, 1, 2, \ldots$$

These procedures give

$$\begin{aligned}
F_1(y) &= 1.00841\big\{\theta(y)\,\mathrm{Ai}(-02.33811 + y) - \theta(-y)\,\mathrm{Ai}(-02.33811 - y)\big\}\\
F_2(y) &= 0.88046\big\{\theta(y)\,\mathrm{Ai}(-04.08795 + y) - \theta(-y)\,\mathrm{Ai}(-04.08795 - y)\big\}\\
F_3(y) &= 0.81727\big\{\theta(y)\,\mathrm{Ai}(-05.52056 + y) - \theta(-y)\,\mathrm{Ai}(-05.52056 - y)\big\}\\
F_4(y) &= 0.77631\big\{\theta(y)\,\mathrm{Ai}(-06.78671 + y) - \theta(-y)\,\mathrm{Ai}(-06.78671 - y)\big\}\\
F_5(y) &= 0.74642\big\{\theta(y)\,\mathrm{Ai}(-07.94413 + y) - \theta(-y)\,\mathrm{Ai}(-07.94413 - y)\big\}\\
F_{10}(y) &= 0.66221\big\{\theta(y)\,\mathrm{Ai}(-12.82878 + y) - \theta(-y)\,\mathrm{Ai}(-12.82878 - y)\big\}\\
F_{15}(y) &= 0.61808\big\{\theta(y)\,\mathrm{Ai}(-16.90563 + y) - \theta(-y)\,\mathrm{Ai}(-16.90563 - y)\big\}\\
F_{20}(y) &= 0.58874\big\{\theta(y)\,\mathrm{Ai}(-20.53733 + y) - \theta(-y)\,\mathrm{Ai}(-20.53733 - y)\big\}\\
&\vdots
\end{aligned}$$

[32] The *Mathematica* commands are of the form

```
f[y_]:=UnitStep[y] AiryAi[ξ + y] - UnitStep[-y] AiryAi[ξ - y]
```

Do not confuse these f-functions with the bouncer functions f of (69).

$$
\begin{aligned}
G_0(y) &= 1.30784\big\{\theta(y)\,\mathrm{Ai}(-01.01879+y)+\theta(-y)\,\mathrm{Ai}(-01.01879-y)\big\}\\
G_1(y) &= 0.93634\big\{\theta(y)\,\mathrm{Ai}(-03.24820+y)+\theta(-y)\,\mathrm{Ai}(-03.24820-y)\big\}\\
G_2(y) &= 0.84666\big\{\theta(y)\,\mathrm{Ai}(-04.82010+y)+\theta(-y)\,\mathrm{Ai}(-04.82010-y)\big\}\\
G_3(y) &= 0.79581\big\{\theta(y)\,\mathrm{Ai}(-06.16331+y)+\theta(-y)\,\mathrm{Ai}(-06.16331-y)\big\}\\
G_4(y) &= 0.76081\big\{\theta(y)\,\mathrm{Ai}(-07.37218+y)+\theta(-y)\,\mathrm{Ai}(-07.37218-y)\big\}\\
G_9(y) &= 0.66813\big\{\theta(y)\,\mathrm{Ai}(-12.38479+y)+\theta(-y)\,\mathrm{Ai}(-12.38479-y)\big\}\\
G_{14}(y) &= 0.62168\big\{\theta(y)\,\mathrm{Ai}(-16.52050+y)+\theta(-y)\,\mathrm{Ai}(-16.52050-y)\big\}\\
G_{19}(y) &= 0.58630\big\{\theta(y)\,\mathrm{Ai}(-20.18863+y)+\theta(-y)\,\mathrm{Ai}(-20.18863-y)\big\}\\
&\vdots
\end{aligned}
$$

Straightforward modification of Gea-Banacloche's asymptotic description of the bouncer normalization factors (page 38) leads us to anticipate that for odd wedge functions we can write

$$N_n^{\text{odd}} \sim \Big[\frac{\pi}{2\sqrt{-\xi_n}}\Big]^{\frac{1}{2}} \approx \Big[\frac{\pi^2}{3(4n-1)}\Big]^{\frac{1}{6}} \tag{73.1}$$

and in support of that expectation I offer the following data:

$$
\begin{aligned}
\Big[\tfrac{\pi}{2\sqrt{02.33811}}\Big]^{\frac{1}{2}} &= 1.01355, \quad \Big[\tfrac{\pi^2}{3(4\cdot1-1)}\Big]^{\frac{1}{6}} = 1.01549: \quad \text{compare } 1.00841\\
\Big[\tfrac{\pi}{2\sqrt{04.08795}}\Big]^{\frac{1}{2}} &= 0.88142, \quad \Big[\tfrac{\pi^2}{3(4\cdot2-1)}\Big]^{\frac{1}{6}} = 0.88175: \quad \text{compare } 0.88046\\
\Big[\tfrac{\pi}{2\sqrt{05.52056}}\Big]^{\frac{1}{2}} &= 0.81764, \quad \Big[\tfrac{\pi^2}{3(4\cdot3-1)}\Big]^{\frac{1}{6}} = 0.81777: \quad \text{compare } 0.81727\\
\Big[\tfrac{\pi}{2\sqrt{06.78671}}\Big]^{\frac{1}{2}} &= 0.77651, \quad \Big[\tfrac{\pi^2}{3(4\cdot4-1)}\Big]^{\frac{1}{6}} = 0.77657: \quad \text{compare } 0.77632\\
\Big[\tfrac{\pi}{2\sqrt{07.94413}}\Big]^{\frac{1}{2}} &= 0.74653, \quad \Big[\tfrac{\pi^2}{3(4\cdot5-1)}\Big]^{\frac{1}{6}} = 0.74657: \quad \text{compare } 0.74642\\
\Big[\tfrac{\pi}{2\sqrt{012.82878}}\Big]^{\frac{1}{2}} &= 0.66224, \quad \Big[\tfrac{\pi^2}{3(4\cdot10-1)}\Big]^{\frac{1}{6}} = 0.66225: \quad \text{compare } 0.66221\\
\Big[\tfrac{\pi}{2\sqrt{016.90563}}\Big]^{\frac{1}{2}} &= 0.61809, \quad \Big[\tfrac{\pi^2}{3(4\cdot15-1)}\Big]^{\frac{1}{6}} = 0.61809: \quad \text{compare } 0.61808\\
\Big[\tfrac{\pi}{2\sqrt{020.53733}}\Big]^{\frac{1}{2}} &= 0.58874, \quad \Big[\tfrac{\pi^2}{3(4\cdot20-1)}\Big]^{\frac{1}{6}} = 0.58874: \quad \text{compare } 0.58874
\end{aligned}
$$

It is not so obvious—yet perhaps not too surprising—that this obvious variant of (73.1) does the job for *even* wedge functions:

$$N_n^{\text{even}} \sim \Big[\frac{\pi}{2\sqrt{-\eta_n}}\Big]^{\frac{1}{2}} \approx \Big[\frac{\pi^2}{3(4n+1)}\Big]^{\frac{1}{6}} \tag{73.2}$$

That claim is supported by the numerical data shown on the next page:

$$\Big[\tfrac{\pi}{2\sqrt{01.01879}}\Big]^{\frac{1}{2}} = 1.24749\,, \quad \Big[\tfrac{\pi^2}{3(4\cdot0+1)}\Big]^{\frac{1}{6}} = 1.21954: \quad \text{compare } 1.30784$$
$$\Big[\tfrac{\pi}{2\sqrt{03.24820}}\Big]^{\frac{1}{2}} = 0.93358\,, \quad \Big[\tfrac{\pi^2}{3(4\cdot1+1)}\Big]^{\frac{1}{6}} = 0.93261: \quad \text{compare } 0.93634$$
$$\Big[\tfrac{\pi}{2\sqrt{04.82010}}\Big]^{\frac{1}{2}} = 0.84586\,, \quad \Big[\tfrac{\pi^2}{3(4\cdot2+1)}\Big]^{\frac{1}{6}} = 0.84558: \quad \text{compare } 0.84666$$
$$\Big[\tfrac{\pi}{2\sqrt{06.16331}}\Big]^{\frac{1}{2}} = 0.79544\,, \quad \Big[\tfrac{\pi^2}{3(4\cdot3+1)}\Big]^{\frac{1}{6}} = 0.79532: \quad \text{compare } 0.79581$$
$$\Big[\tfrac{\pi}{2\sqrt{07.37218}}\Big]^{\frac{1}{2}} = 0.76061\,, \quad \Big[\tfrac{\pi^2}{3(4\cdot4+1)}\Big]^{\frac{1}{6}} = 0.76054: \quad \text{compare } 0.76081$$
$$\Big[\tfrac{\pi}{2\sqrt{012.38479}}\Big]^{\frac{1}{2}} = 0.66809\,, \quad \Big[\tfrac{\pi^2}{3(4\cdot9+1)}\Big]^{\frac{1}{6}} = 0.66808: \quad \text{compare } 0.66813$$
$$\Big[\tfrac{\pi}{2\sqrt{016.52050}}\Big]^{\frac{1}{2}} = 0.62166\,, \quad \Big[\tfrac{\pi^2}{3(4\cdot14+1)}\Big]^{\frac{1}{6}} = 0.62166: \quad \text{compare } 0.62168$$
$$\Big[\tfrac{\pi}{2\sqrt{020.18863}}\Big]^{\frac{1}{2}} = 0.59127\,, \quad \Big[\tfrac{\pi^2}{3(4\cdot19+1)}\Big]^{\frac{1}{6}} = 0.59126: \quad \text{compare } 0.59127$$

I find it fairly amazing that the construcions (73) work as well as they do (which is to say: *quite* well, even when n is small) ... and utterly amazing that (on numerical evidence that is consistent with quantum mechanical necessity)

- $F_m(x) \perp F_n(x)$ if $m \neq n$;
- $G_m(x) \perp G_n(x)$ if $m \neq n$;
- $F_m(x) \perp G_n(x)$ in all cases.

If the functions are presented to *Mathematica* with only the accuracy expressed on these pages (*i.e.*, if the higher precision data normally concealed within *Mathematica*'s memory is discarded) then one finds the following results

$$\texttt{NIntegrate}[F_1(x)\,F_2(x), \{x, -\infty, +\infty\}] = +1.16 \times 10^{-6}$$
$$\texttt{NIntegrate}[G_0(x)G_1(x), \{x, -\infty, +\infty\}] = +8.11 \times 10^{-7}$$
$$\texttt{NIntegrate}[F_1(x)\,G_1(x), \{x, -\infty, +\infty\}] = -1.09 \times 10^{-17}$$

to be typical (though in some cases, especially cases involving wedge functions of higher order, *Mathematica* complains of "lost precision").

30. Eigenvalues and eigenfunctions for the quantum wedge problem. Those can, in ascending spectral order, be described as follows:

$$\psi_0(x) = \sqrt{k}G_0(kx) \quad \text{with eigenvalue} \quad E_0 = \big(\tfrac{1}{2}mg^2\hbar^2\big)^{\frac{1}{3}} \cdot 1.01879$$
$$\psi_1(x) = \sqrt{k}\,F_1(kx) \quad \text{with eigenvalue} \quad E_1 = \big(\tfrac{1}{2}mg^2\hbar^2\big)^{\frac{1}{3}} \cdot 2.33811$$
$$\psi_2(x) = \sqrt{k}G_1(kx) \quad \text{with eigenvalue} \quad E_2 = \big(\tfrac{1}{2}mg^2\hbar^2\big)^{\frac{1}{3}} \cdot 3.24820$$
$$\psi_3(x) = \sqrt{k}\,F_2(kx) \quad \text{with eigenvalue} \quad E_3 = \big(\tfrac{1}{2}mg^2\hbar^2\big)^{\frac{1}{3}} \cdot 4.08795$$
$$\psi_4(x) = \sqrt{k}G_2(kx) \quad \text{with eigenvalue} \quad E_4 = \big(\tfrac{1}{2}mg^2\hbar^2\big)^{\frac{1}{3}} \cdot 4.82010$$
$$\psi_5(x) = \sqrt{k}\,F_3(kx) \quad \text{with eigenvalue} \quad E_5 = \big(\tfrac{1}{2}mg^2\hbar^2\big)^{\frac{1}{3}} \cdot 5.52056$$
$$\psi_6(x) = \sqrt{k}G_3(kx) \quad \text{with eigenvalue} \quad E_6 = \big(\tfrac{1}{2}mg^2\hbar^2\big)^{\frac{1}{3}} \cdot 6.16331$$
$$\vdots$$

The red entries exactly reproduce the bouncer spectrum. In the next pair of figures I provide graphical representations of the wedge eigenfunctions described above:

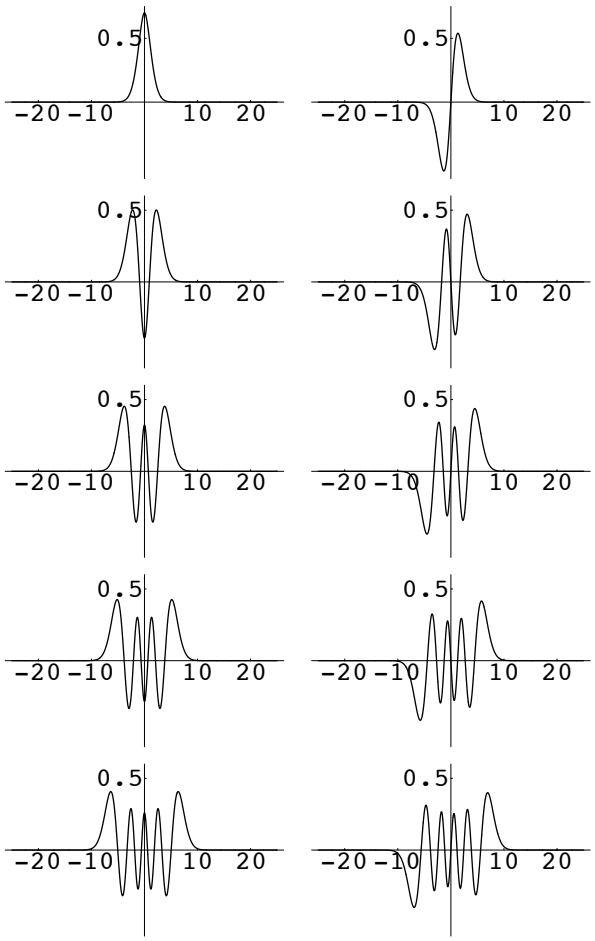

FIGURE 17: *Wedge eigenfunctions $\psi_0(x), \ldots, \psi_9(x)$, displayed in ascending order (figure to be read "like a book"). Even G-functions are seen in the left column, odd F-functions in the right column. With a little practice one can discover the identity of any such figure by counting zero-crossings and local extrema.*

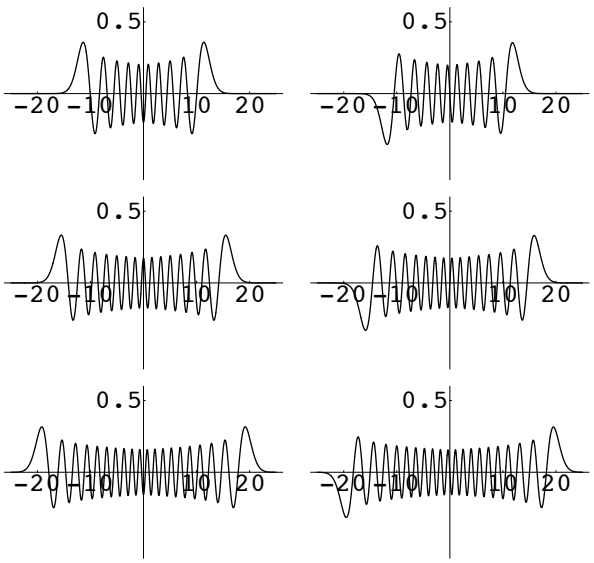

FIGURE 18: *Wedge eigenfunctions $\psi_{18}(x)$ & $\psi_{19}(x)$ (top row, constructed from G_9 & F_{10}), $\psi_{28}(x)$ & $\psi_{29}(x)$ (middle row, constructed from G_{14} & F_{15}) and $\psi_{38}(x)$ & $\psi_{39}(x)$ (bottom row, constructed from G_{19} & F_{20}). Again, the functions in the left column (those with even index) are clearly even, those in the right column (those with odd index) as clearly odd functions of x.*

31. Probabilistic aspects of the wedge problem. An obvious adjustment of the argument that gave (40) gives

$$Q_{\text{wedge}}(x) = \begin{cases} \dfrac{1}{4\sqrt{x_{\max}}\sqrt{x_{\max} - |x|}} & : \quad 0 \leqslant |x| \leqslant x_{\max} \\ \\ 0 & : \quad \text{elsewhere} \end{cases} \tag{74}$$

In Figure 19 (next page: compare Figure 8 on page 20) that distribution is superimposed upon its quantum counterpart in the case ψ_{20}.

32. Comparison with the result of Planck quantization. An obvious adjustment of the argument that led in §14 to

$$\begin{aligned} \oint p\,dx &= \tfrac{4}{3} p_0 x_{\max} \\ &= \tfrac{4}{3}\sqrt{2mE}\,(E/mg) \quad : \quad \text{BOUNCER} \end{aligned}$$

now gives

$$\begin{aligned} &\downarrow \\ &= \tfrac{8}{3}\sqrt{2mE}\,(E/mg) \quad : \quad \text{WEDGE} \end{aligned}$$

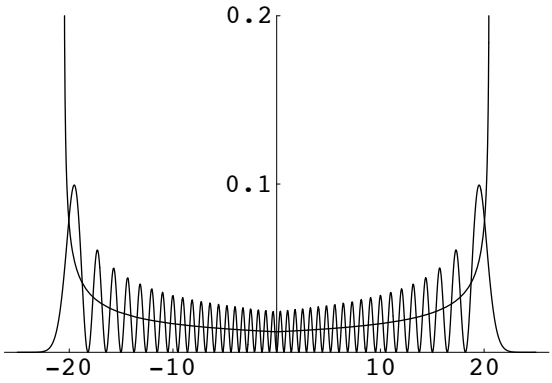

FIGURE 19: *Superimposed displays of* $|\psi_{20}(x)|^2$ *and its classical counterpart* $Q_{\rm wedge}(x)$. *In constructing the figure I have both* k *and* mg *to unity, so* $x_{\rm max} = 20.53733$.

so Planck's quantization condition[33] gives

$$\begin{aligned} E_{n-1} &= \left[\tfrac{9}{128}\right]^{\frac{1}{3}} (mg^2\hbar^2)^{\frac{1}{3}} n^{\frac{2}{3}} \quad : \quad n = 1, 2, 3, \ldots \\ &= \left[\tfrac{72\pi^2}{128}\right]^{\frac{1}{3}} (\tfrac{1}{2} mg^2\hbar^2)^{\frac{1}{3}} n^{\frac{2}{3}} \\ &= 1.77068\, (\tfrac{1}{2} mg^2\hbar^2)^{\frac{1}{3}} n^{\frac{2}{3}} \end{aligned}$$

In particular, for the ground state we have (looking back again to page 47 for the exact data)

$$E_0/(\tfrac{1}{2} mg^2\hbar^2)^{\frac{1}{3}} = \begin{cases} 1.77068 & : \quad \text{PLANCK} \\ 1.01879 & : \quad \text{SCHRÖDINGER} \end{cases}$$

which (see again footnote [30] on page 47) now *do* stand in the naively anticipated relationship.

That the wedge problem is in some respects "nicer/better-behaved" than the bouncer is a point remarked already by J. J. Sakurai,[34] whose interest in

[33] It was actually Sommerfeld & Wilson who, in 1915, first wrote $\oint p dx = nh$ as an expression of Planck's idea.

[34] *Modern Quantum Mechanics* (revised edition 1994), pages 107–109. It is a special pleasure for me to recall memories of John Sakurai, for he and I were first-year graduate students together at Cornell in 1955–1956, and used to play flute and double bass duets together in the physics library in dead of night. The contempt for theoretical fine points, the preoccupation with the *physics* of physics that was then (and remains) a tradition at Cornell ... caused me to flee to Brandeis, but was precisely what John (who had spent his undergraduate years at Harvard, in the shade of Schwinger) sought. In 1970 he left the University of Chicago to rejoin Schwinger at UCLA. He died in 1982 while visiting CERN (from which I had departed in 1962), decades before his time.

the role of gravity in quantum mechanics was so well developed (see his pages 126–129[35]) that it was probably no accident that he selected the bouncer/wedge problems to illustrate the practical application of the WKB approximation.[36]

33. Why the "bounced Gaussian" presents a problem. PROBLEM #1 is *How to describe the initial wavepacket*? One might be tempted, in imitation of (60), to write

$$\psi(x,0) = \tfrac{1}{\sqrt{\sigma\sqrt{2\pi}}}\, e^{-\frac{1}{4}\left[\frac{x-a}{\sigma}\right]^2} \tag{75}$$

But that function (i) does not vanish at $x = 0$, and (ii) is normalized on the wrong base (which is to say: on $(-\infty, \infty)$ instead of on $(0, \infty)$). On account of (i) the Gaussian (75) does not describe a possible *state* of the bouncer, though it *nearly* does if $a \gg \sigma$: for example, if $a = 10\sigma$ then $\psi(0,0) = 1.39\times10^{-11}\psi(a,0)$.

We might resolve point both difficulties by writing

$$\psi(x,0) = N \cdot \left\{ e^{-\frac{1}{4}\left[\frac{x-a}{\sigma}\right]^2} - e^{-\frac{1}{4}\left[\frac{x+a}{\sigma}\right]^2} \right\} \tag{76.1}$$

and setting

$$\begin{aligned} N &= \left[\sigma\sqrt{2\pi}\Big(1 - e^{-\frac{1}{2}[a/\sigma]^2}\Big)\right]^{-\frac{1}{2}} \qquad (76.2)\\ &\downarrow \\ &= \begin{cases} \frac{1}{\sqrt{\sigma\sqrt{2\pi}}} & \text{for } a \gg \sigma;\ \textit{i.e.}, \text{ as } a \uparrow \infty \\ \infty & \text{for } a \ll \sigma;\ \textit{i.e.}, \text{ as } a \downarrow 0 \end{cases} \end{aligned}$$

On its face, (76) appears to assume the improper form $\infty \cdot 0$ at $a = 0$, but by l'Hôspital's Rule we are led actually to the quite unpathological function

$$\lim_{a\downarrow 0} \psi(x,0) = \left[\tfrac{2}{\pi}\right]^{\frac{1}{4}} \left[\tfrac{1}{\sigma}\right]^{\frac{3}{2}} x\, e^{-\frac{1}{4}\left[\frac{x}{\sigma}\right]^2} \tag{77}$$

and confirm that indeed $\int_0^\infty (\text{etc.})^2\, dx = 1$.

It should be noted that J. Gea-Banacloche[27] omits the preceding discussion: he is content to proceed from (75) and to work in the approximation $a \gg \sigma$ (*i.e.*, to assume that the wavepacket is dropped from a height large compared to its width). And that none of the problems discussed above arise in connection with the wedge problem: in that context (75) serves perfectly well as it stands.

---

[35] The ALbert OVErhauser whose beautiful neutron diffraction experiment he cites was our teacher (of solid state theory) at Cornell . . . and the father of a lady physicist who called herself ALOVE, and who taught for one year at Reed College, where she created the optics lab.

[36] The upshot of Sakurai's discussion is posed as Problems ****8.5** and ***8.6** in Griffiths' *Introduction to Quantum Mechanics* (1994).

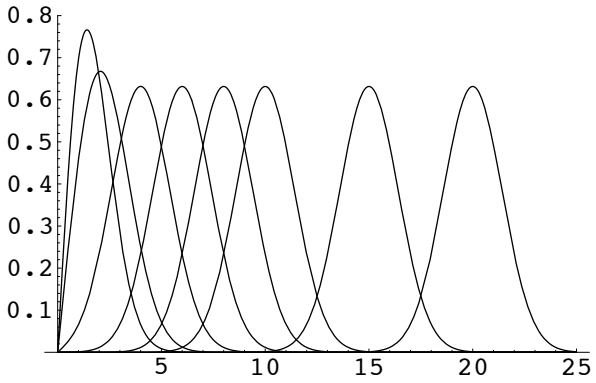

FIGURE 20: *"Pinched Gaussian" wavepackets obtained from (76) and (77), in which I have set* $\sigma = 1$ *and* $a = 0, 2, 4, 6, 8, 10, 15, 20$.

PROBLEM #2: To describe the dynamically evolved wavepacket we have—in principle—only to write

$$\psi(x,t) = \sum_n c_n \psi_n(x) e^{-\frac{i}{\hbar}E_n t} \tag{78.1}$$

$$c_n = \int_0^\infty \psi_n(\xi)\,\psi(\xi,0)\,d\xi \tag{78.2}$$

but this is more easily said than done: the program presumes that

- that we possess exact descriptions of all eigenfunctions/eigenvalues; *i.e.*, of all the zeros of $\mathrm{Ai}(x)$, and all normalization factors;
- that we are able to perform the $\int$'s;
- that we are able to perform the final $\sum_n$.

Reverse the order of integration and summation. One then has

$$\psi(x,t) = \int_0^\infty K(x,t;\xi,0)\psi(\xi,0)\,d\xi \tag{79.1}$$

$$K(x,t;\xi,0) = \sum_n e^{-\frac{i}{\hbar}E_n t}\,\psi_n(x)\psi_n(\xi) \tag{79.2}$$

and sees that those same difficulties beset the spectral construction and use of the propagator.

Identical difficulties attach to the wedge problem.

PROBLEM #3: We have no alternative but to resort to various approximation schemes, but confront then the *problem of distinguishing real/physical results from artifacts*, and here it is easy to stumble. For example: from (78.1) it follows that the frequencies present in the motion of

$$|\psi(x,t)|^2 = \sum_{m,n} c_m^* c_n \psi_m(x)\,\psi_n(x) e^{\frac{i}{\hbar}(E_m - E_n)t}$$

are given (see again page 41) by

$$\omega_{mn} \equiv -\tfrac{1}{\hbar}\mathcal{E}\cdot\xi_{mn} \quad \text{with} \quad \xi_{mn} \equiv \xi_m - \xi_n$$

where now $\mathcal{E} \equiv \big(\frac{1}{2}mg^2\hbar^2\big)^{\frac{1}{3}}$. But the numbers

$$\begin{array}{cccc} \xi_{12} & \xi_{13} & \xi_{14} & \cdots \\ & \xi_{23} & \xi_{24} & \cdots \\ & & \xi_{34} & \cdots \\ & & & \cdots \end{array}$$

are (I assert in the absence of proof) *irrational multiples of one another*.[37] It becomes therefore difficult to understand how the resonances ("revivals") which Geo-Banacloche claims to observe can be real.

34. Approximate development of a Gaussian wavepacket as a superposition of bouncer eigenfunctions. For the purposes of this discussion I will take the bouncer eigenfunctions to be given by[38]

$$\begin{aligned} \psi_1(x) &= \sqrt{k}\,(1.4261)\,\mathrm{Ai}(kx - 2.3381) \\ \psi_2(x) &= \sqrt{k}\,(1.2452)\,\mathrm{Ai}(kx - 4.0879) \\ \psi_3(x) &= \sqrt{k}\,(1.1558)\,\mathrm{Ai}(kx - 5.5206) \\ \psi_4(x) &= \sqrt{k}\,(1.0979)\,\mathrm{Ai}(kx - 6.7867) \\ \psi_5(x) &= \sqrt{k}\,(1.0556)\,\mathrm{Ai}(kx - 7.9441) \end{aligned}$$

and, for $n > 5$, by[39]

$$\psi_n(x) = \sqrt{k}\Big[\frac{8\pi^2}{3(4n-1)}\Big]^{\frac{1}{6}}\mathrm{Ai}\big(kx - \big[\tfrac{3\pi}{8}(4n-1)\big]^{\frac{2}{3}}\big)$$

To describe our initial Gaussian wavepacket we adopt a "bouncer adapted" version of (75), writing

$$\psi(x,0;a,\sigma) = \sqrt{k}\,\tfrac{1}{\sqrt{k\sigma\sqrt{2\pi}}}e^{-\frac{1}{4}\left[\frac{k(x-a)}{k\sigma}\right]^2} \quad : \quad a \gg \sigma$$

but notice that in point of fact all the k's spontaneously disappear.

The following figure indicates why we might expect the integrals c_n to be relatively small unless $E_n/mg \approx a \pm \sigma$: if $E_n/mg \ll a - \sigma$ then the integrand

[37] In this respect the bouncer and wedge problems differ profoundly from the harmonic oscillator ($E_n \sim n$), the particle-in-a-box ($E_n \sim n^2$) and the Kepler ($E_n \sim n^{-2}$) problem.

[38] See again (69.2) and page 41.

[39] See again (68.2) and (70) on pages 37/38.

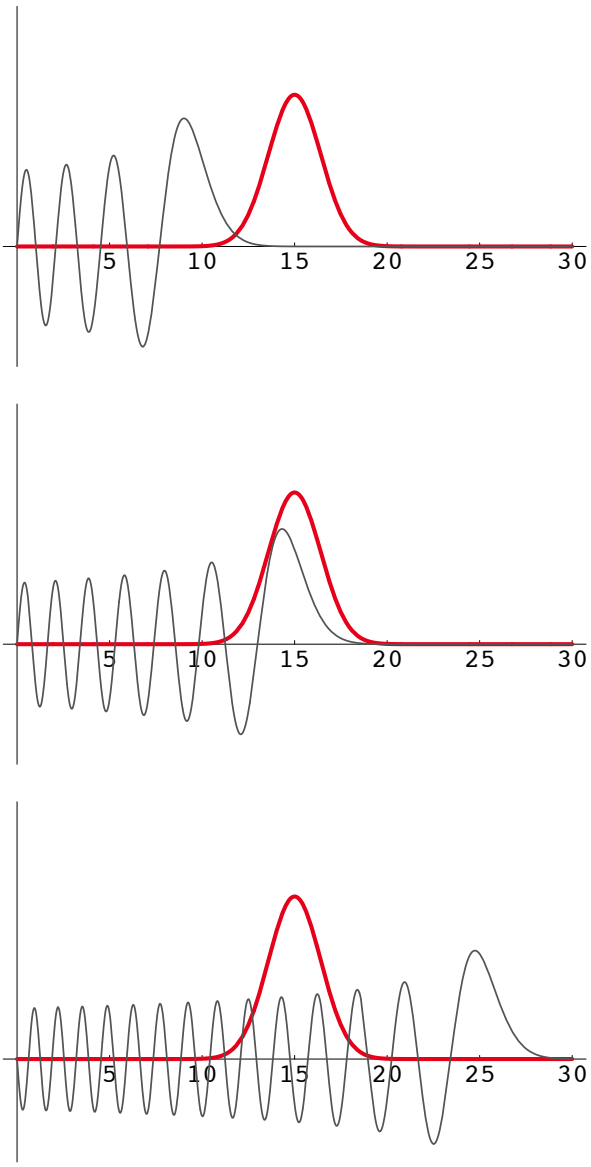

FIGURE 21: *Graphical indication of why—for distinct reasons—we expect the c_n to be small if either $\xi_n \ll ka$ or $\xi_n \gg ka$. To construct the figure I have set $k = 1$.*

never departs much from zero because it is the product of a pair of functions (eigenfunction and Gaussian) that do not overlap much, while if $E_n/mg \gg a+\sigma$ then the Gaussian is "buzzed to death." Moreover, we expect the c_n to be most sharply peaked at $c_{\max}$ when $\sigma \approx \xi_1 - \xi_2$: if $\sigma \ll \xi_1 - \xi_2$ then many

eigenfunctions will be needed to capture the detail written into the Gaussian, while if $\sigma \gg \xi_1 - \xi_2$ then many eigenfunctions will enjoy significant overlap. Those are our broad expectations. The question is: How do they square with the details of the situation?

Look to some illustrative numerical evidence. Take

$$\text{Gaussian wavepacket} = \psi(x, 0; 15, 1.75)$$

where I have set $\sigma = 1.75 \approx \xi_1 - \xi_2 = -2.3381 + 4.0879 = 1.7498$. *Mathematica* responds to the command

$$\texttt{NIntegrate[Evaluate[}\psi(x, 0; 15, 1.75) * \psi_n(x), \{x, 0, \infty\}\texttt{]]}$$

with complaints[40] and this data

$$\begin{aligned}
c_1 &= 0.0000 \\
c_2 &= 0.0001 \\
c_3 &= 0.0008 \\
c_4 &= 0.0034 \\
c_5 &= 0.0113 \\
c_6 &= 0.0300 \\
c_7 &= 0.0664 \\
c_8 &= 0.1251 \\
c_9 &= 0.2041 \\
c_{10} &= 0.2920 \\
c_{11} &= 0.3703 \\
c_{12} &= 0.4191 \\
c_{13} &= 0.4259 = c_{\max} \\
c_{14} &= 0.3902 \\
c_{15} &= 0.3233 \\
c_{16} &= 0.2427 \\
c_{17} &= 0.1653 \\
c_{18} &= 0.1021 \\
c_{19} &= 0.0572 \\
c_{20} &= 0.0290 \\
c_{21} &= 0.0132 \\
c_{22} &= 0.0054 \\
c_{23} &= 0.0020 \\
c_{24} &= 0.0006 \\
c_{25} &= 0.0002
\end{aligned}$$

[40] "Underflow occurred in computation," "NIntegrate failed to converge to prescribed accuracy after 7 recursive bisections ..."

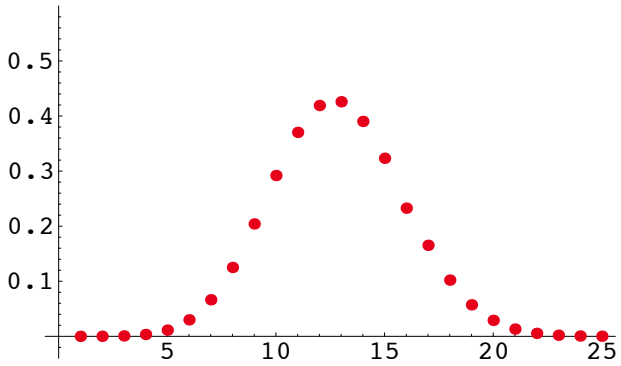

FIGURE 22: `ListPlot` *display of the data tabulated on the preceding page. The* c_n*'s* • *that contribute significantly to the representation of that particular Gaussian wavepacket are seen to have*

$$4 = 13 - 9 \leqslant n \leqslant 13 + 9 = 22$$

That **it works!** is convincingly demonstrated below:[41]

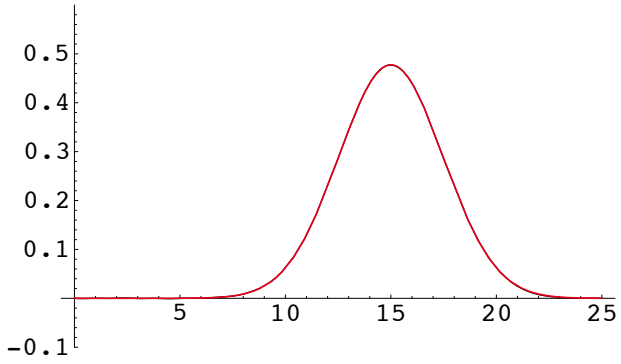

FIGURE 23: *Superimposed graphs of*

$$\psi(x, 0; 15, 1.75) \quad \textit{and} \quad \sum_{n=4}^{22} c_n \psi_n(x)$$

with c's taken from the data displayed in Figure 22. The difference is impreceptible.

In Figures 24 I display data taken from another pair of Gaussians—one fatter, one thinner than the case $\sigma = 1.75$ discussed above. The result is in one respect surprising, as noted in the caption.

[41] I am encouraged on this evidence to think that *Mathematica* supplies good data even when she complains.

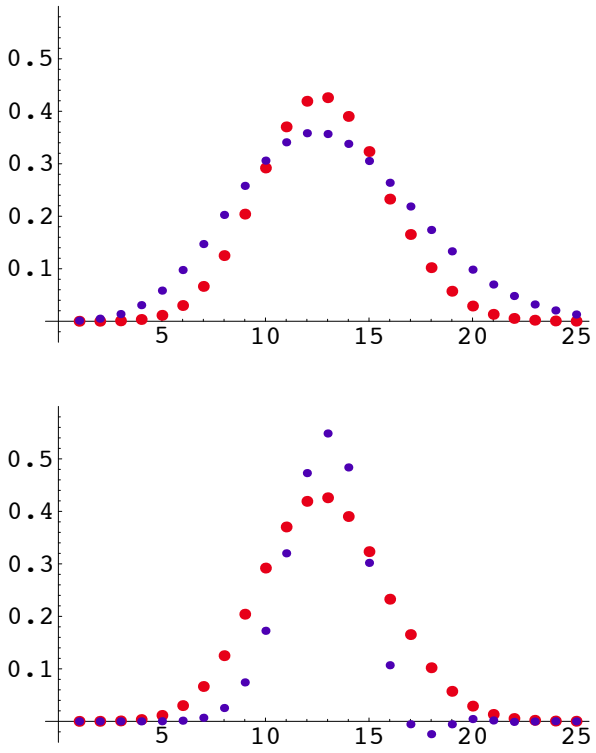

FIGURE 24 (UPPER): *Here superimposed upon the data • of the preceding figure is data • associated with the relatively fatter Gaussian* $\sigma = 2.5$*: the c's are more broadly distributed about* $c_{\max}$ *—precisely as anticipated.*

FIGURE 24 (LOWER): *Here the superimposed data • is associated with the relatively sharper Gaussian* $\sigma = 1.0$*. Contrary to what we anticipated, the c's are now still more narrowly distributed about* $c_{\max}$*. This is a development that awaits explanation.*

We have proceeded thus far numerically. I turn now to discussion of some analytical aspects of the situation.[42] Drawing upon the integral representation (52) of the Airy function, we by (78.2) have

$$c_n = \tfrac{1}{\pi} N_n \frac{1}{\sqrt{\sigma\sqrt{2\pi}}} \int_0^\infty \left\{ \int_0^\infty \cos\left([y+\xi_n]u + \tfrac{1}{3}u^3\right) e^{-\frac{1}{4}\left[\frac{y-a}{\sigma}\right]^2} du \right\} dy$$

Reverse the order of integration, and (on the assumption that $a \gg \sigma$) replace

[42] The pattern of the argument was sketched already by Gea-Banacloche near the end of his §2.

$\int_0^{+\infty} dy$ by $\int_{-\infty}^{+\infty} dy$: *Mathematica* then supplies

$$\Big\{\text{etc.}\Big\} = 2\sigma\sqrt{\pi}\, e^{-\sigma^2 u^2} \cos\big([a+\xi_n]u + \tfrac{1}{3}u^3\big)$$

whence

$$c_n = \Big[\tfrac{4\sigma}{\pi\sqrt{2\pi}}\Big]^{\frac{1}{2}} N_n \int_0^{\infty} e^{-\sigma^2 u^2} \cos\big([a+\xi_n]u + \tfrac{1}{3}u^3\big) du \tag{80}$$

As a check on the accuracy of this result I set $a = 15$, $\sigma = 1.75$ and $n = 13$ (whence $N_{13} = 0.8956$ and $\xi_{13} = -15.3403$) and by numerical evaluation of the integral obtain $c_{13} = 0.4529$, in precise agreement with the value tabulated on page 55. I am confident that one would enjoy the same success with other values of n.

If σ is large—which is (in dimensionless physical variables) to say: if

$$ka \gg k\sigma \gg 1 \quad : \quad \text{entails} \quad \sigma \gg k^{-1} \equiv \big(\tfrac{\hbar^2}{2m^2 g}\big)^{\frac{1}{3}}$$

—then the Gaussian $e^{-\sigma^2 u^2}$ dies so fast that only small u-values contribute to the $\int$ in (80): to exploit the implications of this fact we adopt the abbreviation $A \equiv a + \xi_n$ and write

$$\begin{aligned}\cos\big(Au + \tfrac{1}{3}u^3\big) &= \cos Au \cdot \frac{\cos\big(Au + \frac{1}{3}u^3\big)}{\cos Au} \\ &= \cos Au \cdot \Big\{1 - \tfrac{1}{3}u^3 \tan Au - \tfrac{1}{18}u^6 + \tfrac{1}{162}u^9 \tan Au + \cdots\Big\}\end{aligned}$$

Mathematica now supplies

$$\begin{aligned}\int_0^{\infty} e^{-\sigma^2 u^2} \cos Au\, du &= \tfrac{\sqrt{\pi}}{2\sigma} e^{-\frac{1}{4}A^2/\sigma^2} \\ -\int_0^{\infty} e^{-\sigma^2 u^2} \tfrac{1}{3}u^3 \sin Au\, du &= \tfrac{\sqrt{\pi}}{2\sigma} e^{-\frac{1}{4}A^2/\sigma^2} \cdot \frac{A^3 - 6A\sigma^2}{24\sigma^6} \\ &\vdots \text{ subsequent integrals are also "elementary"}\end{aligned}$$

on which basis we have

$$c_n = \tfrac{1}{\sqrt{\sigma\sqrt{2\pi}}}\, N_n\, e^{-[a+\xi_n]^2/4\sigma^2} \cdot \Big\{1 + \frac{[a+\xi_n]^3 - 6[a+\xi_n]\sigma^2}{24\sigma^6} + \cdots\Big\} \tag{81}$$

This result accounts nicely for the Gaussian patterns evident in Figure 22 and Figure 24 (upper), and provides insight into the circumstance responsible for the slight deviations from "Gaussianness" evident in Figure 24 (lower). I have been working with $k = 1$: one should insert k's in the obvious way to restore dimensional consistency to the $\big\{\text{etc.}\big\}$ in (81).

35. See the dropped wavepacket bounce. Generally, to launch

$$\psi(x,0) = \sum_n c_m \psi_n(x)$$

into dynamical motion we have only to let the individual eigenfunctions start buzzing, each with its own characteristic eigenfrequency $\omega_n = E_n/\hbar$:

$$\psi(x,t) = \sum_n c_m \psi_n(x)\, e^{-i\omega_n t} \qquad (82)$$

We have special interest in the motion of the associated probability density[43]

$$\begin{aligned} |\psi(x,t)|^2 &= \sum_m \sum_n c_m c_n \psi_m(x)\psi_n(x)\, e^{i(\omega_m - \omega_n)t} \\ &= \sum_m \sum_n c_m c_n \psi_m(x)\psi_n(x) \cos\omega_{mn} t \quad \text{with} \quad \omega_{mn} \equiv \omega_m - \omega_n \\ &= \sum_n \big[c_n \psi_n(x)\big]^2 + 2\sum_{m>n} \sum_n c_m c_n \psi_m(x)\psi_n(x) \cos\omega_{mn} t \end{aligned} \qquad (83)$$

Notice that if only two eigenstates enter into the construction of $\psi(x,0)$

$$\psi(x,0) = c_1\psi_1(x) + c_2\psi_2(x)$$

then (83) becomes

$$|\psi(x,t)|^2 = \big[c_1\psi_1(x)\big]^2 + \big[c_2\psi_2(x)\big]^2 + 2\, c_1 c_2 \psi_1(x)\psi_2(x) \cos\big\{(\omega_1 - \omega_2)\, t\big\}$$

Such motion is necessarily *periodic*. But if three (or more) eigenstates enter into the construction of $\psi(x,0)$ then the description of $|\psi(x,t)|^2$ involves terms proportional to each of the following

$$\cos\big\{(\omega_1 - \omega_2)\, t\big\} \qquad \cos\big\{(\omega_1 - \omega_3)\, t\big\} \qquad \cos\big\{(\omega_2 - \omega_3)\, t\big\}$$

and will, in general, be *aperiodic*: periodicity in such a circumstance requires the existence of integers p, q and r such that it is possible to write

$$\left.\begin{aligned} (\omega_1 - \omega_2)\,\tau &= p \cdot 2\pi \\ (\omega_1 - \omega_3)\,\tau &= q \cdot 2\pi \\ (\omega_2 - \omega_3)\,\tau &= r \cdot 2\pi \end{aligned}\right\} \quad \text{with some appropriately selected } \tau$$

Which is to say:

$$\frac{\omega_1 - \omega_2}{\omega_1 - \omega_3}, \quad \frac{\omega_1 - \omega_2}{\omega_2 - \omega_3} \text{ and } \frac{\omega_1 - \omega_3}{\omega_2 - \omega_3} \text{ must all be } \underline{\text{rational numbers}}$$

[43] The applications of specific interest to us present only real ψ_n's and real c_n's, so I omit all of the anticipated *'s from my equations.

Of course, if two of those ratios are rational then the rationality of the third is *automatic*, but that does not diminish the force of the preceding periodicity condition. (Generally, for what it's worth: from ν frequencies one can construct $\frac{1}{2}\nu(\nu-1)$ frequency differences, and $\frac{1}{2}\nu(\nu-1)-1$ independent ratios of differences, in terms of which all other such ratios can be expressed.)

Returning now from generalities to the bouncer: From (see again page 42 and recall that all the zeros ξ_n of $\text{Ai}(x)$ are negative)

$$E_n = -mg\left(\tfrac{\hbar^2}{2m^2g}\right)^{\frac{1}{3}}\xi_n \quad : \quad \text{BOUNCER EIGENVALUES} \tag{84.1}$$

we have

$$\omega_n = -\left(\tfrac{mg^2}{2\hbar}\right)^{\frac{1}{3}}\xi_n \tag{84.2}$$

giving

$$\frac{\omega_p-\omega_q}{\omega_r-\omega_s} = \frac{\xi_p-\xi_q}{\xi_r-\xi_s}$$

I have no idea how to prove[44] so must be content to

$$\text{CONJECTURE: All ratios } \frac{\xi_p-\xi_q}{\xi_r-\xi_s} \text{ are irrational} \tag{85}$$

and on this basis to conclude that the motion of $|\psi(x,t)|^2$ is (except in trivial cases of the sort described above) aperiodic.[45] The recurrent "collapses" and "revivals" which are the subject of Gea-Banacloche's §4 must evidently be subtle phenomena, related only distantly to the familiar "periodicity of a bouncing ball" ... but I get ahead of myself: we must first *expose* those (surprising) phenomena before it will make sense to try to understand them.

From (83) it follows that

$$\langle x\rangle_{\text{at time } t} = \sum_m \sum_n c_m c_n \langle x\rangle_{mn} \cos\omega_{mn}t \tag{86}$$

$$\langle x\rangle_{mn} \equiv \int_0^\infty \psi_m(x)\, x\, \psi_n(x)\, dx$$

Generally, we look to $\langle x\rangle$ because it is an object of direct physical/intuitive interest, and because its t-dependence is something we can graph (whereas to graph $|\psi(x,t)|^2$ we must run a movie, and the graphical display of $\psi(x,t)$ is even more awkward). We might in the same spirit look to the t-dependence of $\Delta x \equiv \sqrt{\langle (x-\langle x\rangle)^2\rangle}$, and have diminishing interest also in the moving higher

[44] I will pay $100 for either a proof or a counterexample!

[45] Of course, the ratios $(\xi_p-\xi_q)/(\xi_r-\xi_s)$ are *always* rational when the ξ's are described only to finitely many decimal places. As in practice they always will be. The implication is that *we must be alert to the psuedo-periodicity which is an artifact of numerical calculation*.

moments of $|\psi(x,t)|^2$. Thus, in the case of the bouncer, do we acquire interest in the integrals

$$\langle x\rangle_{mn} = k\int_0^\infty \mathrm{Ai}(kx+\xi_m)\,\mathrm{Ai}(kx+\xi_n)\,x\,dx \tag{87}$$

which I will discuss in the case $k=1$. The essentials of the analytical problem now before us are developed very nicely by Gea-Banacloche in his §3, and I am content here to follow his lead.

Gea-Banacloche begins—because it lends significance to some expressions that turn up also in the quantum problem—with the observation that the classical motion

$$x(t) = \tfrac{1}{2}g(\tfrac{1}{2}\tau+t)(\tfrac{1}{2}\tau-t)\ :\ -\tfrac{1}{2}\tau < t < +\tfrac{1}{2}\tau \text{ (repeated periodically)}$$

of a bouncing ball (see Figure 25) yields very naturally to Fourier analysis:

$$= B_0 + \sum_{p=1}^{\infty} B_p \cos\left[2p\pi(t/\tau)\right] \tag{88.1}$$

where[46]

$$\begin{aligned} B_0 &= (1/\tau)\int_{-\frac{1}{2}\tau}^{+\frac{1}{2}\tau} x(u)\,du \\ &= \tfrac{1}{12}g\tau^2 \\ &= \tfrac{2}{3}x_{\max} \\ &= \text{time-averaged value of } x(t) \\ &= \int_0^{x_{\max}} Q(x)x\,dx\ :\ Q(x) \text{ given by (40)} \end{aligned} \tag{88.2}$$

and

$$\begin{aligned} B_p &= (2/\tau)\int_{-\frac{1}{2}\tau}^{+\frac{1}{2}\tau} x(u)\cos\left[2p\pi(u/\tau)\right]du \\ &= -(-)^p\tfrac{1}{2p^2\pi^2}g\tau^2 \\ &= -(-)^p\tfrac{4}{p^2\pi^2}x_{\max} \end{aligned} \tag{88.3}$$

The remarkable efficiency of (88)—which can be written

$$x(t) = \left[\tfrac{2}{3} + \tfrac{4}{\pi^2}\left\{\tfrac{1}{1^2}\cos\left[2\pi\tfrac{t}{\tau}\right] - \tfrac{1}{2^2}\cos\left[4\pi\tfrac{t}{\tau}\right] + \tfrac{1}{3^2}\cos\left[6\pi\tfrac{t}{\tau}\right] - \cdots\right\}\right]\cdot\tfrac{1}{8}g\tau^2$$

—is indicated in Figure 25, while in Figure 26 I look to

$$\dot{x}(t) = -\tfrac{1}{\pi}\left\{\tfrac{1}{1^2}\sin\left[2\pi\tfrac{t}{\tau}\right] - \tfrac{1}{2^2}\sin\left[4\pi\tfrac{t}{\tau}\right] + \tfrac{1}{3^2}\sin\left[6\pi\tfrac{t}{\tau}\right] - \cdots\right\}\cdot g\tau \tag{89.1}$$

$$\ddot{x}(t) = -2\left\{\tfrac{1}{1^2}\cos\left[2\pi\tfrac{t}{\tau}\right] - \tfrac{1}{2^2}\cos\left[4\pi\tfrac{t}{\tau}\right] + \tfrac{1}{3^2}\cos\left[6\pi\tfrac{t}{\tau}\right] - \cdots\right\}\cdot g \tag{89.2}$$

with results that serve to underscore some of the subtle limitations of the Fourier representation. The lower part of Figure 26 acquires special interest from the

[46] Compare K. Rektorys (editor), *Survey of Applicable Mathematics* (1969), page 709.

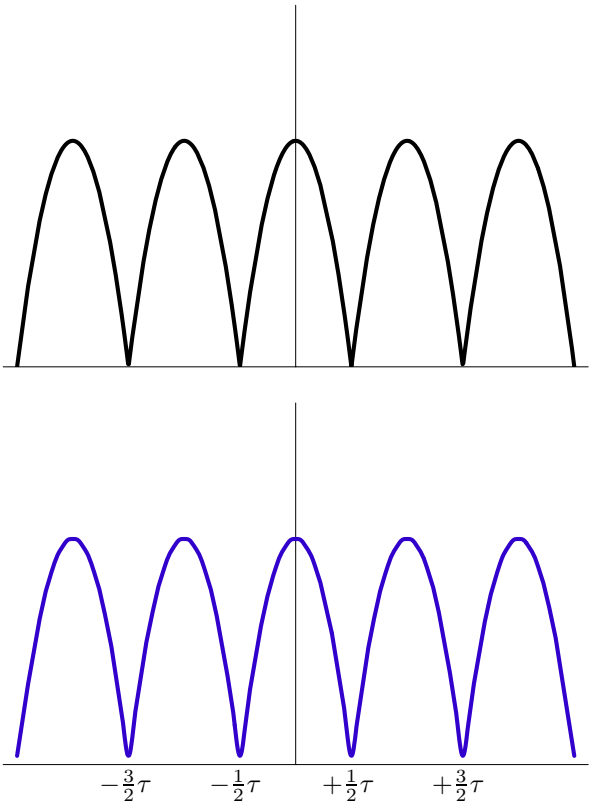

FIGURE 25: *Graphs (above) of the classical bouncing ball trajectory that during the central bounce* $-\frac{1}{2}\tau < t < +\frac{1}{2}\tau$ *is described*

$$x(t) = \tfrac{1}{2}g(\tfrac{1}{2}\tau + t)(\tfrac{1}{2}\tau - t)$$

[*in constructing the figure I set* $g = \tau = 1$] *and (below) the sum of only the first 10 terms of the Fourier representation* (88) *of* $x(t)$. *To all appearances, the inclusion of higher-order terms serves only to sharpen detail "at the bounce."*

following circumstance: our bouncing ball moves as described by an equation of motion of the form

$$m\ddot{x}(t) = \mathcal{F} \cdot \sum_{n=-\infty}^{\infty} \delta(t - \tfrac{1}{2}\tau + n\tau)$$

where in order to achieve the right impulse (abrupt change of momentum) at each bounce we must set $\mathcal{F} = 2mg\tau$.[47] The implication is that we can write

[47] From this point of view, τ controls the strength of the impulsive kick, which determines the height of the flight, and shows up finally as the period.

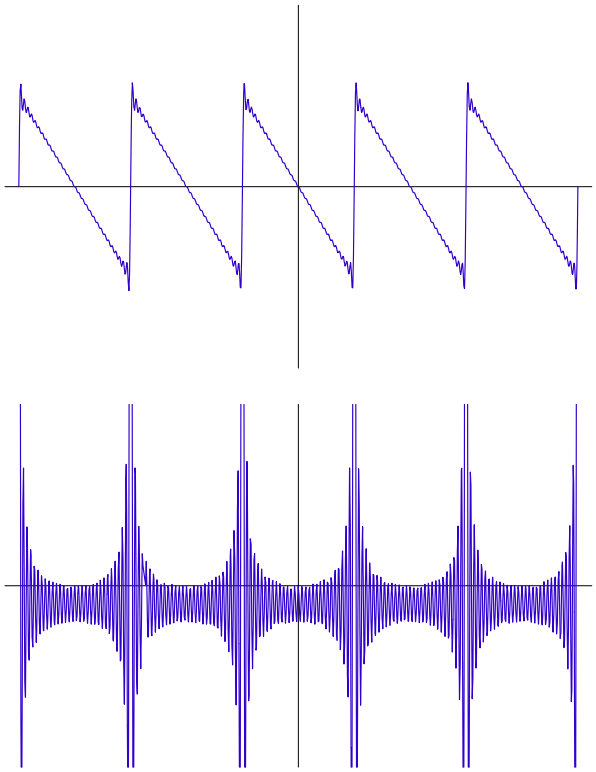

FIGURE 26: *Above: the result (compare Figure 6) of retaining the first 30 terms in the Fourier representation* (89.1) *of* $\dot{x}(t)$. *Notice the overshoot ("Gibbs' phenomenon") at the beginning and end of each descending ramp. The Fourier representation of the sawtooth waveform is, of course, an exercise familiar to engineers. Below: the result of retaining the first 30 terms in the representation* (89.2) *of* $\ddot{x}(t)$. *The interesting feature of the figure is that it is a mess: 30 terms is far too few to capture the exquisitely fine detail written into the design of the "Dirac comb" that, for the reason explained in the text, we might have expected to see.*

$$\text{Dirac comb} \equiv \sum_{k=-\infty}^{\infty} \delta(t - \tfrac{1}{2}\tau + k\tau) = \tfrac{1}{\tau} \sum_{p=1}^{\infty} (-)^p \tfrac{1}{p^2} \cos\left[2p\pi \tfrac{t}{\tau}\right] \qquad (90)$$

but it is the lesson of the figure that *truncated versions of the sum at right are not good for much*! The Fourier representation (90) of the Dirac comb may, nevertheless, prove useful (indeed: may already be known) to engineers with "tick, tick, tick, ..." on their minds.

We owe much to Gea-Banacloche the remarkable discovery that if $f_n(\xi)$ refers to the normalized bouncer functions described at (69.2) on page 37 then

$$\int_0^\infty f_n(\xi)\,\xi\,f_{n+p}(\xi)\,d\xi = \begin{cases} \frac{2}{3}|\xi_n| & : \quad p=0 \\ (-)^{p-1}\dfrac{2}{(\xi_{n+p}-\xi_n)^2} & : \quad p=1,2,3,\ldots \end{cases} \tag{91}$$

which he "was only able to guess at by considering the classical limit," for which he can provide no analytical proof, but which he considers—on convincing numerical evidence—to be *exact*. Taking my data from (69.2) on page 37, I provide an illustrative sample of that evidence:

$$\begin{aligned}
\texttt{NIntegrate}[f_4(\xi)\,\xi\,f_4(\xi),\ \{\xi,0,\infty\}] &= 4.52447 \\
\tfrac{2}{3}\xi_4 &= 4.52447 \\
\texttt{NIntegrate}[f_4(\xi)\,\xi\,f_5(\xi),\ \{\xi,0,\infty\}] &= 1.49294 \\
(-)^{1-1}2(\xi_5-\xi_4)^{-2} &= 1.49294 \\
\texttt{NIntegrate}[f_4(\xi)\,\xi\,f_6(\xi),\ \{\xi,0,\infty\}] &= -0.400045 \\
(-)^{2-1}2(\xi_6-\xi_4)^{-2} &= -0.400045 \\
\texttt{NIntegrate}[f_4(\xi)\,\xi\,f_7(\xi),\ \{\xi,0,\infty\}] &= 0.188946 \\
(-)^{3-1}2(\xi_7-\xi_4)^{-2} &= 0.188946 \\
\texttt{NIntegrate}[f_4(\xi)\,\xi\,f_8(\xi),\ \{\xi,0,\infty\}] &= -0.112210 \\
(-)^{4-1}2(\xi_8-\xi_4)^{-2} &= -0.112210
\end{aligned}$$

$$\begin{aligned}
\texttt{NIntegrate}[f_5(\xi)\,\xi\,f_5(\xi),\ \{\xi,0,\infty\}] &= 5.29609 \\
\tfrac{2}{3}\xi_5 &= 5.29609 \\
\texttt{NIntegrate}[f_5(\xi)\,\xi\,f_6(\xi),\ \{\xi,0,\infty\}] &= 1.71940 \\
(-)^{1-1}2(\xi_6-\xi_5)^{-2} &= 1.71940 \\
\texttt{NIntegrate}[f_5(\xi)\,\xi\,f_7(\xi),\ \{\xi,0,\infty\}] &= -0.455230 \\
(-)^{2-1}2(\xi_7-\xi_5)^{-2} &= -0.455230 \\
\texttt{NIntegrate}[f_5(\xi)\,\xi\,f_8(\xi),\ \{\xi,0,\infty\}] &= 0.212982 \\
(-)^{3-1}2(\xi_8-\xi_5)^{-2} &= 0.212982 \\
\texttt{NIntegrate}[f_5(\xi)\,\xi\,f_9(\xi),\ \{\xi,0,\infty\}] &= -0.125509 \\
(-)^{4-1}2(\xi_9-\xi_5)^{-2} &= -0.125509
\end{aligned}$$

Gea-Banacloche writes $(-)^p$ where he must have intended to write $(-)^{p-1}$, but apart from that trivial defect it would be difficult in the face of such evidence to deny either the accuracy of (91) or that the resourceful Dr. Gea-Banacloche

is to be applauded for an enviable stoke of genius.[48]

We are in possession now of all the information we need to plot the dynamical motion of $\langle x\rangle$ that proceeds from any prescribed initial wavefunction $\psi(x,0)$. To illustrate the point I return to the Gaussian wavepacket $\psi(x,0;a,\sigma)$ described near the bottom of page 53. More particularly, we look to the case

$$\psi(x,0;15,1.75) = \sum_{n=4}^{22} c_n\psi_n(x) \quad \text{in good approximation}$$

plotted in Figure 23. We have this data already in hand:

$$\begin{aligned}
c_4 &= 0.0034 & \xi_4 &= 6.7867\\
c_5 &= 0.0113 & \xi_5 &= 7.9441\\
c_6 &= 0.0300 & \xi_6 &= 9.0227\\
c_7 &= 0.0664 & \xi_7 &= 10.0402\\
c_8 &= 0.1251 & \xi_8 &= 11.0085\\
c_9 &= 0.2041 & \xi_9 &= 11.9360\\
c_{10} &= 0.2920 & \xi_{10} &= 12.8288\\
c_{11} &= 0.3703 & \xi_{11} &= 13.6915\\
c_{12} &= 0.4191 & \xi_{12} &= 14.5278\\
c_{13} &= 0.4259 & \xi_{13} &= 15.3408\\
c_{14} &= 0.3902 & \xi_{14} &= 16.1327\\
c_{15} &= 0.3233 & \xi_{15} &= 16.9056\\
c_{16} &= 0.2427 & \xi_{16} &= 17.6613\\
c_{17} &= 0.1653 & \xi_{17} &= 18.4011\\
c_{18} &= 0.1021 & \xi_{18} &= 19.1264\\
c_{19} &= 0.0572 & \xi_{19} &= 19.8381\\
c_{20} &= 0.0290 & \xi_{20} &= 20.5373\\
c_{21} &= 0.0132 & \xi_{21} &= 21.2248\\
c_{22} &= 0.0054 & \xi_{22} &= 21.9014
\end{aligned}$$

[48] It was today (9 June 2002) brought to my attention by Tomoko Ishihara that all of the pretty Airy relations that came originally to Gea-Banacloche's attention as results of numerical experimentation were promptly established *analytically* by David M. Goodmanson ("A recursion relation for matrix elements of the quantum bouncer. Comment on 'A quantum bouncing ball,' by Julio Gea-Banacloche," AJP **68**, 866 (2000)). In view of the fact that Gea-Banacloche's paper was published in the September 1999 issue of AJP, it is remarkable that Goodmanson's comment was stamped "received 28 September 1999." Goodmanson appears to have no institutional affiliation.

The c_n-values reproduce data presented already on page 55, and as a check on the accuracy/sufficiency of that data we compute

$$\sum_4^{22}(c_n)^2 = 0.9999 \approx 1.0000$$

The ξ_n-values are abbreviations of data presented on page 36, to which I have added two entries computed with the aid of (68.1). Several additional preparatory steps are necessary if we are to make effective use of *Mathematica* and to make sense of the results to which we will be led. We agree, as several times before, to adopt the dimensionless position coordinate

$$\xi \equiv kx = \left(\tfrac{2m^2g}{\hbar^2}\right)^{\frac{1}{3}} x \tag{92.1}$$

and, taking inspiration from (84.2)—*i.e.*, in order to be able to write

$$\omega_n t = \left(\tfrac{mg^2}{2\hbar}\right)^{\frac{1}{3}} |\xi_n| t = |\xi_n|\theta$$

—we adopt also the dimensionless time coordinate

$$\theta \equiv \left(\tfrac{mg^2}{2\hbar}\right)^{\frac{1}{3}} t \tag{92.2}$$

Notice that in this notation the classical statement

$$x_{\max} = \tfrac{1}{2}g(t_{\text{half-period}})^2$$

becomes

$$\xi_{\max} = \left(\tfrac{2m^2g}{\hbar^2}\right)^{\frac{1}{3}} \tfrac{1}{2} g \left(\tfrac{mg^2}{2\hbar}\right)^{-\frac{2}{3}} (\theta_{\text{half-period}})^2 = (\theta_{\text{half-period}})^2$$

giving

$$\theta\text{-period} = 2\sqrt{\xi_{\max}}$$

Our chosen example involves really a Gaussian *distribution* of $\xi_{\max}$-values, but if we assign to $\xi_{\max}$ its *most probable* value we obtain

$$\theta\text{-period} = 2\sqrt{15} = 7.746$$

On the other hand, we might, with equal plausibility, compute the

$$\textit{expected } \theta\text{-period} \equiv \int_0^\infty \left[\frac{1}{\sqrt{1.75\sqrt{2\pi}}} e^{-\frac{1}{4}\left[\frac{\xi-15}{1.75}\right]^2}\right]^2 2\sqrt{\xi}\, d\xi = 7.733$$

If we adopt the former hypothesis then in dimensionless (ξ, θ)-coordinates the classical bounce-bounce-bounce... can be described

$$\xi(\theta) = \left(\sqrt{\xi_{\max}} + \theta\right)\left(\sqrt{\xi_{\max}} - \theta\right) = \xi_{\max} - \theta^2 \quad : \quad -\sqrt{\xi_{\max}} < \theta < +\sqrt{\xi_{\max}}$$

which is to be repeated periodically: in the case of interest we therefore have

$$\xi(\theta) = \sum_k \left[15 - (\theta - k2\sqrt{15})^2\right] \cdot \texttt{UnitStep[}15 - (\theta - k2\sqrt{15})^2\texttt{]} \tag{93}$$

Organizing (86) to conform to our conventions and to what—especially in view of (91)—we now understand to be the facts of the situation, we write

$$\langle\xi\rangle_\theta = \tfrac{2}{3}\sum_4^{22} c_n c_n|\xi_n| - 4c_4\sum_5^{22}(-)^{n-4}c_n\frac{\cos[(\xi_n-\xi_4)\theta]}{(\xi_n-\xi_4)^2} \tag{94}$$
$$- 4c_5\sum_6^{22}(-)^{n-5}c_n\frac{\cos[(\xi_n-\xi_5)\theta]}{(\xi_n-\xi_5)^2} - \cdots + 4c_{21}c_{22}\frac{\cos[(\xi_{22}-\xi_{21})\theta]}{(\xi_{22}-\xi_{21})^2}$$

and are led to the following portfolio of figures:

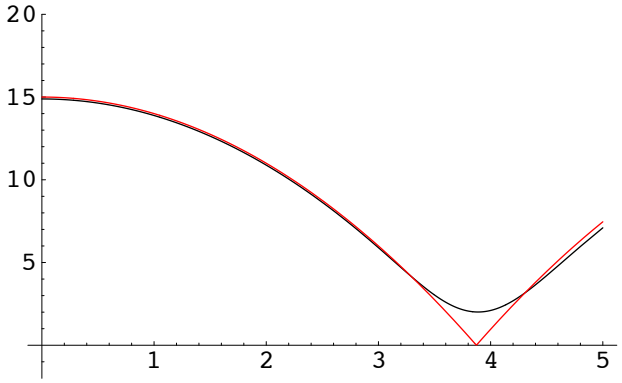

FIGURE 27: *Here and in subsequent figures, the black curve derives from* (94)*, the red curve from its classical counterpart* (93)*. The* θ*-axis runs* $\rightarrow$*, the* ξ*-axis runs* $\uparrow$*. We see that initially* $\langle\xi\rangle_\theta$ *moves along the classical parabola, but rebounds before it quite reaches the reflective barrier at* $\xi = 0$*.*

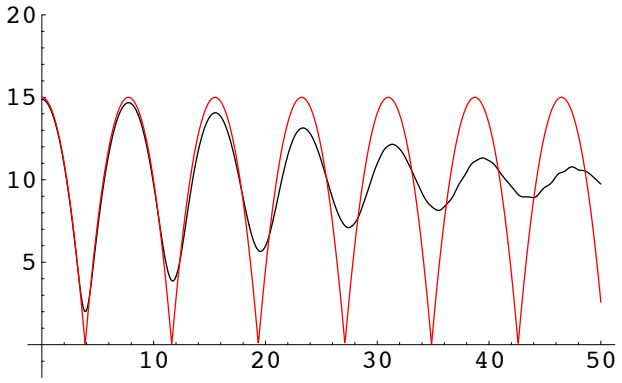

FIGURE 28: *The oscillation of* $\langle\xi\rangle_\theta$ *is seen over a longer initial interval to diminish in both amplitude and frequency.*

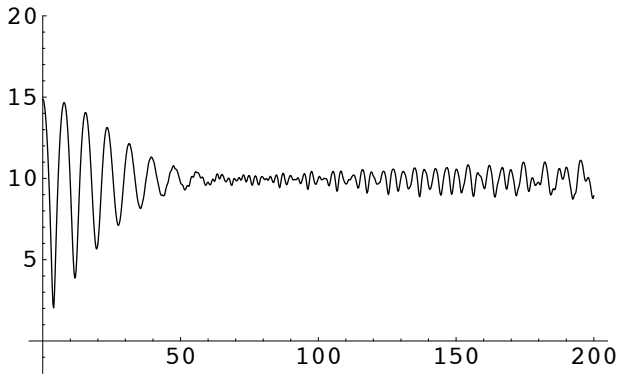

FIGURE 29: *Over a still longer time interval the* $\langle \xi \rangle_\theta$ *is seen to become nearly quiescent, and then to begin small oscillation at a higher frequency. It becomes clear on this longer time base that the*

$$\text{mean value of } \langle \xi \rangle_\theta = 10 = \tfrac{2}{3} \cdot 15$$
$$= \text{classical mean value: see (88.2)}$$

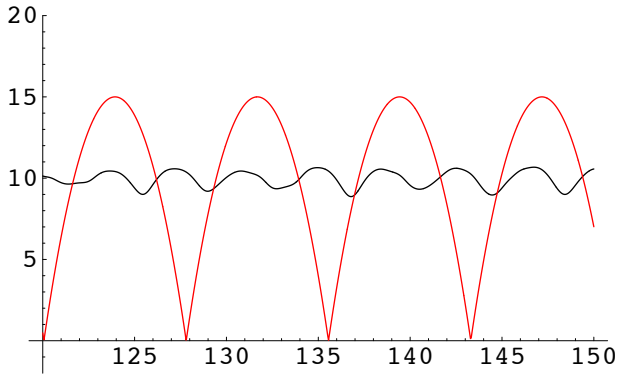

FIGURE 30: *Magnified central region of the preceding figure. The higher frequency of the reborn oscillations invites description as a kind of "frequency doubling."*

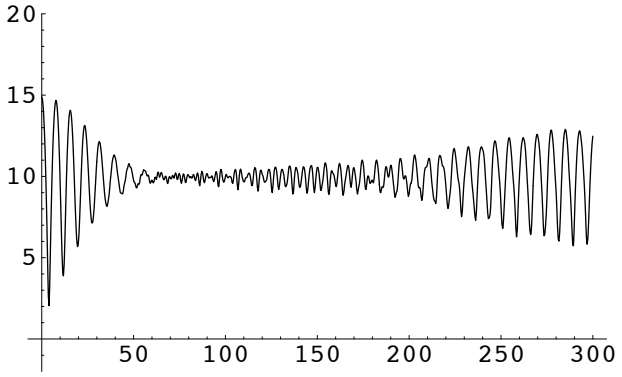

FIGURE 31: *In time the reborn oscillations grow in amplitude and revert to something like their former amplitude/frequency relation.*

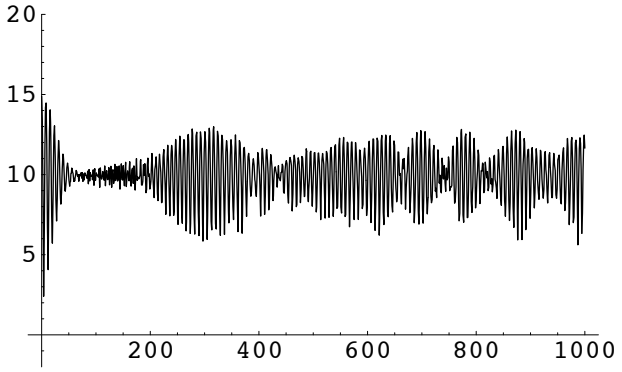

FIGURE 32: *The oscillations of* $\langle \xi \rangle_\theta$ *are seen over long times to display semi-random (chaotic?) extinctions and rebirths. This is a clear example of the* **collapse & revival phenomenon** *that has recently been recognized to be a ubiquitous feature of semi-classical quantum physics. The "quantum motion of the mean" shown here is in marked contrast to what one might have anticipated from a naive application of Ehrenfest's theorem.*

36. Things to do. The preceding discussion raises so many questions, opens so many doors ... that it seems well to attempt to construct a semi-rationally ordered list of the issues now before us, to take stock of where we are before plunging on.

• We have been watching the motion of $\langle x \rangle_t$ that follows upon "dropping" a *particular* Gaussian wavepacket: $\psi(x, 0; 15, 1.75)$. To what extent are our results typical? It would be useful to devise *Mathematica* commands that

permit one to range easily over the generality of cases $\psi(x,0;a,\sigma)$. This, I suspect, would be easy for anyone with a command of *Mathematica programing* techniques. When we wrote

$$a = 15 \cdot \left(\tfrac{\hbar^2}{2m^2 g}\right)^{\frac{1}{3}}$$

we placed ourselves deep within the quantum realm: we would have special interest, therefore, in cases where m and a are so large as to be "classical."

• In some other contexts (free particle, particle in free fall, oscillator) it proves very instructive to watch the motion of $\langle x^2\rangle_t$ and of $\sqrt{\langle x^2\rangle_t - (\langle x\rangle_t)^2}$; *i.e.*, to watch the motion of the *second* moment of $|\psi(x,t)|^2$. We are in position to do so with the quantum bouncer, for Goodmanson has supplied us with a description of the matrix elements $(\psi_m|x^2|\psi_n)$.

• $\langle x\rangle_t$ and $\langle x^2\rangle_t$ capture only *some* of the information written into $|\psi(x,t)|^2$ (which in turn captures only some of the information borne by $\psi(x,t)$). We are in position to use animation techniques to illustrate the motion of $|\psi(x,t)|^2$. Just such an animation is provided by Gea-Banacloche at the following web site: http://www.uark.edu/misc/julio/bouncing_ball/bouncing_ball.html. It is informative in a qualitative, gee-whizz kind of way, but difficult to interpret and impossible to capture on the printed page. It does, however, bring to mind this question:

• *In what respects is a "bouncing Gaussian" similar to/different from a Gaussian that smacks into a barrier and recoils*? One should track down the papers/animations/textbooks that refer to the latter (much more studied) problem. The point at issue: How does "hitting your head on a wall" differ from doing so again and again . . . unceasingly? Notice that it is very easy to devise a potential from which *all* such problems can be recovered as special cases:

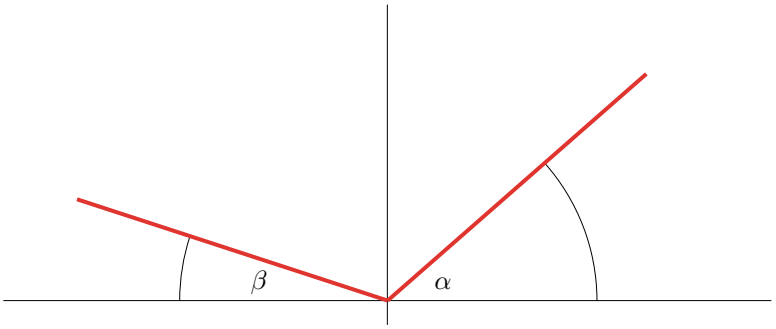

FIGURE 33: *Description of the potential $U(x;\alpha,\beta)$. By assigning suitably-selected values to α and β one can recover the free particle, free fall, bouncer, wedge, brick wall, Crandall ramp—all of the systems of present interest. I call this the "asymmetric wedge" potential. See again the figure on page 43.*

• It would be interesting to do for the wedge what we have recently done for the bouncer; *i.e.*, to construct wedge analogs of Figures 27–32. What effect does the relatively benign form of the wedge potential have on the collapse/revival phenomenon? (Certainly it has a profound effect in the free particle limit $\alpha = \beta = 0$.)

• Finally the deep question: **What has become of Ehrenfest's theorem?** We know that the motion of $\langle x \rangle$ and $\langle p \rangle$ is—for all quantum states—*exactly* classical when the Hamiltonian $H(p,x)$ depends at most quadratically on its arguments . . . as it does, for example, in the case of free fall:

$$H(p,x) = \tfrac{1}{2m}p^2 + mgx$$

The problem—for the bouncer, more clearly for the wedge—must have to do with the funny things happening at $x = 0$; *i.e.*, with the fact that our potential is defined sector-wise (though linear on each sector). In this connection it may be useful to notice that the $U(x;\alpha,\beta)$ illustrated in Figure 33 can be described

$$U(x;\alpha,\beta) = \alpha x \cdot \theta(x) - \beta x \cdot \theta(-x)$$

and if represent the unit step function $\theta(x)$ as the limit of a *differentiable* function—this can be done in many ways, of which this[49]

$$\theta(x) = \lim_{\kappa\uparrow\infty} \tfrac{1}{2}\big[1 + \tanh(\kappa x)\big]$$

is an illustrative example—then we have

$$U(x;\alpha,\beta) = \lim_{\kappa\uparrow\infty} \mathcal{U}(x;\alpha,\beta;\kappa)$$

$$\mathcal{U}(x;\alpha,\beta;\kappa) \equiv \alpha x \cdot \tfrac{1}{2}\big[1 + \tanh(\kappa x)\big] - \beta x \cdot \tfrac{1}{2}\big[1 + \tanh(-\kappa x)\big]$$

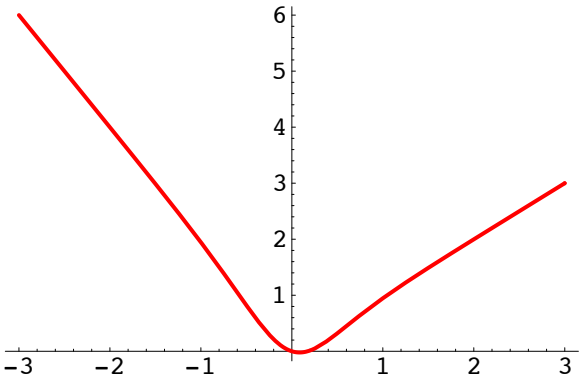

FIGURE 2: *Graph of the differentiable potential* $\mathcal{U}(x;1,2;2)$.

[49] See Spanier & Oldham, *An Atlas of Functions* (1987), page 67.

Each of the resulting Hamiltonians

$$\mathcal{H}(p,x;\alpha,\beta;\kappa) = \tfrac{1}{2m}p^2 + \mathcal{U}(x;\alpha,\beta;\kappa)$$

has the merit of being (for every finite value of κ) infinitely differentiable, and therefore well-adapted to the argument upon which Ehrenfest's theorem is based. Note, however, that the Hamiltonian $\mathcal{H}(p,x;\bullet,\bullet;\bullet)$ does *not* depended "at most quadratically on its arguments."

37. Goodmanson's analytical proof/extension of Gea-Banacloche's emperical discoveries. My source here is the short paper[48] by David M. Goodmanson that was mentioned already on page 65. I will adopt a slight modification of Goodmanson's notation.

Let the zeros of $\mathrm{Ai}(x)$ be notated $-x_n : \cdots - x_3 < -x_2 < -x_1 < 0$, the point to notice being that the x_n themselves are now *positive* numbers. Define

$$A_n(x) \equiv \mathrm{Ai}(x - x_n) \quad : \quad \begin{cases} \text{translated Airy function with} \\ n^{\text{th}} \text{ zero sitting at the origin} \end{cases}$$

and agree to work on the "bouncer half-line" $x \geqslant 0$: all $\int$'s will be understood therefore to mean $\int_0^\infty$. $\mathrm{Ai}(x)$ is a solution of Airy's differential equation(50)

$$\mathrm{Ai}\,''(x) = x\,\mathrm{Ai}(x)$$

so we have

$$A_n''(x) = (x - x_n)A_n(x) \tag{95.1}$$

and

$$A_n(x_n) = 0 \tag{95.2}$$

Notice that equations (95) do not require that the x_n be explicitly *known*.

Goodmanson's ingenious point of departure is the trivial identity

$$\Big[-f''(A_mA_n)' + 2f'A_m'A_n' \Big]_0^\infty = \int_0^\infty \big[-f''(A_mA_n)' + 2f'A_m'A_n' \big]'\,dx \tag{96}$$

where $f(x)$ is a generic placeholder that will acquire enforced properties as we proceed: our interest will attach ultimately to the cases $f(x) = x^p : p \geqslant 0$.

Look to the integrand on the right: we have

$$\begin{aligned} \big[-f''(A_mA_n)' + 2f'A_m'A_n' \big]' = -f'''(A_mA_n)' + f''\big[2A_m'A_n' - (A_mA_n)''\big] \\ + 2f'(A_m''A_n' + A_m'A_n'') \end{aligned}$$

Using (95.1) to eliminate all the A''-terms, we obtain

$$\begin{aligned} = &-f'''(A_mA_n)' - f''A_mA_n(2x - x_m - x_n) \\ &+ 2f'\big[A_mA_n'(x - x_m) + A_nA_m'(x - x_n)\big] \end{aligned}$$

Integration by parts gives

$$\int_0^\infty \big[- f'''(A_m A_n)' \big]\, dx = -f'''(A_m A_n)\Big|_0^\infty + \int_0^\infty f'''' A_m A_n\, dx$$

where the leading term on the right drops away because $A_n(0) = A_n(\infty) = 0$. We now have

$$\begin{aligned} \text{left side of (96)} = \int_0^\infty A_m A_n \big[f'''' - 2(x - x_{\rm ave}) f'' \big]\, dx \\ + \int_0^\infty 2f' \big[A_m A_n'(x - x_m) + A_n A_m'(x - x_n) \big]\, dx \end{aligned} \tag{97}$$

where with Goodmanson we have written

$$(2x - x_m - x_n) = 2\Big(x - \frac{x_m + x_n}{2} \Big) \equiv 2(x - x_{\rm ave})$$

The resourceful Dr. Goodmanson uses the identity

$$ab + cd = \tfrac{1}{2}(a + c)(b + d) + \tfrac{1}{2}(a - c)(b - d)$$

to bring the second of the preceding integrals to the form

$$\int_0^\infty \big[2f'(A_m A_n)'(x - x_{\rm ave}) - f'(A_m A_n' - A_n A_m')(x_m - x_n) \big]\, dx$$

and after an integration by parts obtains

$$\int_0^\infty \Big\{ A_m A_n \big[- 2f''(x - x_{\rm ave}) - 2f' \big] + f(A_m A_n'' - A_n A_m'')(x_m - x_n) \Big\}\, dx$$

which, if we again use (95.1) to eliminate the A''-terms, becomes

$$\int_0^\infty A_m A_n \big[- 2f''(x - x_{\rm ave}) - 2f' + f(x_m - x_n)^2 \big]\, dx$$

Returning with this information to (97) we have what I will call "Goodmanson's identity"

$$\begin{aligned} \Big[- f''(A_m A_n)' + 2f' A_m' A_n' \Big]_0^\infty \\ = \int_0^\infty A_m A_n \big[f'''' - 4(x - x_{\rm ave}) f'' - 2f' + (x_m - x_n)^2 f \big]\, dx \end{aligned} \tag{98}$$

It is from (98) that Goodmanson extracts all of his remarkable conclusions:

Set $m = n$ and $f(x) = x$ Then (98) reads

$$\Big[2A_n' A_n' \Big]_0^\infty = \int_0^\infty A_n A_n \big[- 2 \big]\, dx$$

which by $A_n^{'}(\infty)=0$ becomes

$$\int_0^\infty A_n^2(x)\,dx=\big[A_n^{'}(0)\big]^2$$

The normalized bouncer eigenfunctions can therefore be described

$$\begin{aligned}\psi_n(x)=&N_nA_n(x)\\ &N_n=\big(|A_n^{'}(0)|\big)^{-1}\equiv\big(|A^{'}(-x_n)|\big)^{-1}\quad\text{(exactly!)}\end{aligned}\tag{99}$$

But we are informed by Abramowitz & Stegun (**10.4.96**) that

$$\begin{aligned}A^{'}(-x_n)=&(-)^{n-1}f_1\big[\tfrac{3\pi}{8}(4n-1)\big]\\ &f_1(z)\equiv\pi^{-\frac{1}{2}}z^{\frac{1}{6}}\big(1+\tfrac{5}{48}z^{-2}-\tfrac{1525}{4608}z^{-4}+\cdots\big)\end{aligned}$$

so *in leading order* we have

$$N_n=\big[\tfrac{3}{8\pi^2}(4n-1)\big]^{-\frac{1}{6}}$$

In thus accounting for Gea-Banacloche's emperical formula (70) Goodmanson has greatly improved upon it ... and at the same time fulfilled the hope that inspired Gea-Banacloche to write his Appendix. But Goodmanson at a single stroke also accomplished much more:

Multiply (98) by N_mN_n to obtain

$$\begin{aligned}&\Big[-f^{''}(\psi_m\psi_n)^{'}+2f^{'}\psi_m^{'}\psi_n^{'}\Big]_0^\infty\\ &\quad=\int_0^\infty\psi_m\psi_n\big[f^{''''}-4(x-x_{\rm ave})f^{''}-2f^{'}+(x_m-x_n)^2f\big]\,dx\\ &\quad\equiv\langle m|\big[f^{''''}-4(x-x_{\rm ave})f^{''}-2f^{'}+(x_m-x_n)^2f\big]|n\rangle\end{aligned}$$

and notice that

$$\Big[-f^{''}(\psi_m\psi_n)^{'}\Big]_0^\infty=\Big[2f^{'}\psi_m^{'}\psi_n^{'}\Big]^\infty=0\quad\text{by established properties of }\psi_n(x)$$

So we have

$$\langle m|\big[f^{''''}-4(x-x_{\rm ave})f^{''}-2f^{'}+(x_m-x_n)^2f\big]|n\rangle=-2f^{'}\psi_m^{'}\psi_n^{'}\Big|_0\tag{100}$$

Set $f(x)=x^p$ with $p\geqslant 0$ and notice that the expression on the right side of (100) now vanishes unless $p=1$. In this specialized instance of (100) we have

$$\begin{aligned}p(p-1)(p-2)(p-3)\langle m|x^{p-4}|n\rangle&\\ +4p(p-1)x_{\rm ave}\langle m|x^{p-2}|n\rangle&\\ -2p(2p-1)\langle m|x^{p-1}|n\rangle&\\ +(x_m-x_n)^2\langle m|x^{p-0}|n\rangle=-2\delta_{1p}\psi_m^{'}(0)\psi_n^{'}(0)&\\ =2\delta_{1p}(-)^{m-n+1}&\end{aligned}\tag{101}$$

where the factor $(-)^{m-n}=(-)^{m+n}$ arose from the "dangling Abramowitz & Stegun signs" that were discarded when we constructed N_n, and where it is understood that terms of the form $\langle m|x^{\text{negative power}}|n\rangle$ are to be abandoned. It is as implications of (101) that Goodmanson obtains his results:

Set $m = n$ and $p = 0, 1, 2, 3, \ldots$ and read off statements which after easy serial simplifications become

$$\begin{aligned}
p = 0 \quad &: \quad 0 = 0 \\
p = 1 \quad &: \quad \langle n|n\rangle = 1 \qquad (102.1)\\
p = 2 \quad &: \quad \langle n|x|n\rangle = \tfrac{2}{3}x_n \qquad (102.2)\\
p = 3 \quad &: \quad \langle n|x^2|n\rangle = \tfrac{4}{5}x_n\langle n|x|n\rangle = \tfrac{8}{15}x_n^2 \qquad (102.3)\\
&\vdots
\end{aligned}$$

Of these, (102.1) reasserts the normalization of the bouncer state $|n\rangle$, (102.2) reproduces a result to which Gea-Banacloche was led "experimentally" on the basis of a classical guess,[50] and (102.3) is new (but would doubtless have been guessed by Gea-Banacloche if he had had any *interest* in $\langle n|x^2|n\rangle$).

Set $m \neq n$ and $p = 0, 1, 2, 3, \ldots$ Goodmanson is led to

$$\begin{aligned}
p = 0 \quad &: \quad \langle m|n\rangle = 0 \qquad (103.0)\\
p = 1 \quad &: \quad \langle m|x|n\rangle = 2(-)^{m-n+1}(x_m - x_n)^{-2} \qquad (103.1)\\
p = 2 \quad &: \quad \langle m|x^2|n\rangle = 12\langle m|x|n\rangle(x_m - x_n)^{-2}\\
&\qquad\qquad = 24(-)^{m-n+1}(x_m - x_n)^{-4} \qquad (103.2)\\
&\vdots
\end{aligned}$$

Of these, (103.0) asserts the orthogonality of the bouncer eigenstates, (103.1) establishes the exactness of a relation that Gea-Banacloche had discovered experimentally and *guessed* to be exact, and (103.2) is again new.

Goodmanson has managed by a cunning argument that, however, employs only the simplest of technical means (integration by parts) to establish an infinitude of exact formulæ that involve the transcendental zeros of the Airy function but *do not presume those x_n to be explicitly known*. His argument appears to hinge essentially on the simplicity of Airy's differential equation (*i.e.*, upon (95)), and would not appear to be applicable within a wider context —would not appear to have things to say about (say) the functions defined

$$J_n(x) \equiv J_0(x - x_n) \quad \text{where} \quad J_0(x_n) = 0$$

—so it seems unlikely that he adapted his argument from some established source: how he managed to come up with (96) as a point of departure remains therefore a mystery.

38. Motion of the second moment. Goodmanson has placed us in position to study the motion of $\langle x^2\rangle_t$, which we do by looking graphically to the motion of $\langle \xi^2\rangle_\theta$. To that end we have only to make the substitutions

[50] See again (91) on page 64. The result is foreshadowed by (88.2), page 61.

$$\begin{aligned} \tfrac{2}{3}|\xi_n| &\longmapsto \tfrac{8}{15}\xi_n^2 \\ 2(-)^{n-p}(\xi_n-\xi_p)^{-2} &\longmapsto 24(-)^{n-p}(\xi_n-\xi_p)^{-4} \end{aligned}$$

in (94). That procedure gives

$$\begin{aligned} \langle\xi^2\rangle_\theta = \tfrac{8}{15}\sum_4^{22} c_n c_n \xi_n^2 - 48c_4 \sum_5^{22}(-)^{n-4} c_n \frac{\cos[(\xi_n-\xi_4)\theta]}{(\xi_n-\xi_4)^4} \\ - 48c_5 \sum_6^{22}(-)^{n-5} c_n \frac{\cos[(\xi_n-\xi_5)\theta]}{(\xi_n-\xi_5)^4} - \cdots + 48c_{21}c_{22}\frac{\cos[(\xi_{22}-\xi_{21})\theta]}{(\xi_{22}-\xi_{21})^4} \end{aligned} \tag{104}$$

But before we look to the graphical implications of (104) we pause to acquire some benchmarks:

From the bouncer-adapted Gaussian

$$\psi(\xi,0;a,\sigma) = \tfrac{1}{\sqrt{\sigma\sqrt{2\pi}}} e^{-\frac{1}{4}\left[\frac{(\xi-a)}{\sigma}\right]^2} \quad : \quad a \gg \sigma > 0$$

we have

$$\begin{aligned} \langle\xi^0\rangle &= 1 \\ \langle\xi^1\rangle &= a \\ \langle\xi^2\rangle &= a^2+\sigma^2 \\ (\Delta\xi)^2 \equiv \langle(\xi-\langle\xi\rangle)^2\rangle &= \langle\xi^2\rangle - \langle\xi\rangle^2 = \sigma^2 \end{aligned}$$

which in the case of immediate interest—the case $\psi(\xi,0;15,1.75)$—should mark the *initial* values

$$\left.\begin{aligned} \langle\xi^1\rangle_0 &= 15 \\ \langle\xi^2\rangle_0 &= 228.063 \\ (\Delta\xi)_0^2 &= (1.75)^2 = 3.06250 \end{aligned}\right\} \tag{105.1}$$

of such curves as we will be examining—as, indeed, $\langle\xi^1\rangle_0 = 15$ does already mark the initial values of the curves shown in Figures 27, 28, 29, 31 & 32. Now let the classical bouncer distribution (40) be written

$$Q(\xi) = \frac{1}{2\sqrt{a(a-\xi)}}$$

and look to the associated *classical* moments $\langle\xi^p\rangle_{\text{classical}} \equiv \int_0^a \xi^p Q(\xi)\,d\xi$. By computation we find

$$\begin{aligned} \langle\xi^0\rangle_{\text{classical}} &= 1 \\ \langle\xi^1\rangle_{\text{classical}} &= \tfrac{2}{3}a \quad : \quad \text{compare (104.2)!} \\ \langle\xi^2\rangle_{\text{classical}} &= \tfrac{8}{15}a^2 \quad : \quad \text{compare (104.3)!} \\ (\Delta\xi)^2_{\text{classical}} &= \tfrac{4}{45}a^2 \end{aligned}$$

which at $a = 15$ become

$$\left.\begin{aligned} \langle\xi^1\rangle_\infty &= 10 \\ \langle\xi^2\rangle_\infty &= 120 \\ (\Delta\xi)^2_\infty &= 20 \end{aligned}\right\} \tag{105.2}$$

We have learned to anticipate that these are the numbers about which our quantum curves will asymptotically dither (whence the subscript $_\infty$) ... and indeed: the curves in Figures 27–32 are in fact seen to dither about $\langle\xi^1\rangle_\infty = 10$.

I present now a portfolio of figures—based upon (104)—which illustrate aspects of the time-dependence of the second moment $\langle\xi^2\rangle_\theta$, followed by a second portfolio—based jointly upon (104) and (94)—showing the motion of the "squared uncertainty" $(\Delta\xi)^2_\theta$.

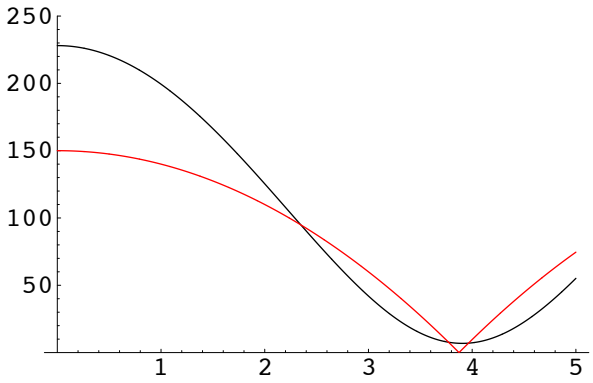

FIGURE 35: *Early motion of* $\langle\xi^2\rangle$. *From the fact that the initial value is in agreement with* (105.1) *we conclude that the truncations built into* (104) *do not introduce significant inaccuracies. Here and in subsequent figures, the red curve is an amplified trace of the classical motion* $\xi_{\text{classical}}(\theta)$, *and is intended to serve only as a clock.*

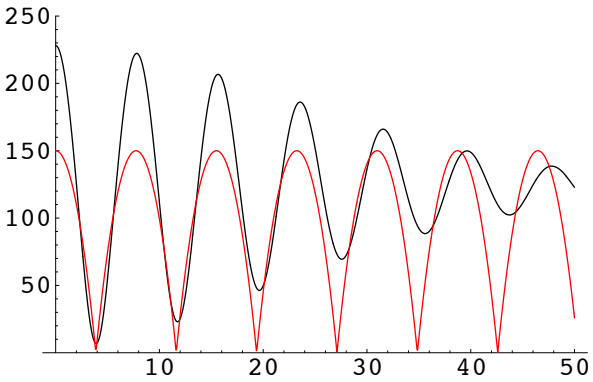

FIGURE 36: *Motion of* $\langle\xi^2\rangle$ *over the longer term. See Figure 28.*

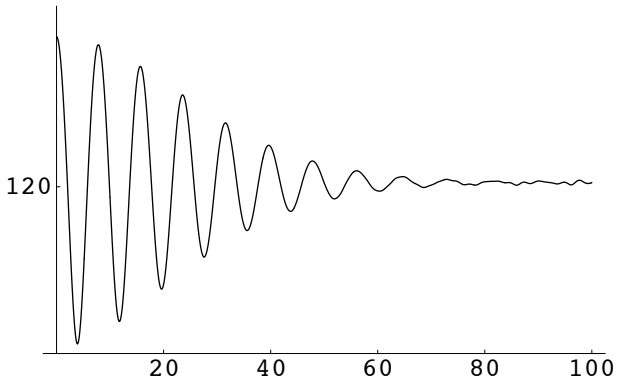

FIGURE 37: *The motion of* $\langle \xi^2 \rangle$ *"collapses" to the value anticipated at* (105.2).

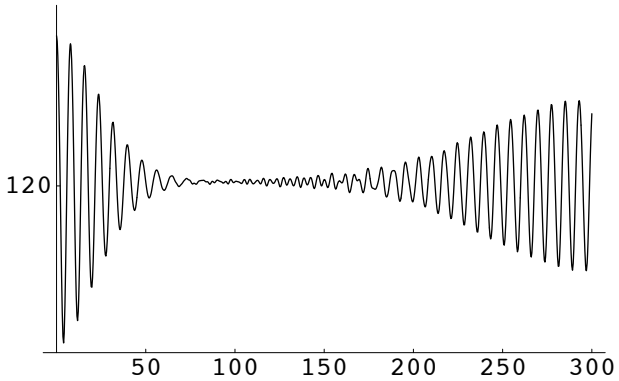

FIGURE 38: *Collapse is followed by a "revival" even more distinct than that exhibited by the first moment (Figure 31).*

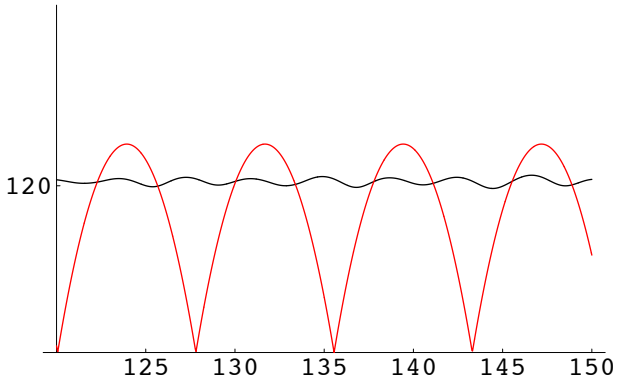

FIGURE 39: *The phase shift and frequency doubling encountered already in Figure 30 show up also in the motion of* $\langle \xi^2 \rangle$.

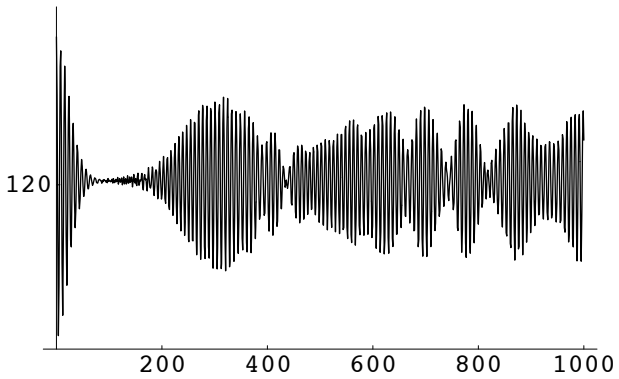

FIGURE 40: *Semi-chaotic motion of* $\langle \xi^2 \rangle$ *in the long term. This ends the set of figures relating to the motion of* $\langle \xi^2 \rangle$*: we turn now to the motion of* $(\Delta\xi)^2$*.*

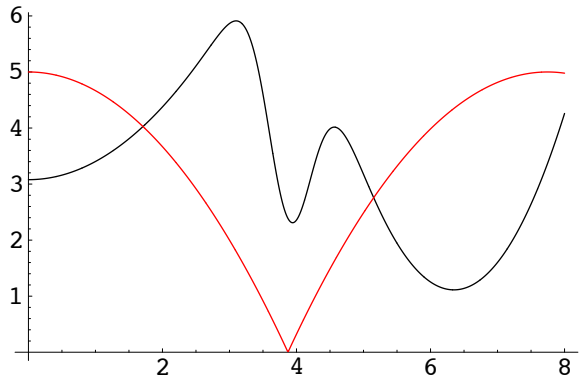

FIGURE 41: *Initial motion of* $(\Delta\xi)^2$*. The initial value conforms to* (105.1)*, and during the first part of the first bounce the growth of* $(\Delta\xi)^2$ *is plausibly hyperbolic, as for a particle in free fall.*

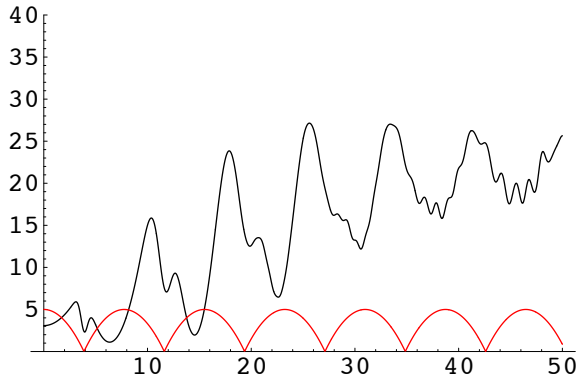

FIGURE 42: *Motion of* $(\Delta\xi)^2$ *in the longer term. Note the details coincident with the classical bounce points, other details that slightly anticipate the top of the classical flight.*

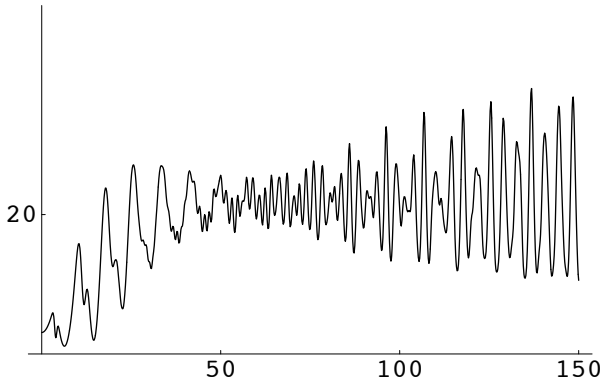

FIGURE 43: *The motion of* $(\Delta\xi)^2$ *in the still longer term does not display a conspicuous collapse, but does asymptotically dither about the classical value given in* (105.2).

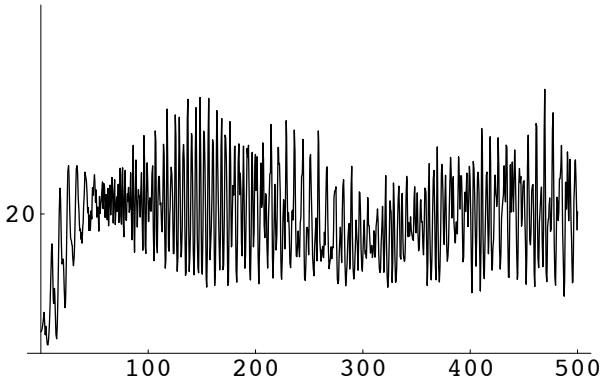

FIGURE 44: *The motion of* $(\Delta\xi)^2$ *in the still longer term does not display a conspicuous collapse, but does asymptotically dither about the classical value given in* (105.2).

39. Collapse & revival. The figures, though they pertain to an arbitrarily-selected particular case, establish the *existence* of a "collapse/revival phenomenon"—quite pronounced during the "adolescence" of $\langle\xi^1\rangle_\theta$ and $\langle\xi^2\rangle_\theta$, semi-random and less pronounced when those (also other?) moments have reached a riper old age. Can the gross features of the phenomenon be understood theoretically?